

AD _____

Award Number: DAMD17-98-1-8526

TITLE: An Innovative Strategy for the Prevention and Treatment
of Metastatic Prostate Cancer: Modified Tetracycline as
Chemotherapeutics

PRINCIPAL INVESTIGATOR: Balakrishna L. Lokeshwar, Ph.D.

CONTRACTING ORGANIZATION: University of Miami School of Medicine
Miami, Florida 33136

REPORT DATE: October 2002

TYPE OF REPORT: Annual

PREPARED FOR: U.S. Army Medical Research and Materiel Command
Fort Detrick, Maryland 21702-5012

DISTRIBUTION STATEMENT: Approved for Public Release;
Distribution Unlimited

The views, opinions and/or findings contained in this report are
those of the author(s) and should not be construed as an official
Department of the Army position, policy or decision unless so
designated by other documentation.

20041112 029

REPORT DOCUMENTATION PAGE			Form Approved OMB No. 074-0188	
Public reporting burden for this collection of information is estimated to average 1 hour per response, including the time for reviewing instructions, searching existing data sources, gathering and maintaining the data needed, and completing and reviewing this collection of information. Send comments regarding this burden estimate or any other aspect of this collection of information, including suggestions for reducing this burden to Washington Headquarters Services, Directorate for Information Operations and Reports, 1215 Jefferson Davis Highway, Suite 1204, Arlington, VA 22202-4302, and to the Office of Management and Budget, Paperwork Reduction Project (0704-0188), Washington, DC 20503				
1. AGENCY USE ONLY (Leave blank)	2. REPORT DATE October 2002	3. REPORT TYPE AND DATES COVERED Annual (1 Oct 01 - 30 Sep 02)		
4. TITLE AND SUBTITLE An Innovative Strategy for the Prevention and Treatment of Metastatic Prostate Cancer: Modified Tetracycline as Chemotherapeutics		5. FUNDING NUMBERS DAMD17-98-1-8526		
6. AUTHOR(S): Balakrishna L. Lokeshwar, Ph.D.				
7. PERFORMING ORGANIZATION NAME(S) AND ADDRESS(ES) University of Miami School of Medicine Miami, Florida 33136 E-Mail: blokeshw@med.miami.edu		8. PERFORMING ORGANIZATION REPORT NUMBER		
9. SPONSORING / MONITORING AGENCY NAME(S) AND ADDRESS(ES) U.S. Army Medical Research and Materiel Command Fort Detrick, Maryland 21702-5012		10. SPONSORING / MONITORING AGENCY REPORT NUMBER		
11. SUPPLEMENTARY NOTES				
12a. DISTRIBUTION / AVAILABILITY STATEMENT Approved for Public Release; Distribution Unlimited			12b. DISTRIBUTION CODE	
13. Abstract (<i>Maximum 200 Words</i>) (<i>abstract should contain no proprietary or confidential information</i>) In this second year (months 12-24) of the Phase II of the project, the molecular basis of chemoresistance in prostate tumor cells, acquired due to their interaction with stromal cells was explored. Both biochemical and molecular biological approaches using quantitative mRNA expression analysis by cDNA Microarray, Quantikine mRNA ELISA, and stable transfection with anti-sense cDNA were undertaken to analyze the role of three pro-inflammatory cytokines in the modulation of tumor cells' response to chemotherapeutic drugs. These studies revealed that in addition to chemodrugs induced increase in the expression levels of three cytokines IL-1 β , IL-6 and IL-8, Cyclooxygenase-II (COX-2), the key enzyme in the classical inflammatory response, in also highly elevated. Inhibition of the expression of IL-1 β , IL-6 and IL-8, not only increased response chemotherapy drug-induced cytotoxicity and apoptosis but also showed an interlinking relationship between the three cytokines. Inhibition of COX-2 by specific inhibitors such as Celecoxib or NS 398 also induced apoptosis mediated cytotoxicity in CaP cells. A combination of COX-2 inhibition and CMT-3 revealed synergistic increase in cytotoxicity and apoptosis. Furthermore, a combined treatment modality, using Celecoxib and CMT-3, in mice bearing human tumor xenografts produced an increased tumor growth delay, without any adverse effect on the host, suggesting increased efficacy.				
14. SUBJECT TERMS: CMT-3, COL-3, celecoxib, prostate cancer, metastasis, neo-adjuvant, chemotherapy, antisense therapy			15. NUMBER OF PAGES 49	
			16. PRICE CODE	
17. SECURITY CLASSIFICATION OF REPORT Unclassified	18. SECURITY CLASSIFICATION OF THIS PAGE Unclassified	19. SECURITY CLASSIFICATION OF ABSTRACT Unclassified	20. LIMITATION OF ABSTRACT Unlimited	

Table of Contents

Cover.....	1
SF 298.....	2
Table of Contents.....	3
Introduction.....	4
Body	5
Key Research Accomplishments.....	12
Reportable Outcomes.....	13
Conclusions.....	14
References.....	14

Appendices

1. Lokeshwar BL, Selzer MG, Zhu B, Block NL, Golub LM. Int J Cancer. 98:297-309, 2002.
2. Lokeshwar BL, Dandekar DS, Lopez M. Miami Nature Biotechnology Short Reports .Vol 14, 109a, 2003.
3. Lokeshwar BL, Dandekar DS, Lopez M. AACR Proceedings, Vol. 44, 3723a, 2003.
4. Dandekar DS, Lokeshwar VB, Cevallos-Arelano E, Soloway MS, Lokeshwar BL. Cancer Chemo. Pharm. Vol. 51 (in press).

Title: Title: An innovative strategy for the prevention and treatment of metastatic prostate cancer: chemically modified tetracycline as chemotherapeutics-Phase II.

A. Introduction and background: The overall goal of this funded project is to determine the utility of non-antibiotic forms of chemically modified tetracycline (CMT) against metastatic prostate cancer, with specific emphasis on prostate cancer-metastasis to bone. During the first phase of this project after screening about 10 analogues of CMTs, we identified a non-antimicrobial CMT, 6-deoxy, 6-demethyl, 4-dedimethylamino tetracycline (CMT-3, COL-3) as a potent orally bioavailable anti-neoplastic and anti-metastatic agent. Although we had initially hypothesized CMTs as anti-metastatic agents due to their strong anti-metalloproteinase (anti-collagenase) activity in several systems [1-3], we discovered some of the CMTs have activities similar to cytotoxic chemotherapeutic agents. We found, CMTs inhibit cell proliferation via mitochondrial permeabilization, induction of apoptosis and by arresting cells at G1/S boundary [4-6]. These properties combined with their strong affinity for bone matrix led us to test the efficacy of CMT-3 on bone metastasis. We reported that when tested on a highly aggressive prostate cancer model, induced to form skeletal/lumbar bone metastasis, CMT-3 was able to inhibit development of paraplegia and cause a significant delay in development of morbidity associated with lung metastasis [7].

The compound was tested in the clinic (Phase I) independent of this research group and was recommended for Phase II and III trials. However, its clinical efficacy was modest (28% disease stabilization, and 13% remission [8]. The major dose-limiting toxicity was development of photosensitivity at doses above 70 mg/day, and drug-induced lupus (7%). Several derivatives of CMT-3s, with modifications to Carbon-7 and carbon-9 positions of the CMT-3 was developed and tested for similar activities. We reported earlier that functionally, CMT-303 (9-Nitro CMT-3), and CMT-308 (9-aminoCMT-3) resemble CMT-3 activity without photo toxicity [5]. We had three objectives in this second phase of the project. These are: (1) Test the efficacy of CMT-3 and CMT-308 on tumor growth and metastasis, either alone or combined with other therapeutic modality; such as cytotoxic chemotherapeutic drugs (e.g., docetaxel or doxorubicin) or radiation, (2) Test the cytotoxic and antimetastatic activity of halofuginone - a novel collagenase and collagen synthesis inhibitor halofuginone (Stenorol) [9-11] - and (3) Determine how stromal cells modify the cytotoxic response of tumor cells to CMT-3 and other chemotherapeutic drugs (chemodrugs).

The findings related to the effect of halofuginone (HF) and CMT-3 either alone or in combination was reported last year (2002 progress report). We discontinued the work with HF for two reasons. One, CMT-3 and HF did not provide any additional cytotoxicity than either agent alone. Two, HF is not readily available, it is now a property of COLGARD Inc, a startup company in Israel. Researchers associated with COLGARD have published interesting results on the effect of HF on prostate cancer models. However, other groups have published that HF is not effective in laboratory animals when administered orally and minimally effective against a few cancers in experimental models [12-13]. Due to these contested findings we did not pursue the combination studies during this reporting period (March 2002-April 2003). However, this principal investigator (B. Lokeshwar) is in contact with Dr. Arnon Nagler of COLGARD (and Chaim Sheba Medical Center, Tel-Hashomer, Israel), to pursue the project if needed.

We focused our effort to work proposed under task 3, namely acquired drug resistance and role of stroma-derived cytokines in the modification of chemotherapeutic drug sensitivity. We investigated the role of Interleukin-1 β (IL-1 β), interleukin-6 and Interleukin-8 (IL-8) in chemo sensitivity and chemo invasion of prostate cancer cells using stable transfectants of PC-3MI cells with each of the three cytokines. In addition, we discovered during the last year or so, that CMT-3 and specific inhibitors of cyclooxygenase-2 (COX-2) increase the cytotoxicity in an additive to synergistic fashion. Particularly interesting COX-2 inhibitor was Celecoxib (CXB) that increased the cytotoxicity of CMT-3 by more than 2-fold, and depending on which drug was added first, CMT-3 and CXB synergistically (>2x) increased drug-induced apoptosis. We investigated the in vitro and in vivo sensitivity of the single chemotherapeutic drug (CMT-3 or doxorubicin (DXR)) or CXB or in vivo sensitivity to combined agents (CMT-3+CXB). These results are succinctly described in the following pages.

Progress Report:

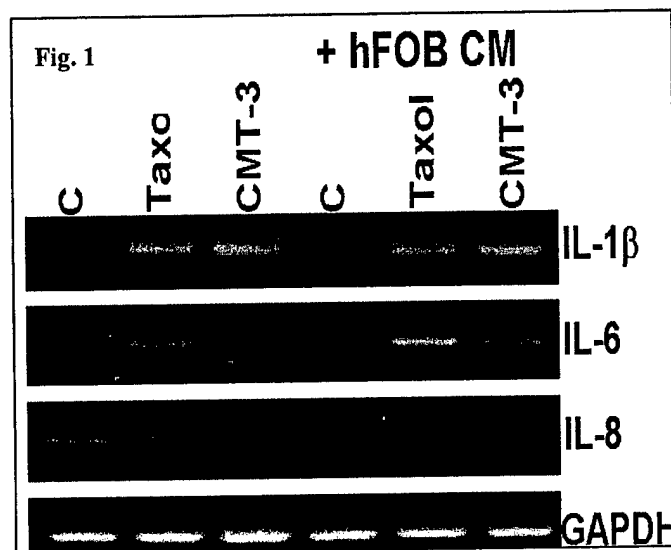
B1. Cytokines modulate drug sensitivity in CaP cells: We reported previously that stromal cell culture-conditioned medium (S-CCM) from diverse sources alter the cytotoxic response of CaP cells

Treatment	IL-1 β (ng/ml)
Growth medium	42.5 \pm 8.2
CMT-3	16.9 \pm 3.2
Taxol	13.4 \pm 2.5
hFOB	32.7 \pm 2.4
HFOB + Taxol	29.4 \pm 5.2
HFOB + CMT-3	21.8 \pm 1.6

Table 1: IL-1 β in PC-3ML CM

(Reports 2001 and 2002). The stromal cells or cell lines used are: a fetal human osteoblastic cell line (hFOB), a fetal lung fibroblast cell line (HLF), primary prostate fibroblasts and smooth muscle cells, and the mouse NIH 3t3 cell line. Instead of fractionating the concentrated CCM and trying to identify active agent (s), we took an alternate approach. Several reports in recent years suggest that tumor cells respond to anticancer drugs in the similar manner as immune cells respond to environmental stress and release pro-inflammatory cytokines and chemokines [14,15]. The gene expression array study described previously (Report 2002) revealed that expression of pro-inflammatory cytokines such as, IL-1 β , IL-6 and IL-8 is altered in the presence of chemotherapeutic

drugs and stromal CCM. These chemokines have been shown to induce acquired drug resistance or sensitivity in other tumor cells, including DU145 cells exposed to Cis-platin [16]. We analyzed the levels of these three interleukins in CaP cells exposed to chemotherapeutic drugs in the presence or absence of stromal CCM.

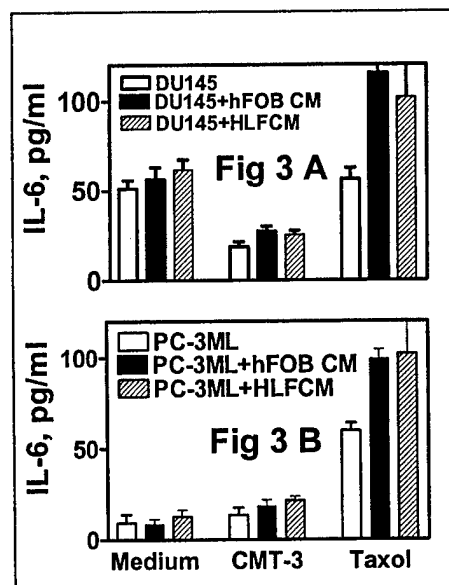
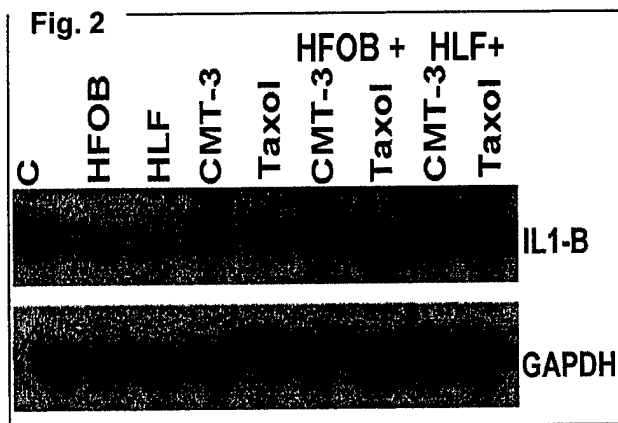


B1.2. Changes in the expression and levels of IL1- β , IL-6 and IL-8 during drug-induced cytotoxicity: We investigated the changes in the expression and secretion of three cytokines IL-1 β , IL-6 and IL-8 after PC3-ML cells exposed to chemotherapeutic drugs in the presence or absence of stromal CCM. **Fig 1** shows semi-quantitative RT-PCR analysis of RNA isolated from PC-3ML cells, cultured in the presence or absence of hFOB CCM for 2 days, followed by treatment with either taxol (0.1 μ g/ml) or CMT-3 (5 μ g/ml) for 3 h, and a recovery period of 24 h. At these doses of drugs, the clonogenic survival was ~50% (data not shown). IL1- β , IL-6 and IL-8 specific primer pairs were used to amplify 297 bp, 291 and 196 bp PCR products, respectively.

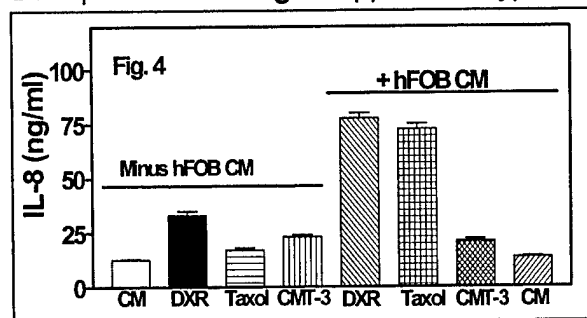
The cycles of PCR amplification were 32, 40, and 36 for IL-1 β , IL-6 and IL-8, respectively. Both taxol and CMT-3 induced IL1- β expression (> 3-fold) and stromal CCM had minimal effect on this increase. While taxol increased IL-6 mRNA expression, in the presence of CMT-3 the expression actually decreased by ~ 40%. IL8 expression decreased in the presence of taxol, however, in the presence of hFOB CCM, the inhibitory effect of taxol on IL-8 mRNA expression was abolished. CMT-3 was effective in reducing IL-8 expression, both in the presence and absence of hFOB CCM. These drugs had similar effects on DU145 cells, treated with hFOB, HLF and 3T3-CCM. Consistent with a published report, LNCaP showed no detectable mRNA expression of the 3 cytokines [15].

We next measured IL1- β , IL-6 and IL-8 levels in the CCM of drug treated PC-3ML and DU145 cells using cytokine specific ELISA kits (Chemicon Inc. San Diego, CA) As shown in **Table 1**, contrary to the PCR results, IL1- β levels secreted in PC-3ML CM decreased by ~ 70%, following CMT-3 and taxol treatment. In the presence of hFOB CCM, IL1- β secretion returned to normal in taxol treated cells and modestly in CMT-3 treated cells. To understand the cause of this disparity, we performed northern blot analysis on the total RNA from PC-3ML cells, following various treatments, using IL-1 β cDNA probe as described above. As shown in **Fig. 2**, the northern blot results mirrored the PCR. Cells treated with CMT-3 in the presence or absence of either hFOB or HLF CCM, increased IL1- β mRNA expression.

Therefore, it is possible that although, the secretion of IL-1 β decreases in drug-treated cells, there may be an intracellular accumulation of the pro- IL-1 β form.



examined the alteration in the IL-6 receptor levels in taxol-treated PC-3ML and DU145 cells, using an anti-IL-6R antibody (Chemicon Inc., CA), by flow cytometry. Flow cytometry analysis found no significant changes in the IL-6R specific fluorescence (data not shown). The CCM of CaP cells also showed no alteration in soluble IL-6R (sIL-6R) levels following drug treatment. Therefore, we conclude that although there is an increase in the expression and secretion of IL-6, there is no quantitative change in the cell-surface receptor expression. These results show that to overcome the IL-6-mediated acquired drug resistance, silencing its expression by antisense cDNA transfections may be necessary. Data presented in **Fig 4** support this hypothesis.



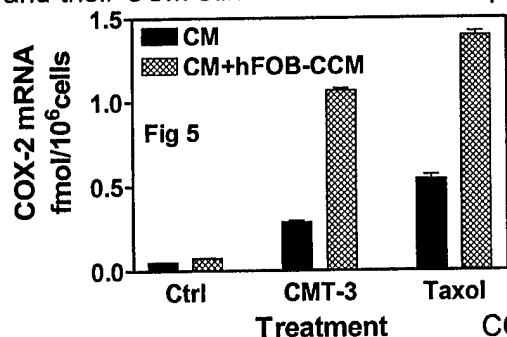
DXR and taxol induced a ~ 4-fold increase in IL-8 secretion, suggesting that stromal-cell induced IL-8 secretion may play a role in acquired resistance to conventional chemotherapeutic drugs. As was the case for IL-6, stromal CCM did not induce IL-8 secretion in CMT-3 treated cells. These results are consistent with the observed effect of CMT-3 on IL-8 mRNA expression analyzed using RT-PCR.

We measured the levels of IL-6 in the CCM of PC-3ML and DU145 with an ELISA kit (Chemicon Inc). As shown in **Fig.3 A, and B**, IL-6 levels are increased by 7 to 10 fold in PC-3ML cells treated with taxol in the presence of hFOB and HLF CCM. The increase in IL-6 levels in the CCM of DU145 cells treated with taxol was not very significant, possibly because DU145 cells secrete constitutively high levels of IL-6 (unpublished observation). None-the-less, in the presence of stromal CCM, taxol treatment resulted in a 2-fold increase in IL-6 secretion. These results are consistent with the RT-PCR data presented in **Fig. 1**. Similar results were also obtained when DU145 and PC-3ML cells were treated with DXR (0.2 μ g/ml). These results suggest that IL-6 may participate in the development of acquired drug resistance (ADR) in CaP cells. This may be through the interaction of CaP cells with stromal cells in tumor environment. However, CMT-3 tempered the stimulatory effect of hFOB and HLF CCM on the secretion of IL-6 by DU145 and PC-3 ML cells. This suggests that CMT-3 may be a better drug in overcoming the acquired chemoresistance, in the sense that stromal influence on its cytotoxic effect may be minimal.

We also examined whether external addition of IL-6 (0.1 to 1 ng/ml) or neutralizing antibody to IL-6 (5 –10 μ g/ml) will affect chemoresistance in DU145 and PC-3ML cells. This external addition of either IL-6, or antibody addition did not alter stromal-cell induced chemoresistance to taxol, as determined by cell proliferation assays (data not shown). Therefore, it is likely that an **"intracrine" mechanism** is involved in intracellular activation of IL-6 receptor (IL-6R) and the associated GP130 protein [16]. We also

We measured the secretion of IL-8 by CaP cell lines treated with chemotherapeutic drugs in the presence or absence of stromal CCM using a human-IL-8 ELISA kit (R&D Systems). As shown in **Fig. 4**, the amount of IL-8 secreted into culture medium by PC-3ML cells was almost 100-fold higher than IL-6. PC-3ML cells secreted IL-8 at the rate of 12 ng/10⁶ cells/6-cm dish and treatment with chemotherapeutic drugs (i.e., DXR, taxol or CMT-3) did not significantly alter IL-8 secretion. However, in the presence of hFOB CM, both

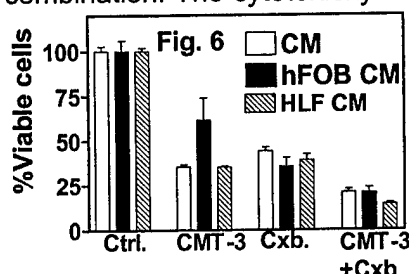
B2. a. Induction of COX-2 by stromal cells and antitumor drugs: Since we found that stromal cells and their CCM stimulate a number of prominent pro-inflammatory cytokines in CaP cells, we examined



whether the classical inflammatory response is also affected when CaP cells are exposed to cytotoxic drugs. Since COX-1 is constitutively expressed and total inhibition of COX-1 is not desirable, due to its gastric cytoprotective function [17], we focused on the inducible COX, i.e., COX-2. We used a quantitative species-specific Quantikine COX-2 mRNA ELISA (R&D Systems, MN) to measure the inducible expression of COX-2 in PC-3ML cells exposed to chemotherapeutic drugs.

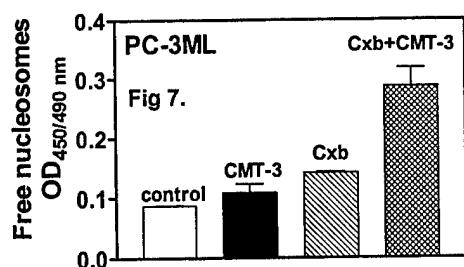
PC-3ML cells cultured in the presence or absence of hFOB CCM were exposed to CMT-3 (5 μ g/ml) and Taxol (0.1 μ g/ml) for 24 hours. Total RNA was extracted, and 2.5 μ g total RNA from each treatment group was analyzed for the amount of COX-2 mRNA. As shown in Fig 5, there was a 5-fold (CMT-3 treated) to 10-fold (taxol treated) increase in the COX-2 mRNA levels when PC-3 cells were exposed to drugs. This increase was even more in the presence of hFOB CCM (i.e., 10-fold in CMT-3 and 15-fold in taxol-treated cells). These results are consistent with our hypothesis that stromal cells may induce chemoresistance in CaP cells by inducing a classical inflammatory response.

B2.b. Inhibition of PC-3 proliferation by Celecoxib, a preferential COX-2 inhibitor: Celecoxib (Cxb) an NSAID, has been approved as a selective inhibitor of COX-2 and has found wide application in inflammatory diseases [18]. Cxb and another COX-2 inhibitor, NS398 (Calbiochem Corp., CA) have been shown to inhibit cell proliferation, tumor growth and metastasis [19-21]. We examined a possible additive or synergistic cytotoxic activity of CMT-3 and Cxb in PC-3ML cells. PC-3ML cells, cultured with or without hFOB or HLF CCM for 48 hr were exposed to CMT-3 (5 μ g/ml) or CXB (10 μ M) and their combination. The cytotoxicity was determined by MTT assay. As shown in Fig. 6, Cxb was significantly

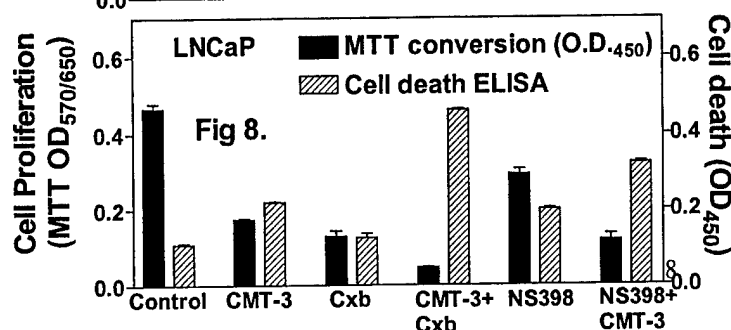


cytotoxic to PC-3ML cells, and neither hFOB nor HLF CCM alters its toxicity. A combination of CXB and CMT-3 found to have an additive response on the cytotoxicity.

We examined whether increased cytotoxic activity of CMT-3 + Cxb combination is due to an increase in apoptotic cell death. PC-3ML cells incubated with CMT-3 (5 μ g/ml), Cxb (10 μ M) or their combination, were assayed for apoptotic activity using the Cell death ELISA-plus kit (Roche Molecular Diagnostics, IN). The assay detects free-histone H1 resulting from nucleosome fragmentation during apoptosis. Free H1 histones are detected using a polyclonal antibody in the ELISA. We observed a 1.2-fold increase in apoptotic activity (Fig 7), in CMT-3 treated cells, and 1.6-fold increase in Cxb treated cells. Furthermore, the combination increased apoptotic activity by 3.5-fold, more than the sum of CMT-3 and Cxb effects alone. Thus, CMT-3 and Cxb are likely to have a synergistic effect on inducing apoptosis in PC-3ML.



We next examined whether CMT-3 and Cxb combination has similar cytotoxic and apoptosis-inducing activity in the androgen-sensitive cell line LNCaP. LNCaP cells (10⁴/well; 48-well plate) were incubated with CMT-3 (5 μ g/ml), Cxb (10 μ M), NS398 (10 μ M) or their combination for 24h. Cell proliferation was measured by MTT assay and apoptotic activity was measured using Cell death ELISA kit. As shown in Fig 8,



CMT-3 inhibited cell proliferation (62%) and induced apoptosis (2-fold). Although, Cxb and NS398 inhibited cell proliferation (73% and 35%, respectively) neither Cxb nor NS398 induced significant apoptosis. However, CMT-3 and Cxb combination inhibited cell proliferation by 90% and caused a 4.6-fold increase in apoptosis. Similarly, CMT-

3+NS398 combination inhibited cell proliferation by 71% and caused a 2.9-fold increase in apoptosis. Based on these results **CMT-3+Cxb combination appears to be superior to CMT-3+NS398** for inducing apoptosis and inhibiting cell proliferation.

In addition, we examined the effect of CMT-3 and Cxb combination treatment on cell-cycle

Gene	Changes in mRNA Expression		
	CMT-3	Cxb	CMT-3+Cxb
IL1- β	-	\uparrow 1.8	\downarrow 7.6
IL-8	-	-	\downarrow 2.5
IL13-R alpha 2	-	\uparrow 3.2	-
C-X-C cytokine 5		\uparrow 2.7	\downarrow 14.4
C-X-C member 6		\uparrow 5.9	\downarrow 8.1
C-X3-C R1			\downarrow 2.0
CP-4	\uparrow 4.0	-	-
COX-2	-	-	\downarrow 4.2
Prostate diff. factor (PLAB)	\uparrow 2.7	\downarrow 2.1	\downarrow 3.0
Cyclin D1 & E1	\downarrow 4.0	\downarrow 2.1	\downarrow 2.1
UPA	-	\uparrow 1.8	\downarrow 2.9
IGF BP 1	\uparrow 11.0	-	-
IGF BP 3		\uparrow 1.8	\downarrow 2.9

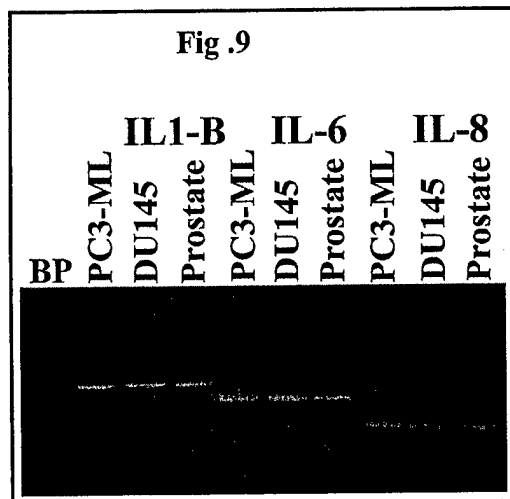
Table 4: Differential gene expression in drug-treated PC-3ML cells. \uparrow and \downarrow arrows

phase progression in PC-3ML cells. PC-3ML cells cultured in 60 mm dishes at 2×10^5 cells/dish were treated with CMT-3 ($5 \mu\text{g/ml}$), CXB, $10 \mu\text{M}$, and CXB + CMT-3 together ($10 \mu\text{M}$ each) for 24 h. Following the incubation, cells were simultaneously lysed, stained with propidium iodide ($50 \mu\text{g/ml}$), and the nuclei suspension was analyzed in a flow cytometer (Coulter XL). Data collected using a long-pass filter (620 nm) were analyzed for cell cycle analysis using the MODFIT (Verity Software, ME) program for determining the

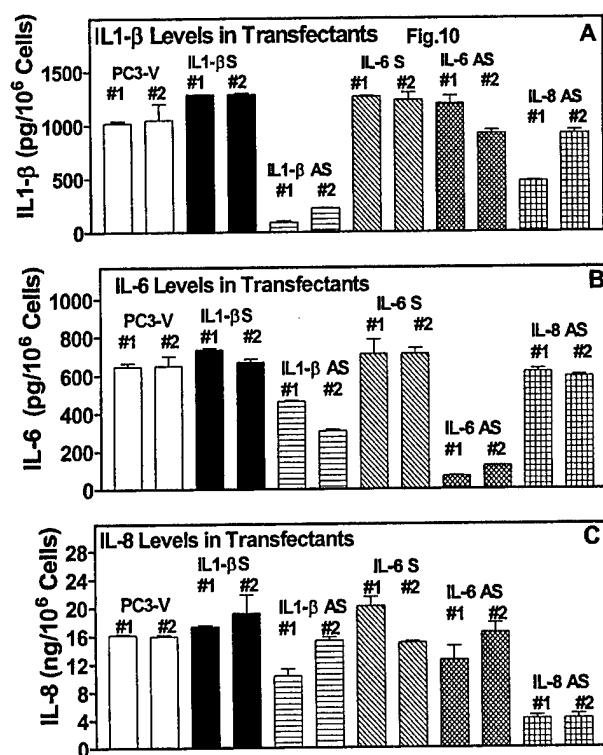
proportion of cells in various phases of cell cycle. The fraction of cells in G0/G1 phase in CMT-3 ($5 \mu\text{g/ml}$) treated samples ($75.6 \pm 6.5\%$) was significantly higher compared to untreated control ($54.4 \pm 3.4\%$). Cxb ($10 \mu\text{M}$) also caused some G0/G1 phase arrest (63.2 ± 5.0). However, the G0/G1 fraction of Cxb+CMT-3 combination (78.9 ± 5.2) was not significantly different than that of CMT-3 treated samples. These results suggest that the higher cytotoxicity of CMT-3+Cxb combination may not be due to their effect on cell cycle arrest alone. Based on the biochemical analysis of cytotoxicity of either CMT-3 or CXB, we were not convinced that only a handful of genes are responsible for the added cytotoxicity of CMT-3plus CXB. We chose to analyze the changes in the gene expression profile of cells treated with CMT-3, CXB alone or in combination.

B2.c. Comparison of differential gene expression in CMT-3, Cxb and CMT3 + Cxb treated PC-3ML cells: cDNA microarray analysis was carried out in the DNA Microarray facility (Univ. Miami). In this facility, cDNA micro arrays are printed in-house with the Gene Machines Omni grid-arraying robot. The cDNA sequences used for arraying are exclusively licensed from Agilent Technologies, which has licensed the full Incyte gene content to our facility. PC-3ML cells were treated with CMT-3 ($5 \mu\text{g/ml}$), Cxb ($10 \mu\text{M}$) or their combination for 24 h. Poly A+ RNA was isolated from drug treated cells using the Oligotex mRNA isolation kit (Qiagen, CA) and analyzed for quality using the Agilent 2100 Bioanalyzer. Poly A+ RNA (200 ng) was subjected to reverse transcription, to generate labeled Cy3 or Cy5 probes, using the Incyte Genomics Life Array probe labeling kit. The combined Cy3 (untreated)/Cy5 (drug-treated) probes were hybridized to the GEMTM microarray slide (**10800 cDNA sequences/slide**) at $60^\circ \text{C}/6 \text{ h}$ and the slide was washed as per the manufacturer's instructions. The hybridization arrays were scanned on the Axon GenePix 4000 scanner and analyzed by Incyte's GEMTools application. Each analysis was repeated twice using 2 independent preparations of mRNA from drug treated and untreated cells. Genes that were differentially expressed by 2-fold or more were considered "hits". There were 29 hits including 13 up-regulated and 16 down-regulated genes in CMT-3 treated cells. There were 142 hits (26 up regulated and 116 down-regulated genes) in Cxb treated cells. In CMT-3+Cxb treated cells, 11 up regulated and 117 down-regulated genes were identified. As shown in **Table 2** several cytokines and their receptors, including IL1- β and IL-8, expression was decreased in CMT-3+Cxb treated PC-3ML cells when compared to CMT-3 or Cxb treated cells. Interestingly, the combination and not Cxb treatment alone decreased COX-2 expression. These results demonstrate that a combination of cytotoxic and anti-inflammatory drugs is likely to overcome acquired drug

resistance induced due to over-production of pro-inflammatory cytokines. We were now convinced that analyzing the response of tumor cells to anticancer drugs in the absence of inducible cytokines such as IL-1 β , IL-6 and IL-8 and also COX-2. To achieve these we decided to produce stable cell lines of PC-3ML that constitutively express anti-sense IL-1 β , IL-6, IL-8 as well as COX-2. By creating stable transfectants of these antisense plasmids, we could delineate the underlining mechanism of cytokine mediated drug sensitization or resistance. To understand the consequence of over-expressing either one or more of these pro-inflammatory proteins, we decided to create both sense- and anti-sense transfectants.



5'CAGCTATGAACTCCTTCTCC3'. IL6 (727) R: 5'ACAACAACATCTGAGGTGC3'. 3. IL-8 (72) L: 5'AGGAACCATCTCACTGTGTG3' IL-8 (417) R: 5'GGCATCTTCACTGATTCTTG 3'. The PCR amplification was carried out using Ampli TaqGold (Applied Biosystems/Perkin Elmer) as follows: 95 $^{\circ}$ C/10 min. 2. 10 cycles of 94 $^{\circ}$ C/30 sec, (70 $^{\circ}$ C - 60 $^{\circ}$ C/30 sec) and 72 $^{\circ}$ C/1min. 3. 35 cycles of 94 $^{\circ}$ C/30 sec, 60 $^{\circ}$ C/30 sec and 72 $^{\circ}$ C/1min. 4. 72 $^{\circ}$ C/7 min extensions. As shown in **Fig. 9**, IL1- β , IL-6 and IL-8 primer pairs amplified 870 bp, 669 bp and 346 bp PCR amplimers representing the entire coding regions of IL1- β , IL-6 and IL-8, respectively. The amplimers were cloned into a eukaryotic expression vector pEF6/V5-His TOPO. This vector allows bi-directional cloning of the PCR products. Thus each of the PCR cloned cDNA had a 50:50 chance of insertion into the vector in the sense and antisense orientation with respect to the enhancer/promoter elements from the human elongation factor 1 α subunit (hEF-1 α). The vector contains blasticidin resistance gene for selecting stable mammalian cell transfectants and an ampicillin resistance gene for bacterial selection. Sequencing of the cloned cDNAs (DNA Core Facility, U. Miami) confirmed their identity to the known IL1- β , IL-6 or IL-8 cDNAs and confirmed their orientation in the sense or antisense direction.



B2.d. Generation of stable cell lines expressing Interleukins (IL-1 β , IL-6 and IL-8) sense and antisense cDNA constructs:

We obtained published cDNA sequences of the three cytokines from the Genbank data base obtained via the NCBI ENTREZ-search and retrieval portal (ENTREZ-PUBMED) and deduced PCR primers for amplification. Total RNA was isolated from CaP cells (PC-3ML, DU145 and primary prostate tumor tissues) and reverse transcribed using Superscript II reverse transcription kit (Invitrogen/Life Technology). The first strand cDNA was PCR amplified by using primer sets to amplify full length cDNAs of IL1- β , IL-6 and IL-8 using the following set of primers: 1. IL1 β (70) L: 5'AAGTGTCTGAAGCAGCCATG3'. IL β (939) R: 5'TTGAGTCCACATTCAGCAC3' 2. IL6 (59) L: 5'CAGCTATGAACTCCTTCTCC3'. IL6 (727) R: 5'ACAACAACATCTGAGGTGC3'. 3. IL-8 (72) L: 5'AGGAACCATCTCACTGTGTG3' IL-8 (417) R: 5'GGCATCTTCACTGATTCTTG 3'. The PCR amplification was carried out using Ampli TaqGold (Applied Biosystems/Perkin Elmer) as follows: 95 $^{\circ}$ C/10 min. 2. 10 cycles of 94 $^{\circ}$ C/30 sec, (70 $^{\circ}$ C - 60 $^{\circ}$ C/30 sec) and 72 $^{\circ}$ C/1min. 3. 35 cycles of 94 $^{\circ}$ C/30 sec, 60 $^{\circ}$ C/30 sec and 72 $^{\circ}$ C/1min. 4. 72 $^{\circ}$ C/7 min extensions. As shown in **Fig. 9**, IL1- β , IL-6 and IL-8 primer pairs amplified 870 bp, 669 bp and 346 bp PCR amplimers representing the entire coding regions of IL1- β , IL-6 and IL-8, respectively. The amplimers were cloned into a eukaryotic expression vector pEF6/V5-His TOPO. This vector allows bi-directional cloning of the PCR products. Thus each of the PCR cloned cDNA had a 50:50 chance of insertion into the vector in the sense and antisense orientation with respect to the enhancer/promoter elements from the human elongation factor 1 α subunit (hEF-1 α). The vector contains blasticidin resistance gene for selecting stable mammalian cell transfectants and an ampicillin resistance gene for bacterial selection. Sequencing of the cloned cDNAs (DNA Core Facility, U. Miami) confirmed their identity to the known IL1- β , IL-6 or IL-8 cDNAs and confirmed their orientation in the sense or antisense direction.

We used the previously established PC-3ML cells expressing high levels of Enhanced Green Fluorescence protein (EGFP-PC3ML cells). EGFP-PC3ML cells; 2 x 10⁵ cells/dish) were transfected with 1 μ g DNA of various constructs (i.e., IL1- β sense (IL1- β S), IL1- β -antisense (IL1- β AS), IL-6 sense (IL-6S), IL-6 antisense (IL-6AS) and IL8-antisense) or vector DNA using the Effectene transfection reagent as per the manufacturer's protocol (Qiagen Inc, CA). We decided not to create

IL-8 sense PC-3ML transfectants, since PC-3ML already secrete abundant amount of IL-8 (~20 ng/10⁶ cells). After 48 h incubation, the transfectants were selected in the growth medium containing blasticidin (5 µg/ml) and hygromycin (100 µg/ml). Individual clones were picked and expanded. Culture-conditioned media (CCM) from 48 to 72 clones were assayed for the expression or the inhibition of respective cytokine proteins using cytokine-specific ELISAs (Quantikine ELISA kits, R&D systems). Data on two representative clones from each construct are shown here.

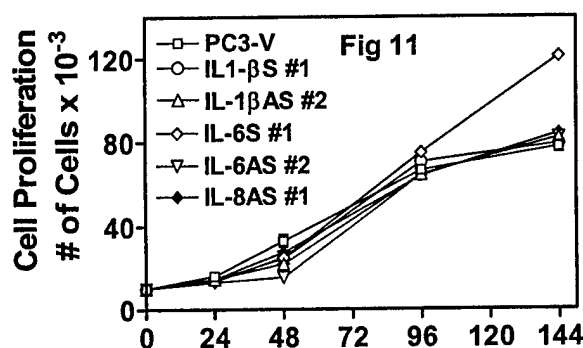
B2.e. Production of IL1-β, IL-6 and IL-8 in transfectants: Since the production of IL1-β, IL-6 and IL-8 may be inter-linked we assayed the production of these three cytokines in the CCM of various sense, antisense and vector transfectants using cytokine specific ELISAs (R&D Systems). As shown in **Fig. 10 A**, both PC3-V (i.e., PC3 vector only transfectants) secrete ~ 1000 pg/10⁶ cells IL1-β. The IL1-βS transfectants secreted ~ 35% more IL1-β (1368 pg/10⁶ cells). A ~ 90% reduction in IL1-β production was observed in both IL1-βAS transfectants (90-150 pg/10⁶ cells). IL1-β production was not significantly different among IL-6S and IL-6AS transfectant #1. However, IL6-AS clone #2, and both IL-8AS clones showed a 30% to 50% reduction in IL1-β production.

Fig. 10 B shows secretion of IL-6 by various transfectants. IL-6S and IL1-βS transfectants secreted comparable levels of IL-6 (743-768 pg/10⁶ cells), which were slightly greater than IL-6 levels in PC3-V transfectants (650 pg/10⁶ cells). IL-6 secretion was ~ 85-90% decreased in IL-6AS transfectants (66-120 pg/10⁶ cells). Interestingly, IL1-βAS transfect #1 and # 2 secreted 24% and 47% less IL-6 in their conditioned media, respectively, when compared with PC3-V transfectants (**Fig. 20 B**). IL-6 levels in IL-8AS transfectants were similar to those found in PC3-V transfectants.

As shown in **Fig. 10 C**, PC3-V and IL1-βS transfectants secreted similar levels of IL-8 in their conditioned media (16.5 – 21.8 ng/10⁶ cells). As expected IL-8AS transfectants secreted 75% - 82% less IL-8 when compared to PC3-V transfectants. As observed for IL-6 production, IL1-βAS transfectants secreted 25% (clone # 2) and 51% (clone #2) less IL-8, respectively, when compared to PC3-V and IL1-β S transfectants.

These results show the following: 1. Cytokine expression can be constitutively down regulated in PC-3ML cells by antisense transfections, 2. IL1-β expression partially regulates the expression of IL-6 and IL-8 in PC-3ML cells; 3. Blocking IL-8 expression appears to partially inhibit IL1-β production.

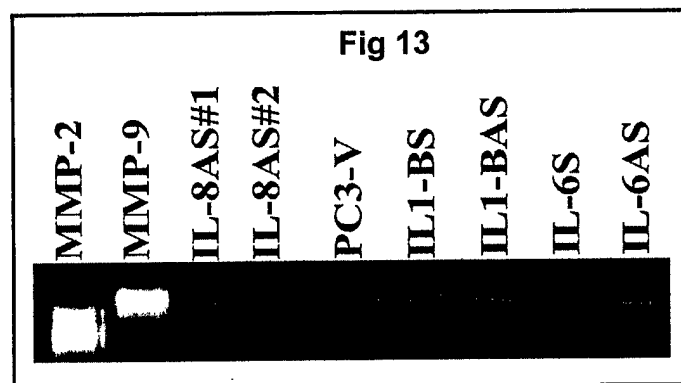
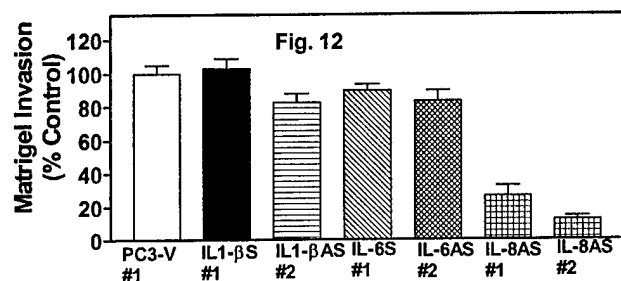
B2.f. Characterization of sense and antisense cytokine cDNA stable transfectants for cell proliferation and invasion: We next examined the growth characteristics of various clones to identify whether antisense cytokine cDNA transfectants have altered growth rate. For determining growth rate, 10,000 cells were plated in 35-mm dishes in replicates in complete medium containing 5 µg/ml blasticidin. Every 24 h, for a total period of 6 days (i.e., 0-144 h) cells were trypsinized, trypan blue stained and counted. Counts were done from 3 separate dishes/transfectant, in 2 separate experiments. The growth kinetics of various sense and antisense cytokine transfectants was similar, suggesting that cytokine expression is unlikely to regulate PC3 cell proliferation (**Fig. 11**).



The growth kinetics of various sense and antisense cytokine transfectants was similar, suggesting that cytokine expression is unlikely to regulate PC3 cell proliferation (**Fig. 11**).

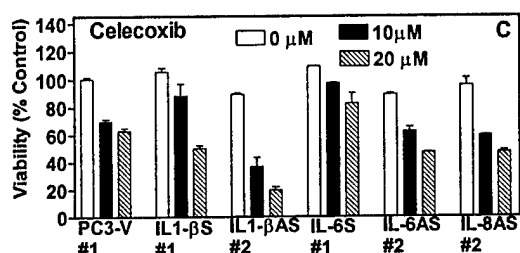
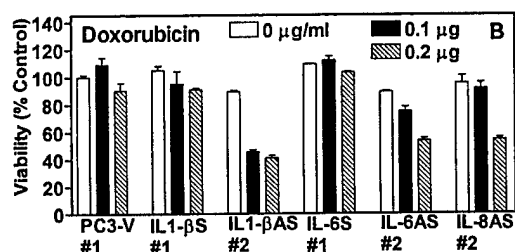
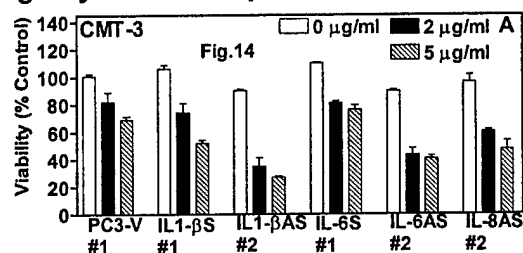
To study invasive profiles of various transfectants we assayed their invasive potential *in vitro* by Matrigel invasion assay [2]. Matrigel (50 µg/cm²)-coated 12-well Transwell plates were seeded with 4 x 10⁵ cells of various transfectants. The bottom well contained a 50:50 mix of hFOB CCM and CM.

Following 48 h incubation, invasion of cells through Matrigel into the bottom chamber was quantified using the MTT assay. The invasion index was defined as a % ratio of O.D. in the bottom well to the O.D. of bottom + top well. The invasion index of PC3-V # 1 transfectant (17.2 ± 4.5) was taken as 100%. As shown in **Fig. 12**, invasion indices were similar in IL1-βS, IL1-βAS, IL-6S and IL-6AS transfectants. However, both IL-8 transfectants were 75% (clone # 1) and 88% (clone # 2) less invasive when compared with PC3-V and other cytokine transfectants. These results demonstrate that IL-8



brilliant blue and destaining in 7% acetic acid. As shown in **Fig. 13**, PC3-V and cytokine transfectants primarily express MMP-9, which is consistent with our previous observation (22). However, IL-8AS showed a decrease in MMP-9 production. The MMP secreted by IL-8AS clones was essentially the latent form indicating lack of expression of other MMPs (MMP-3 or MT-MMP-1) in these two clones. No decrease in MMP-9 production was observed in IL1-βS/AS, IL-6S/AS transfectants when compared to that of PC-3v cultures. Clones other than IL-8AS, including PC-3v, also secreted MMP-2. These results suggest that the decreased invasive phenotype of IL-8AS transfectants may be linked to decreased MMP-9 secretion and inhibition of MMP-2 expression.

B2.g. Cytotoxic response of transfectants to anticancer drugs: We investigated the cytotoxic response of various transfectants to CMT-3, DXR and Cxb. Transfectant clones (10,000 cells/well; 48-well plate) were cultured in growth medium for 48 h and exposed to drugs for 48 h. Following incubation, the viability was estimated by MTT-assay. Viability of PC3-V clone # 1 without drug treatment was taken as 100%. As shown in **Fig. 14 A**, IL1-βAS clone # 2 and IL-6AS clone # 2 were 2.5-fold and 1.7-fold more sensitive to CMT-3 (5 μg/ml) when compared to PC3-V, respectively. In case of DXR (0.2 μg/ml) as well, IL1-βAS clone # 2 and IL-6AS clone # 2 were 2.2-fold and 2-fold more sensitive, respectively (Fig. 14 B). In case of Cxb (20 μM), a 3.2-fold and 1.5-fold increase in cytotoxicity was observed in these IL1-βAS and IL-6AS clones (Fig. 24 C).



expression may confer invasive phenotype in PC3-V cells. It is noteworthy that the effect of IL-8 on invasion is independent of IL1-β expression. This is because, although IL-8AS transfectants secreted 30% to 50% less IL1-β, IL1-βAS transfectants did not show appreciable reduction in invasion. The observed 18% decrease in the invasive index of IL1-βAS #2 clone may be a reflection of reduced IL-8 production by this clone.

We next examined MMP levels in the CCM of various cytokine sense and antisense transfectants by gelatin zymography (see Appendix 2; [2]). Essentially, 3-day CCM from cells plated at 1×10^6 cells/dish were analyzed on gelatin (1 mg/ml) embedded polyacrylamide gels subjected to SDS-PAGE and incubation in zymography buffer overnight. After SDS-PAGE, followed by incubation in zymography buffer overnight. Areas digested by the MMPs in the gel were made visible by staining the gel in 0.25%

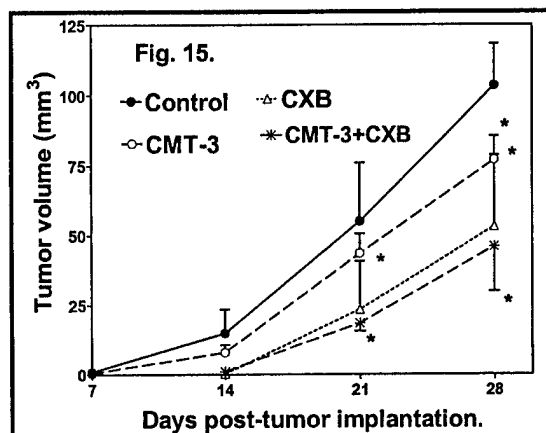
viability was estimated by MTT-assay. Viability of PC3-V clone # 1 without drug treatment was taken as 100%. As shown in **Fig. 14 A**, IL1-βAS clone # 2 and IL-6AS clone # 2 were 2.5-fold and 1.7-fold more sensitive to CMT-3 (5 μg/ml) when compared to PC3-V, respectively. In case of DXR (0.2 μg/ml) as well, IL1-βAS clone # 2 and IL-6AS clone # 2 were 2.2-fold and 2-fold more sensitive, respectively (Fig. 14 B). In case of Cxb (20 μM), a 3.2-fold and 1.5-fold increase in cytotoxicity was observed in these IL1-βAS and IL-6AS clones (Fig. 24 C).

In summary, these results suggest the following: 1. Although, there is some interlinking among IL1-β, IL-6 and IL-8 synthesis, **there does not appear to be a redundancy** among these cytokines with respect to function. 2. IL1-β and IL-6 protect tumor cells against cytotoxic drugs and their down-regulation sensitizes tumor cells to anticancer drugs. The response of IL1-βAS and IL-6AS transfectants to anticancer drugs, as well as, to the combination of anticancer anti-inflammatory drugs may

provide a direct evidence for the role of these cytokines in acquired drug resistance. **3.** IL-8 appears to regulate invasive phenotype of PC-3ML cells, which is apparently independent of IL-1 β and IL-6 expression.

B2.h. In vivo efficacy of CXB and CMT-3 combination therapy on the growth and metastasis of EGFP-PC3ML cells.

The ongoing experiments suggested that a combination treatment in mice bearing PC-3ML tumors with CXB and CMT-3 should reduce the tumor growth more than either agent alone. Instead of using two drugs as oral gavages, we obtained slow release implantable pellets of CMT-3, custom manufactured for us by Innovative Research Inc, Fort Myers, Florida. These pellets containing 10 mg of CMT-3 when implanted subcutaneously, release a steady amount of CMT-3 for at least 21 days. We first analyzed the serum concentration of CMT-3 in mice implanted with one pellet. Mice were bled, 0.2ml/mouse on day 1, 14, 21 and 45 following implantation of the pellet. Serum from three animals were pooled and subjected to HPLC, amount of CMT-3 present in the serum was estimated as described by Li et al [23]. The estimated concentration of CMT-3 was 0.5 μ g/ml on day 1, 3.75 on day 7, 4.95 on d 14, 4.8 and 3.95 μ g/ml on day 21 and undetectable on day 45. These measurements assured us the levels of CMT-3 stayed at or around the cytotoxic levels during the 21-day release period. We next implanted, 2×10^6 cells of EGFP-PC-3ML line at subcutaneous site on the dorsal flank of each nude mouse NuNu (Harlan Sprague Dawley, Indianapolis, IN) under mild anesthesia. Following implantation, mice were randomly divided into 5 groups of 6 animals each. Animals in group 1 and group 2 served as vehicle control, animals in group 1 were implanted with placebo implants and animals from group 2 received 0.5mL 1% carboxymethyl cellulose (CMC) solution (40mg/kg/body weight). Animals in group 3 and group 4 were implanted with continuous release of silastic pellet containing CMT-3 (10mg for 21day continuous release). Fresh suspension of CXB (40mg/kg b.wt) was prepared daily in 1% CMC, animals from group 4 and 5 were gavaged with 0.5mL CXB daily from day 1 of tumor implantation and continued daily 30 days. Tumor growth was examined by palpating the skin around the site of injection. After the tumors became palpable (~ day 7), tumor volumes were measured three times a week, with calipers and tumor growth was estimated using the volume as the dependent parameter, as described before [2]. The observations are summarized in Fig 15.



As shown in Fig 15, there was a delay (7 days) in tumor formation in CXB+CMT-3 treated groups as compared to control. Further, a 56% inhibition in tumor volume of CXB+CMT-3 treated mice was recorded as compared to the control when the size of tumor reached 100 cubic mm. This inhibitory effect was 40% and 15% more than CMT-3 or CXB respectively, when administered singly. These preliminary results suggest that a treatment regimen with a judicious combination of CMT-3 and CXB could lead to improved therapeutic response in hormone-refractory prostate cancer. Current work is focused on identifying a good combination of CMT-3 and CXB to inhibit tumor growth in xenografts of EGFP-PC3ML not only

metastatic to bone but also to treat disseminated metastases.

2. Key Accomplishments:

- An extensive investigation of acquired chemo sensitivity and/or chemoresistance of tumor cells in the presence of organ specific stromal cells were investigated further by molecular biology techniques. Biochemical and gene expression studies (expression arrays) showed that inflammatory cytokines specifically secreted by stromal endothelial cells and fibroblasts induce chemo resistance in tumor cells. An increase in the intra- and extra-cellular levels of IL-1 β , IL-6 and IL-8 were observed and quantified.

- **Role of pro-inflammatory cytokines (IL-1 β , IL-6 and IL-8) in the modulation of chemotherapeutic response in androgen-refractory prostate tumor cells were demonstrated. Using antisense stable transfectants of these three cytokines, a definitive proof was obtained that both IL-1 β , and IL-6 expression increases chemoresistance and blocking their expression sensitizes CaP cells to cytotoxic chemotherapeutic drugs. IL-8 seems to be involved in increasing invasive potential of CaP cells, but does not appear to alter chemo sensitivity to anticancer drugs. There also appear to be an inter-linking between the expression of IL-1 β with that of IL-6 and IL-8. Suppression of IL-1 β mRNA expression reduced the expression of IL-6 and IL-8.**
- **A combination of anti-inflammatory drug (Celecoxib) and anti-metastatic/antiproliferative drug CMT-3 was able to synergistically increase the cytotoxicity on CaP cells. The increase in the cytotoxic efficacy of the drug combination was mediated by a supra-additive increase in apoptotic induction by the two drugs.**
- **The combined oral and subcutaneous administration of Celecoxib and CMT-3 significantly reduced tumor growth in EGFP-PC-3ML tumor xenografts in athymic mice. Further tuning is underway to increase the efficacy of this adjuvant chemotherapeutic modality.**

3. Reportable outcomes:

A. PUBLICATIONS: (i) Published original articles:

1. Lokeshwar BL, Selzer MG, Zhu B-q, Block NL, and Golub LM. Inhibition of cell proliferation, invasion, tumor growth and metastasis by an oral non-antimicrobial tetracycline analog CMT-3 (COL-3) in a metastatic prostate cancer model. *Int. J. Cancer*. 98:297-309, 2002.
2. Dursun D, Wang M, Monroy D, Li DQ, Lokeshwar BL, Stern M, Pflugfelder SC. Experimentally induced dry eye produces ocular surface inflammation and epithelial disease. *Adv Exp Med Biol*. 2002;506(PtA):647-655.
3. Whitlatch LW, Young MV, Schwartz GG, Flanagan JN, Burnstein KL, Lokeshwar BL, Rich ES, Holick MF, Chen TC. 25-Hydroxyvitamin D-1alpha-hydroxylase activity is diminished in human prostate cancer cells and is enhanced by gene transfer. *J Steroid Biochem Mol Biol*. 2002 81:135-40.

(ii). PAPERS IN PRESS:

1. Li, DQ Shang TY, Kim, HS , Solomon A, Lokeshwar, BL, Pflugfelder SC. Regulated expression of collagenases (mmp-1, -8, -13) and stromelysins (mmp-3, -10, -11) by human corneal epithelial cells. *Invest. Ophthalm. Vis. Sci.* (In press).
2. Dandekar, DS, Lokeshwar VB, Cevallos-Arellano, E, Soloway, MS, Lokeshwar BL. A orally active Amazonian plant extract (BIRM) inhibits prostate cancer growth and metastasis. *Cancer Chemoth. Pharma.* (in press).

(iii). OTHER WORKS AND PUBLICATIONS: Published abstracts presented (or to be presented) at the national and international scientific meetings.

1. Lokeshwar BL, Dandekar DS, Lopez M. Miami Nature Biotechnology Short Reports .Vol 14, 109a, 2003.
2. Lokeshwar BL, Dandekar DS , Lopez M. AACR Proceedings , Vol. 44, 3723a, 2003.
3. Dandekar DS, Lokeshwar VB, Cevallos E, Lokeshwar BL. Miami Nature Biotechnology Short Reports .Vol 14, 106a, 2003.
4. Dandekar DS, Lokeshwar VB, Cevallos E., Lokeshwar BL. AACR Proceedings Vol 44, 648a, 2003.

C. Patents: One U.S. Patent was issued on the invention of CMTs efficacy in treating Ocular Rosacea (Meibomium gland disease). Title: **"Method for treating meibomian gland disease"**.

Inventors: S.G. Pflugfelder, B.L. Lokeshwar, M.G. Seizer
U.S. patent No. 6,455,583

D. Clinical Translational research. CMT-3: Several new trials (phase Phase II and I) have begun to test the potential of CMT-3 (COL-3) for treating the Kaposi sarcoma. This investigation has no connection with the clinical trial.

E. Personnel: One full time Research Associate (technician), a part time Research Associate, a post-doctoral associate (October2001-present) and the Principal investigator worked on this project.

F. Conclusions: Stromal modulation of drug sensitivity in tumor cells is mediated by over expression of cytokines, IL-1 β , IL-6 and IL-8. Experiments using stable generation of anti-sense IL-1 β , IL-6, IL-8 showed that pro-inflammatory cytokines indeed modulate chemotherapeutic drug response in androgen refractory prostate tumor cells. Chemotherapeutic drugs induce a strong expression of COX-2 mRNA. Inhibitors of COX-2 are cytotoxic to CaP cells and they enhance the cytotoxicity of both established and novel (e.g., CMT-3, COL-3) chemotherapeutic drugs. Combining an anti-inflammatory drug and chemo/antimetastatic drugs delays tumor growth significantly, without increasing systemic toxicity and hold promise for the development of neo-adjuvant chemotherapy in the battle against prostate cancer metastasis.

G. References:

- 1 Lokeshwar, B.L., Houston-Clark, H. L, Seizer, M.G., Block, N.L., Golub, L. M. Potential application of a chemically modified non-antimicrobial tetracycline (CMT-3) against metastatic prostate cancer. *Adv. Dental. Res.* 12:127-132, 1998.
- 2.Greenwald RA, Golub LM, Ramamurthy NS, Chowdhury M, Moak, SA, Sorsa T. In vitro sensitivity of three mammalian collagenases to tetracycline inhibition: Relationship to bone and cartilage degradation. *Bone*, 22:33-38.1998.
3. Seftor REB, Seftor EA, De Larco JE, Kleiner D, Leferson J, Stetler-Stevenson WG, McNamara TF, Golub LM, Hendrix MJC. Chemically modified tetracyclines inhibit human melanoma cell invasion and metastasis. *Clin. Exp. Metastasis.* 16:217-225,1998.
- 4.Lokeshwar B.L.MMP Inhibition in Prostate Cancer. *Ann. N.Y. Acad Sci.* 878: 71-289,1999.
- 5.Lokeshwar, B.L., Escatel, E., Zhu, B-Q. Novel cytotoxic activity and inhibition of tumor cell invasion by nitro-derivatives of a chemically modified tetracycline CMT-3 (Col-3). *Curr. Med. Chem.* 8:271-279, 2001.
- 6.Lokeshwar B.L., Selzer M.G., Zhu, B-Q., Block, N.L., Golub, L.M. Inhibition of cell-proliferation, invasion, tumor growth and metastasis by an oral non-antimicrobial tetracycline analogue (COL-3) in a metastatic prostate cancer model. *Int. J Cancer.* 2002,98:297-309, 2002.
- 7.Selzer, M.G., Zhu, B-q, Block, N.L., and Lokeshwar, B. L. CMT-3, a chemically modified tetracycline inhibits bony metastases and delays the development of paraplegia in a rat model of prostate cancer. *Ann. NY Acad. Sci.* 878:678-682, 1999.
8. Rudek MA, Figg WB, Dyer C, Dahut W, Turner ML, Steinberg SM, Liewehr DJ, Kohler DR, Pluda JM, Reed E. Phase I clinical trial of oral COL-3, a matrix metalloproteinase inhibitor, in patients with refractory metastatic cancer. *J Clin Oncol.* 19:584-592. 2001.
- 9.Earnst RA, Vohra P, Kratzer FH, Kuhl HJ Jr. Effect of halofuginone (Stenorol) on Chukar partridge (*Alectoris chukar*). *Poult Sci.* 75:1493-5,1996.

10. Pines M, Knopov V, Genina O, Iavelin I, Nagler A. Halofuginone, a specific inhibitor of collagen type I synthesis, prevents diethylnitrosamine-induced liver cirrhosis. *J Hepatol*, 27:391-8, 1997.
11. Elkin M, Reich R, Nagler A, Aingorn E, Pines M, de-Groot N, Hochberg A, Vlodavsky I. Inhibition of matrix metalloproteinase-2 expression and bladder carcinoma metastasis by halofuginone. *Clin Cancer Res*. 5:1982-8, 1999.
12. Gavish Z, Pinthus JH, Barak V, Ramon J, Nagler A, Eshhar Z, Pines M. Growth inhibition of prostate cancer xenografts by halofuginone.
13. Stecklair KP, Hamburger DR, Egorin MJ, Paise RA, Covey JM, Eiseman JL. Pharmacokinetics and tissue distribution of halofuginone (NSC 713205) in CD2F1 mice and Fischer 344 rats. *Cancer Chemother Pharmacol*. 48:375-82, 2001.
14. Xie K. Interleukin-8 and human cancer biology. *Cytokine Growth Factor Rev*. 2001;12(4):375-91.
15. Schneider GP, Salcedo R, Welniak LA, Howard OM, Murphy WJ. The diverse role of chemokines in tumor progression: prospects for intervention (Review). *Int J Mol Med*. 2001;8(3):235-44.
16. Borsellino N, Beldegrun A, Bonavida B. Endogenous interleukin 6 is a resistance factor for cis-diamminedichloroplatinum and etoposide-mediated cytotoxicity of human prostate carcinoma cell lines. *Cancer Res*. 1995; 55(20): 4633-9.
17. Badawi AF. The role of prostaglandin synthesis in prostate cancer. *BJU Int*. 2000 Mar;85(4):451-62.
18. Subbarayan V, Sabichi AL, Llansa N, Lippman SM, Mentor DG. Differential expression of cyclooxygenase-2 and its regulation by tumor necrosis factor- α in normal and malignant prostate cells. *Cancer Res*. 2001, 61:2720-2726.
19. Tjandrawinata RR, Dahiya R, Hughes-Fulford M. Induction of cyclo-oxygenase-2 mRNA by prostaglandin E₂ in human prostate carcinoma cells. *Br. J Cancer* 1997; 75:1111-8.
20. Kirschenbaum A, Liu X, Yao S, Levine AC. The role of cyclooxygenase-2 in prostate cancer. *Urology*. 2001 Aug;58(2 Suppl 1):127-31.
21. Liu XH, Yao S, Kirschenbaum A, Levine AC. NS398, a selective cyclooxygenase-2 inhibitor, induces apoptosis and down-regulates bcl-2 expression in LNCaP cells. *Cancer Res*. 1998; 58(19):4245-9.

INHIBITION OF CELL PROLIFERATION, INVASION, TUMOR GROWTH AND METASTASIS BY AN ORAL NON-ANTIMICROBIAL TETRACYCLINE ANALOG (COL-3) IN A METASTATIC PROSTATE CANCER MODEL

Bal L. LOKESHWAR^{1*}, Marie G. SELZER¹, Bao-Qian ZHU¹, Norman L. BLOCK¹ and Lorne M. GOLUB²

¹Sylvester Comprehensive Cancer Center and Department of Urology, University of Miami School of Medicine, Miami, FL, USA

²Department of Oral Biology and Pathology, School of Dental Medicine, State University of New York at Stony Brook, Stony Brook, NY, USA

Antibiotic forms of tetracycline exhibit antitumor activity in some tumor models. However, their low *in vivo* efficacy and associated morbidity limit their long-term application in cancer therapy. This report appraises the efficacy of doxycycline (DC) and non-antimicrobial, chemically modified tetracyclines (CMTs) against prostate cancer. Both DC and several CMTs inhibited prostate tumor cell proliferation *in vitro*. Some of the CMTs were significantly more potent than DC. One of the CMTs, 6-deoxy, 6-demethyl, 4-de-dimethylamino tetracycline (CMT-3, COL-3), was the most potent inhibitor (50% inhibition dose [GI_{50}] ≤ 5.0 μ g/ml). Exposure of tumor cells to CMT-3 induced both apoptosis and necrosis. Mitochondrial depolarization and increased levels of reactive hydroxyl radicals were also observed in cells treated with CMT-3. Cell cycle arrest at the G_0/G_1 compartment was observed in CMT-3- and DC-treated cells. DC and CMTs also inhibited the invasive potential of the tumor cells *in vitro*, from 10% (CMT-6) to >90% (CMT-3). CMT-3 and DC decreased matrix metalloproteinase (MMP)-2, tissue inhibitor of MMP (TIMP)-1 and TIMP-2 secretion in treated cultures and inhibited activity of secreted MMPs. CMT-3 was a stronger inhibitor. Daily oral gavage of DC and CMT-3 inhibited tumor growth and metastasis in the Dunning MAT LyLu rat prostate tumor. Decreases in tumor growth (27–35%) and lung metastases were observed (28.9 ± 15.4 sites/animal [CMT-3-treated] versus 43.6 ± 18.8 sites/animal [DC-treated] versus 59.5 ± 13.9 [control]; $p < 0.01$). A delay in tumor growth ($27 \pm 9.3\%$, $p < 0.05$), reduction in metastases ($58 \pm 8\%$) and decrease in tumor incidences ($55 \pm 9\%$, CMT-3-treated) were also observed, when rats were predosed for 7 days. No significant drug-induced morbidity was observed in any of the animals. These results, along with a recently concluded clinical trial, suggest a potential use of CMT-3 as an oral, nontoxic drug to treat metastatic prostate and other cancers.

© 2002 Wiley-Liss, Inc.

Key words: tetracycline; chemically modified tetracyclines; COL-3; prostate cancer; metastasis; metalloproteinase inhibitors; therapeutics

Metastasis of initially localized tumor causes much of the pain, suffering and eventual death in about one-third of patients diagnosed with prostate cancer.¹ At present, metastatic prostate cancer is incurable and is poorly palliated. This has created an urgency to find an effective therapy.²

An avenue to prevent the spread of prostate tumor cells is inhibition of their invasive potential. Degradation of basement membrane, which leads to the invasion of tumor cells into the surrounding stroma and blood capillaries, is a critical step in metastasis.³ A repertoire of cell adhesion molecules, proteinases, their activators and their inhibitors participate in this process.^{4–6} The matrix metalloproteinases (MMPs), including stromelysin and gelatinases that degrade the extracellular matrix, are the important enzymes involved in invasion and metastasis.⁷ An imbalance between MMPs and their endogenous inhibitors, the tissue inhibitor of MMPs (TIMPs), has been observed, with the enzymes more active at the invasive front of the tumors.⁸ The paradigm proposed by Liotta *et al.*⁸ that this imbalance may favor invasion and

metastasis of many solid tumors, if not all, has guided many investigations since its proposal.⁹

We previously reported that primary cultures of human prostate tumors secrete high levels of gelatinases (MMP-2 and MMP-9) and low levels of TIMPs.¹⁰ Other studies have also shown high levels of mRNAs for MMPs in prostate tumor tissues.^{11,12} Natural or synthetic inhibitors of MMPs may therefore inhibit or slow tumor metastasis in general and prostate cancer in particular.^{13,14} The antibiotic tetracycline and its chemically modified non-antimicrobial analogs (CMTs) are such agents because they are potent inhibitors of MMPs.^{15–18}

The common tetracyclines such as doxycycline (DC) and minocycline have a variety of antitumor properties such as inhibition of protein synthesis in the mitochondria,^{16,20} collagenolysis¹⁵ and angiogenesis.¹⁸ Because of these activities tetracyclines may be useful as antitumor agents. However, systemic administration of the antibiotic tetracycline over prolonged periods has limitations due to potential emergence of antibiotic-resistant, systemic microbial flora. Furthermore, long-term exposure to tetracycline may also cause additional gastrointestinal and nutritional toxicity due to the destruction of normal beneficial microbial flora. In addition, common tetracyclines have a limited *in vivo* efficacy due to their short life in circulation and rapid elimination, thus requiring relatively large continuous dosing.²⁰

A series of chemically modified tetracyclines (CMTs) have been synthesized and characterized in the hope of overcoming the limitations associated with the antimicrobial forms of tetracycline.^{21–23} Golub *et al.*²¹ reported that removal of the dimethylamino group (CMT-1) from the carbon-4 position of the A-ring of the 4-ringed tetracycline structure (*e.g.*, CMT-1) eliminates the antimicrobial activity of the tetracycline, while retaining the anti-collagenolytic activity. Further modifications of the de-dimethylamino tetracycline have resulted in CMTs with more potent anti-

Abbreviations: CM-DCFDA, carboxyl methyl-2',7'-dichloro-dihydro carboxyl fluorescein diacetate; CMT, chemically modified tetracycline; DC, doxycycline; GI_{50} , 50% inhibition dose; MMP, matrix metalloproteinase; OD, optical density; TIMP, tissue inhibitor of matrix metalloproteinase.

Grant sponsor: Department of Defense, U.S. Army Medical Research Program; Grant sponsor: DAMD 17-98-272; Grant sponsor: PHS; Grant numbers: 1R29-CA 63108, 5R01 CA 63108; Grant sponsor: L. Austin Weeks Endowment Fund of the Department of Urology, University of Miami.

*Correspondence to: Department of Urology, McKnight Vision Research Building, University of Miami School of Medicine, P.O. Box 016960 (D880), Miami, FL 33101, USA. Fax: +305-243-6893. E-mail: BLOKESHW@med.miami.edu

Received 5 July 2001; Revised 5 October 2001; Accepted 12 October 2001

Published online 18 December 2001

collagenolytic activity, oral bioavailability and long-serum half-life.²²⁻²⁴ Previous reports of cytostatic activity and strong MMP inhibition by the antimicrobial and non-antimicrobial forms of tetracyclines motivated us to investigate further the efficacy of these drugs on prostate cancer cells *in vitro* and on a rat model of androgen-insensitive metastatic prostate tumor *in vivo*.

The objective in our study was 2-fold. The first was to test the cytotoxic or cytostatic and antiinvasive activities of a common tetracycline antibiotic, DC, and 1 or more CMTs *in vitro* and *in vivo*. The second objective was to test whether oral administration of 1 or more CMTs with their enhanced anti-MMP activities and longer *in vivo* retention would be therapeutically more effective than that reported before. We report here that although both DC and 1 of the CMTs (CMT-3) show strong antimetastatic activity by oral administration, CMT-3 is significantly more effective as a cytotoxic antitumor and antimetastatic drug.

MATERIAL AND METHODS

Reagents

The following non-antimicrobial CMTs were used in our study: CMT-1 (4-dedimethylamino tetracycline), CMT-2 (tetracycline nitrile), CMT-3 (6-demethyl, 6-deoxy, 4 de-dimethylamino tetracycline), CMT-4 (7-chloro 4-de-dimethylamino tetracycline), CMT-6 (4-hydroxy-4-de-dimethylamino tetracycline), CMT-7 (12- α deoxy 4-de-dimethylamino tetracycline) and CMT-8 (6- α deoxy, 5-hydroxy 4-de-dimethylamino tetracycline). All the CMTs were from the laboratory of 1 of the authors (L.M.G.). Purified, GMP-grade COL-3 (CMT-3) was a generous gift from CollaGenex Pharmaceuticals (Newtown, PA). The characterization of anti-MMP activities of CMTs has been previously described.²¹⁻²⁵ TIMPs and MMP ELISA kits were from Oncogene Sciences/Calbiochem (San Diego, CA). The Cell Death ELISA-Plus kit was from Roche Molecular Biochemicals (Indianapolis, IN). Fluorescent dyes (propidium iodide, JC-1: a membrane potential-sensitive fluorescent dye [5',5',6',6'-tetrachloro-1,1',3,3'-tetraethylbenzimidazole] carbocyanine iodide) and the hydroxyl free radical-reactive dye carboxyl methyl-2',7'-dichloro-dihydro carboxyl fluorescein diacetate [CM-DCFDA] were from Molecular Probes (Eugene, OR). All other reagents were from Sigma (St. Louis, MO), or as indicated.

Cells and tumor lines

Established cell lines used in our study were the Dunning rat prostate tumor line MAT LyLu²⁶ and the human prostate cancer cell lines PC-3ML, LNCaP, DU 145 and TSU PR1. The procurement, culture and maintenance of these cell lines in the authors' laboratory have been described previously.^{26,27} In addition, a non-tumorigenic human prostate epithelial cell line, BPH-1,²⁸ was a gift from Dr. Simon Hayward (University of California, San Francisco, CA). All cultures were maintained in complete medium (RPMI-1640 basal medium with 10% FBS [Atlanta Biological, Atlanta, GA] and 10 μ g/ml gentamicin [Life Technologies, Gaithersburg, MD]). MAT Ly Lu cells were cultured in the complete medium containing 250 nM dexamethasone.²⁶

Cytotoxicity assays

Initially, 2 methods were evaluated for estimating cytotoxicity of CMTs and DC. These included the cellular [³H]thymidine incorporation assay²⁷ and the colorimetric thiazolyl blue (MTT) reduction assay (tetrazolium bromide: [3-(4,5-dimethylthiazol-2-yl)-2,5-diphenyltetrazolium bromide]).²⁹ The details of the procedures for these methods, adapted in the authors' laboratory, have been previously published.^{27,30} Values of growth-inhibitory doses of DC and CMTs evaluated from [³H]thymidine incorporation or the MTT assay were very similar. Subsequently, the nonradioactive MTT assay was used. Drug-induced cytotoxicity was determined in cultures with initial plating density of 2×10^4 cells/well, in 48-well plates as described previously.³⁰ Stock solutions of DC (0.1–5 mg/ml) were prepared in sterile Dulbecco's PBS, pH 7.2.

The CMT stocks (0.1–5 mg/ml) were prepared in sterilized DMSO. The final concentration of DMSO in cultures did not exceed 0.1%, a nontoxic concentration. Cultures incubated with drugs for 48 hr, in replicate wells, were assayed for viability by the MTT assay. All experiments were repeated at least 3 times.

Determination of apoptotic activity

Drug-induced apoptosis was assayed using the Cell Death ELISA-Plus kit (Roche Molecular Biologicals). The assay measures the amount of free nucleosomes in cell lysates and culture supernatants resulting from programmed cell death and necrosis, respectively.³¹ Cell cultures were exposed to drugs in a dose- and time-dependent manner; culture supernatant and cell lysates were assayed separately for apoptotic bodies per the supplier's instructions. Triplicate samples were used for each time- and dose-dependent apoptosis induction experiment. Manufacturer-supplied positive and negative controls and medium blank were used to compare the results from replicate experiments.

Determination of depolarization of mitochondria

We used a mitochondria-specific, lipophilic cationic probe, JC-1,³² to detect changes in mitochondrial membrane potential ($\Delta\Psi$). Polarized mitochondrial membrane (inside negative) permits more accumulation of JC-1 aggregates (J-aggregates) emitting greenish orange fluorescence ($\lambda_{\max} \sim 590$ nm) when excited at 488 nm. Decrease in membrane potential (depolarization) results in increase in green fluorescence (527 nm). This shift in cell fluorescence is measured in a flow cytometer. Cultures were incubated with JC-1 for 30 min after their incubation with CMT-3 or DC for up to 48 hr, as detailed previously.³³ Fluorescence intensity was profiled in a flow cytometer equipped with both a narrow bandpass green filter (FL1) and a long-pass green filter (>575 nm; FL2; EPICS XL, Beckman-Coulter, Palo Alto). Median fluorescence intensity of untreated and treated samples was compared in the green fluorescence channel (log FL1) instead of FL2, as the fluorescence associated with CMT-3 also interfered at the FL2 channel. Increase in green fluorescence intensity (log FL1) was approximated as a decrease in $\Delta\Psi$.

Determination of hydroxyl free radical production

Alteration in the levels of hydroxyl free radicals in drug-treated cells were estimated using oxidation of a nonfluorescent analog of fluorescein, CM-DCFDA. This moderately polar, cell-permeable dye is oxidized by oxygen and hydroxyl free radicals, resulting in oxidized carboxyl fluorescein diacetate. Cytoplasmic esterases convert the carboxyl-fluorescein diacetate to hydrophilic carboxyl-fluorescein.^{34,35} The hydrophilic carboxyl fluorescein is trapped inside intact cells, which now emit bright green fluorescence upon excitation at 488 nm.³⁶ Cellular fluorescence is then quantified by flow cytometry. Cultures treated with CMT-3, DC or 0.1 mM hydrogen peroxide for various periods were incubated with CM-DCFDA (1 μ g/ml) for 60 min. Unreacted DCFDA was rinsed off from culture after 60 min and treated cells were suspended as a single-cell suspension for analysis in a flow cytometer. Median fluorescence intensity of samples treated with drug alone, CM-DCFDA alone or both were compared to estimate the levels of hydroxyl free radicals relative to untreated controls. Relative levels of the free radicals produced by CMT and DC, indicated by the positive shift in median fluorescence channel (log FL1), were also compared against that observed with cells treated with hydrogen peroxide alone.

Determination of cell cycle phase fractions

Drug-induced alteration in cell cycle phase progression was analyzed by determining the percent of cells in each cell cycle phase compartment by flow cytometry as described before,²⁷ with modifications.³⁷ Briefly, CaP cell cultures were treated with various concentrations of CMT-3 or DC for 48 hr, cells were lysed and the nuclei were stained with 50 μ g/ml propidium iodide (PI) simultaneously in a cell lysis buffer (PBS, 0.4% Nonidet p40 (NP40) detergent, 50 μ g/ml PI). DNA contents of the stained

nuclei were profiled in a Coulter XL flow cytometer. The MODFIT LT program (Verity Software House, Topsham, ME) was used for cell cycle analysis of the DNA histograms.³⁸ Experiments were repeated 3 times for each of the 2 cell lines analyzed.

In vitro tumor cell invasion assay

The effects of CMTs and DC on the invasive potential of TSU PR1 and Dunning MAT LyLu cells were tested using the Matrigel assay as described earlier.³⁰ Briefly, the procedure used was a modification of Albini *et al.*³⁹ by Hussain *et al.*⁴⁰: tumor cells, incubated with various drugs for 6 hr, were deposited (4×10^5 cells/filter) in the top wells of Transwell plates (Corning/Costar, Boston, MA). The top wells, made from 12 μ m pore polycarbonate filters, had been previously coated with a layer of Matrigel (0.5 mm, 500 μ g/cm²; Collaborative Research-BD Bioscience, Bedford, MA). The bottom well contained a chemoattractant, a serum-free culture-conditioned medium of human lung fibroblasts (1 ml/well). Percent of cells in each treatment group that invaded through the Matrigel-coated filter in 48 hr was determined by MTT assay as described.³⁰ Invasive activity (% invasion) was defined as the ratio of optical density (OD) from the bottom wells to that of the total OD (OD of bottom plus top wells), multiplied by 100. Use of the MTT assay allowed us to normalize the coincident cytotoxicity of the drugs. All assays were repeated at least 3 times.

Determination of secreted MMP-2 and TIMPs

Culture conditioned medium from a primary culture of a human prostate tumor tissue (Gleason sum 8, preoperation prostate specific antigen [PSA] > 40) was collected and assayed using ELISA kits according to the supplier's instructions (Oncogene Sciences/Cal-Biochem). We have previously reported the establishment and propagation of primary prostate epithelial cells.³⁰ The ELISA was specific for human cell culture-derived MMP-2, TIMP-1 and TIMP-2. Levels of MMP-2 and TIMPs were normalized against total cell proteins, estimated using the Pierce BCA protein assay kit (Pierce Chemicals, Rockford, IL).

Gelatinase activity assay

The activity of gelatinase in the MAT LyLu cell culture-conditioned medium was determined by a modified [³H]gelatin digestion assay of Dean and Woessner.⁴¹ Serum-free culture-conditioned medium, collected from MAT LyLu cells, was chemically reduced (1 mM dithiothreitol) and alkylated (1 mM iodoacetamide), for 30 min at 37°C and dialyzed to destroy any endogenous TIMPs, which could interfere with the MMP assay.^{41,42} The dialyzed medium was assayed for gelatinase activity after activating the latent MMPs with 1 mM p-aminophenyl mercuric acetate (APMA) for 30 min at 37°C. MMP enzyme activity was assayed with 1 or 10 mM CaCl₂, with 2 μ M ZnCl₂ in the assay buffer. We chose 1 mM CaCl₂ because it is closer to the physiological concentration of [Ca²⁺]⁴³ and compared it with the activity obtained using 10 mM CaCl₂, which was reported to be the optimum concentration for assaying MMP activity.⁴¹

SDS-PAGE and zymography

MMPs secreted into the culture medium by cells treated with DC and CMT-3 were identified by electrophoresis and zymography as described previously.¹⁰ Conditioned medium collected from cultures treated with DC or CMT-3 for 2 days were incubated with SDS-gel sample buffer for 30 min at 21°C and analyzed by gel electrophoresis on a 1 mg/ml gelatin-embedded SDS-polyacrylamide gel (8%).¹⁰

In vivo studies

Tumor generation. Dunning MAT LyLu cells harvested from culture flasks in 0.5 ml suspension, containing 2×10^5 to 2×10^6 cells/ml (see Results), were implanted in the dorsal flank of adult male Copenhagen rats (Harlan Sprague-Dawley, Indianapolis, IN). The rats weighed 250–300 g and were 90–100 days old at the time of implanting. Tumor growth was examined by palpating the injection site 5 days after the implant.

Drug treatment. DC and CMT-3 were dissolved in a 2% aqueous solution of carboxymethyl cellulose (Sigma, cat. no. C-5678); a fresh solution was made daily. Rats were dosed by oral gavage with a 4-inch gavage needle daily, with either 1 ml of the drug solution or vehicle (2% carboxymethyl cellulose). Tumor growth was recorded 3 times a week and the rats' weights weekly. The effect of the various treatments on tumor growth was monitored over time by measuring tumor volumes with a caliper; the volume was approximated to an ellipsoid (*i.e.*, volume = length \times width \times height \times 0.5236), as previously reported.²⁷ Tumor growth rate was estimated from a regression analysis of log-transformed tumor volumes *versus* time. The mean tumor growth rates (time to reach a fixed volume) of control and different treatment groups were then compared. The statistical significance of the differences in tumor growth rates was tested by Tukey-Kramer multiple comparisons test. Rats were euthanized when the tumors reached a volume > 10 ml. Necropsy was done, and tumors and lungs were removed and fixed in formalin (tumor tissue) or in Bouin's fixative (lungs). Macroscopic tumor foci on the lungs were counted under a dissecting microscope in a blinded fashion. Fixed tumor and lung specimens were randomly selected for histology. Tissues were sectioned and stained with hematoxylin and eosin solution (Fisher Scientific, Fair Lawn, NJ). A veterinary pathologist examined the slides.

RESULTS

Effect of DC and CMTs on prostate cancer cell proliferation

The effect of CMTs on cell proliferation or viability varied greatly. Some CMTs significantly inhibited cell proliferation, but others did not. As shown in Figure 1, all but CMT-7 was significantly cytotoxic in all 3 cell lines. CMT-3 was the most cytotoxic among all the tetracyclines tested (GI₅₀ 2.3 \pm 0.9 μ g/ml to 6.7 μ g/ml). CMT-7 was nearly nontoxic to all cell lines except the LNCaP, in which it was slightly toxic (GI₅₀ 120 \pm 14.7 μ g/ml). We could not test the toxicity of CMTs at concentrations higher than 50 μ g/ml as they precipitated in the culture medium. DC inhibited the proliferation of LNCaP cells (GI₅₀ 6.3 μ g/ml), but it was much less potent in other cell lines tested (Fig. 1A and Table I). Presence or absence of serum in the culture medium did not alter the cytotoxicity of any of the CMTs or DC in the 3 cell lines tested (data not shown).

Since CMT-3 was the most potent of all CMTs, we compared the cytotoxicity of CMT-3 with that of DC against primary culture CaP 139, derived from a prostate tumor specimen, and the MAT LyLu rat prostatic carcinoma cell line. Cytotoxicity was measured using the MTT assay. As shown in Table I, CMT-3 was up to 8-fold more cytotoxic than DC to these cell cultures. The cellular basis of CMT-3- and DC-induced toxicity was further investigated by examining cytotoxic mechanisms common to other chemotherapeutic drugs.

Cell death induction by CMTs and DC

Due to the contrasting cytotoxic actions of CMT-3 and DC, we chose these 2 drugs for further investigation. We reasoned that observed cytotoxicity may be due to necrotic or apoptotic cell death induced by 1 or more of these agents. Cell death ELISA revealed that cells incubated with CMT-3, and much more weakly with DC, underwent both necrotic and apoptotic cell death in a dose- and time-dependent manner. As shown in Figure 2, cells underwent apoptosis in cultures exposed to CMT-3 for 4 hr and longer. Among the various prostate cell lines tested, the MAT LyLu cell line was the most sensitive. Table II summarizes the results for CMT-3-induced apoptosis in various cell lines. Necrotic cell death was apparent in cultures treated with high concentrations of CMT-3 or DC (>10 μ g/ml for CMT-3 and >20 μ g/ml for DC; Fig. 3). Free nucleosomes were detected by ELISA in both cytoplasmic and culture supernatants at these concentrations, indicating that these drugs induce necrosis and apoptosis at high concentrations (CMT-3 > 5 μ g/ml and DC > 20 μ g/ml). CMT-3-induced

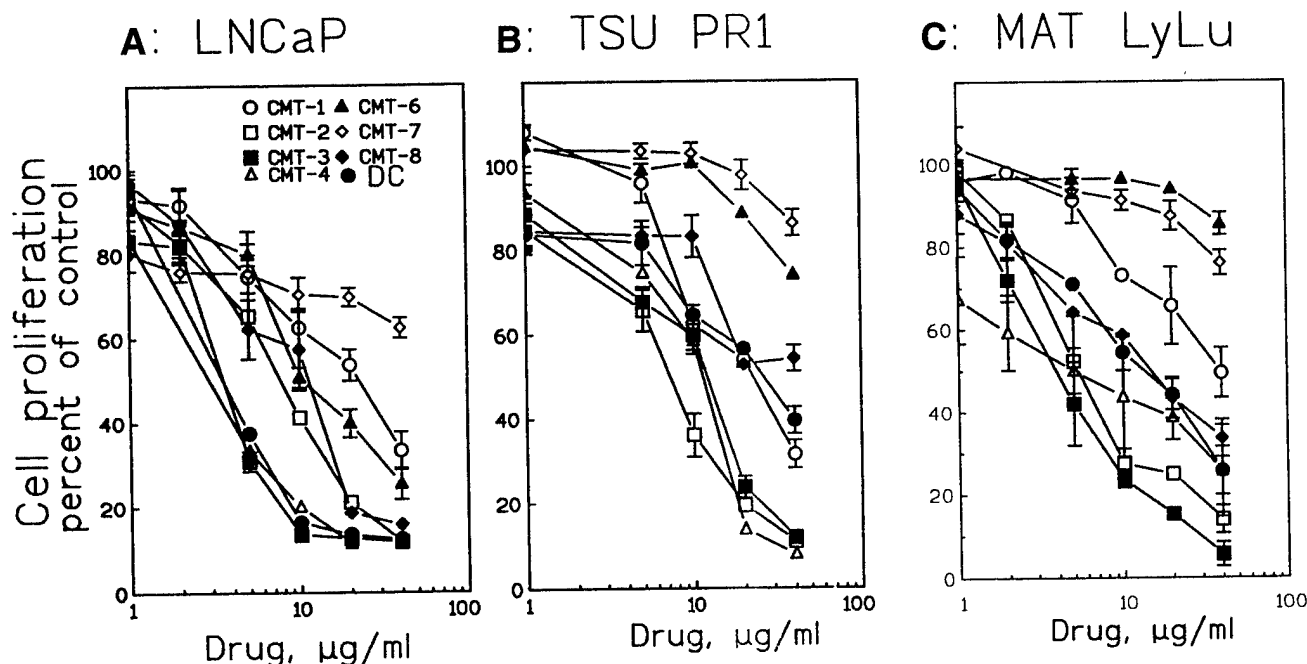


FIGURE 1 – Cytotoxicity of DC and CMTs in prostate tumor cell lines. Two cell lines, an androgen-sensitive, low metastatic potential cell line (LNCaP; *a*), and an androgen receptor-negative, metastatic cell line (TSU PR1; *b*) were exposed to DC or to various CMTs in complete medium for 48 hr. The Dunning MAT LyLu cell line was similarly treated (*c*). Cell proliferation was measured using the MTT assay. Vertical bars represent the mean \pm SEM from 4 independent determinations. Symbols for various CMTs are the same in all panels.

TABLE 1 – CYTOTOXICITY OF DC AND CMT-3 IN PROSTATE CELLS

Cell line ¹	GI ₅₀ ²	
	DC	CMT-3
ALVA 101 (4)	16.67 \pm 1.3 ^b	3.1 \pm 0.34
BPH-1 (3)	9.68 \pm 2.45	4.78 \pm 1.68
CaP 139 (1)	18.7 \pm 3.7	9.3 \pm 2.11
DU 145 (8)	19.8 \pm 4.25	2.3 \pm 0.53
LNCaP (5)	6.3 \pm 1.35	2.29 \pm 0.96
MAT LyLu (7)	9.09 \pm 2.95	2.36 \pm 0.86
PC-3 (5)	16.55 \pm 1.06	4.8 \pm 0.96
TSU PR-1 (5)	18.64 \pm 5.1	6.7 \pm 1.2

¹Numbers of replicate experiments are given in parentheses.

²Growth inhibition was calculated from linear regression of the dose-response curves generated for each experiment using log (dose) vs. cell proliferation (% of control), as shown in Figure 1a–c. Correlation coefficient (*r*) was always ≥ 0.95 (negative). Results are presented as mean \pm SEM μ g/ml (1 μ g/ml = 2.2 μ M) of at least 3 GI₅₀ values calculated from each experiment.

apoptotic activity was significantly higher than that induced by DC at concentrations at which their cytotoxic activity was comparable (Figs. 1,2). A possible pathway to drug-induced apoptosis, commonly mediated by alteration in mitochondrial polarity and permeability was examined next.

Effect of CMT-3 and DC on mitochondrial membrane polarity ($\Delta\psi$) and production of reactive hydroxyl free radical [OH•]

As shown in Figure 4, a significant accumulation of JC-1 was observed in cells treated with CMT-3. In addition, cells treated with CMT-3 for >90 min exhibited an increase in green fluorescence, indicative of lack of J-aggregation (red fluorescence, FL-3), as found in control (Fig. 4). In addition, a stabilization of green-orange fluorescence, accumulated in the long-green fluorescence channels (log FL2), was also observed (data not shown), indicating a decrease in $\Delta\psi$ and leading to increased permeabilization. We next investigated a plausible cause of mitochondrial permeabiliza-

tion. Free radical-induced cellular damage, leading to both necrotic and apoptotic cell death, is 1 of the most common mechanisms of cell kill by antibiotics in bacteria and anticancer drugs in tumor cells.^{45,46} Free-radical-increased generation of hydroxyl free radicals [OH•], in cells exposed to CMT3 and DC, was examined by measuring the oxidative conversion of CM-CFDA to fluorescein. As shown in Figure 5, flow cytometric analysis of cells incubated with the drug revealed elevated production of [OH•] in cells exposed to CMT-3. Cells exposed to DC, however, did not show any appreciable increase in fluorescence intensity (Fig. 5).

CMT-3 and DC affect cell cycle progression

We observed an arrest of cell cycle progression in CaP cells incubated with CMT-3 or DC. Distribution of cells into various cell cycle phase compartments at the end of treatment with DC or CMT-3 is summarized in Table III. Both CMT-3 and DC induced arrest of cells at the G₀/G₁ phase in both the cell lines, DU 145 and LNCaP. There was a significant increase in percent of cells at the G₀/G₁ compartment, from ~50% in the control cell population to up to 85% in cells treated with CMT-3 (10 μ g/ml). Similarly, treatment with DC (≤ 20 μ g/ml) also increased the percent of cells in G₀/G₁ phase up to 79.2% based on the DNA content of the cells. This increase was mainly due to decrease in S-phase fractions, indicating block at the G₁/S boundary. In contrast, there was no significant change in G₂/M fractions in LNCaP cells incubated with CMT-3 or DC. However, incubating DU 145 cells with CMT-3, but not DC, resulted in a significant decrease (from 17.6 \pm 1.8% to 5.6 \pm 5.6% [at CMT-3 of 5 μ g/ml] and 7.0 \pm 5.5% [at CMT-3 of 10 μ g/ml], *p* < 0.003 for both treatment concentrations) in both S-phase and G₂/M phase fractions. Similar results were obtained for another androgen-independent CaP cell line, PC-3 (data not shown).

Effect of DC and CMTs on invasive/metastatic potential of prostate cancer cells

Since tetracycline is a known inhibitor of MMPs, including those associated with invasion and metastasis,¹⁷ we next tested antiinvasive activity of CMTs and DC on a highly invasive human

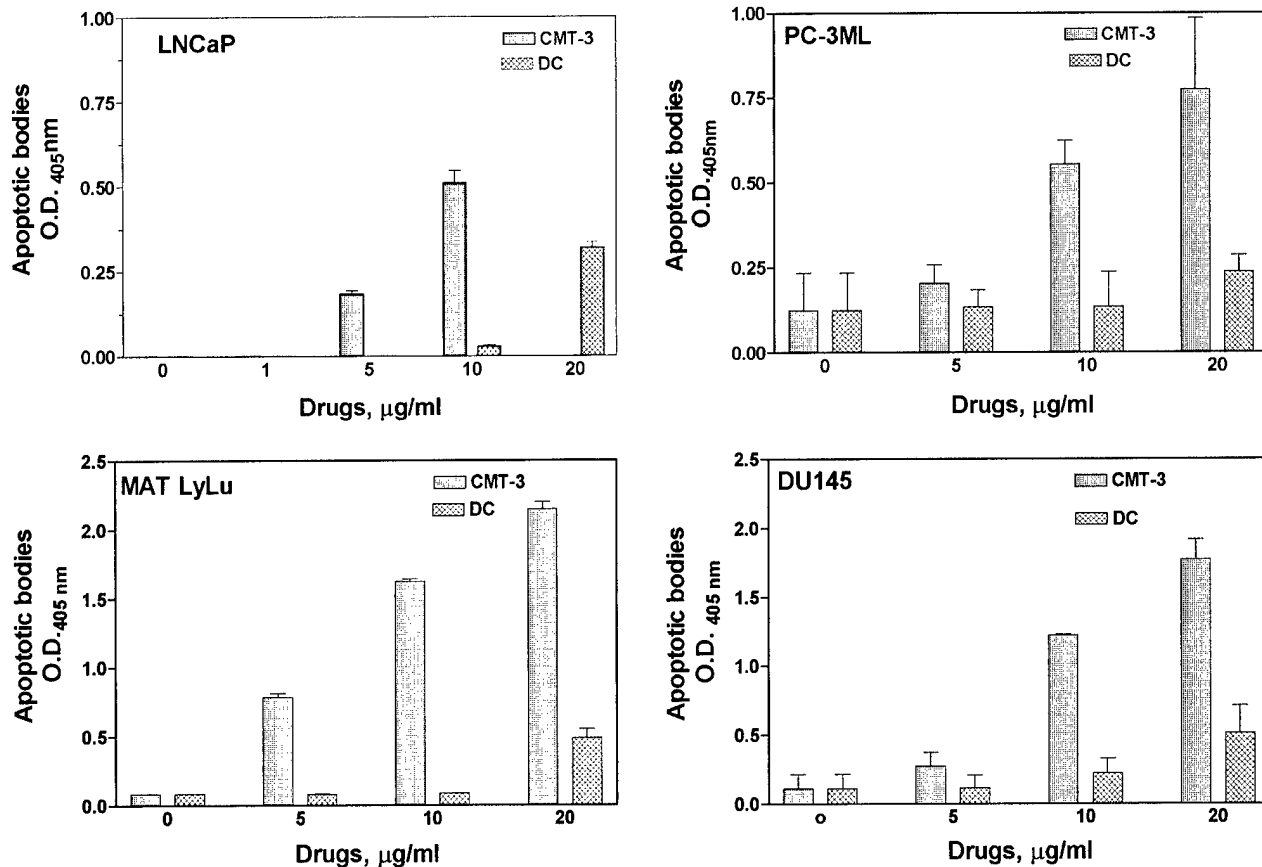


FIGURE 2 – Induction of apoptosis in prostate cancer cells by CMTs. Relative quantities of free nucleosomes in the culture supernatant of CaP cells, incubated with or without CMT-3 and DC for 48 hr, were estimated using the Cell Death ELISA-Plus kit. The ordinate represents specific OD. Note that apoptotic bodies in the culture supernatants of treated LNCaP and PC-3 cells were less than that for DU 145 and MAT LyLu cultures. The data presented for supernatants represent the accumulated free nucleosomes, resulting from apoptosis and necrotic cell death. Data presented are mean \pm SEM (error bars) from 3 independent experiments. [Reprinted from Lokeshwar 1999,⁷⁷ with permission from the publisher.]

TABLE II – CMT-3- AND DC-INDUCED PROGRAMMED CELL DEATH

	Apoptosis detected			
	MAT LyLu	DU 145	PC-3	LNCaP
Range of concentration ¹ (µg/ml)	1–10 (CMT-3) 5–20 (DC)	5–10 (CMT-3) ≥ 20 (DC)	5–10 (CMT-3) ≥ 20 (DC)	2.5–10 (CMT-3) ≥ 20 (DC)
Minimum duration of exposure (hr) ²	4 (CMT-3) 24 (DC)	4 (CMT-3) 24 (DC)	4 (CMT-3) 24 (DC)	4 (CMT-3) 24 (DC)
Replicate experiments	8	4	4	4

¹Free nucleosomes were detected (specific OD > 0.1) in the cell lysates when assayed 48 hr after treatment. ²Cultures were exposed to CMT-3 (5 µg/ml) or DC (10 µg/ml) from 1 to 24 hr, and cell lysates were assayed 24 hr after exposure. An OD of 0.1 from untreated control was taken as the specific due to apoptosis activity.

(TSU PR1) and a rat cell line (MAT Ly Lu) using an *in vitro* (Matrigel) invasion assay.³⁹ As shown in Figure 6, DC and CMTs inhibited invasive activity of these 2 cell lines. However, once again the potency of various CMTs varied greatly (Fig. 6). For example, CMT-3 was the most potent and CMT-7 was the least potent inhibitor of invasive activity of TSU PR1 cells. The 50% inhibition dose (IC_{50}) calculated for various CMTs varied from 1.7 ± 0.31 µg/ml (CMT-3) to >100 µg/ml for CMT-7. DC was not significantly inhibitory in TSU PR1 cells ($IC_{50} = 27 \pm 4.3$ µg/ml). The IC_{50} s of CMT-3 and DC for 3 other invasive human prostate cancer cell lines (DU 145 and PC-3) were also in the same concentration range as that for the TSU PR1 cells (data not shown). CMTs affected the invasive potential of MAT LyLu cells similarly (Fig. 6b). However, compared with the TSU PR1 cells,

DC was significantly more effective in the MAT LyLu cells ($68 \pm 4.2\%$ inhibition at 5 µg/ml; Fig. 6b).

Effect of CMT-3 and DC on gelatinase activity

First we examined whether CMT-3 and DC inhibit the activity of MMPs secreted by the cells into the culture medium. TSU PR1 and MAT LyLu cells were cultured in a serum-free medium for 48 hr. Culture-conditioned media were then assayed for MMP activity using [³H]gelatin as the substrate, in the presence of DC or CMT-3. As shown in Table III, both CMT-3 and DC inhibited MMP activity *in vitro*. At 1 mM $CaCl_2$, the IC_{50} s of CMT-3 and DC were ~ 0.5 and 2.25 µM, respectively. At 10 mM $CaCl_2$, the IC_{50} for CMT-3 was ~ 5.5 µM and that of DC was 10.0 µM (Table IV).

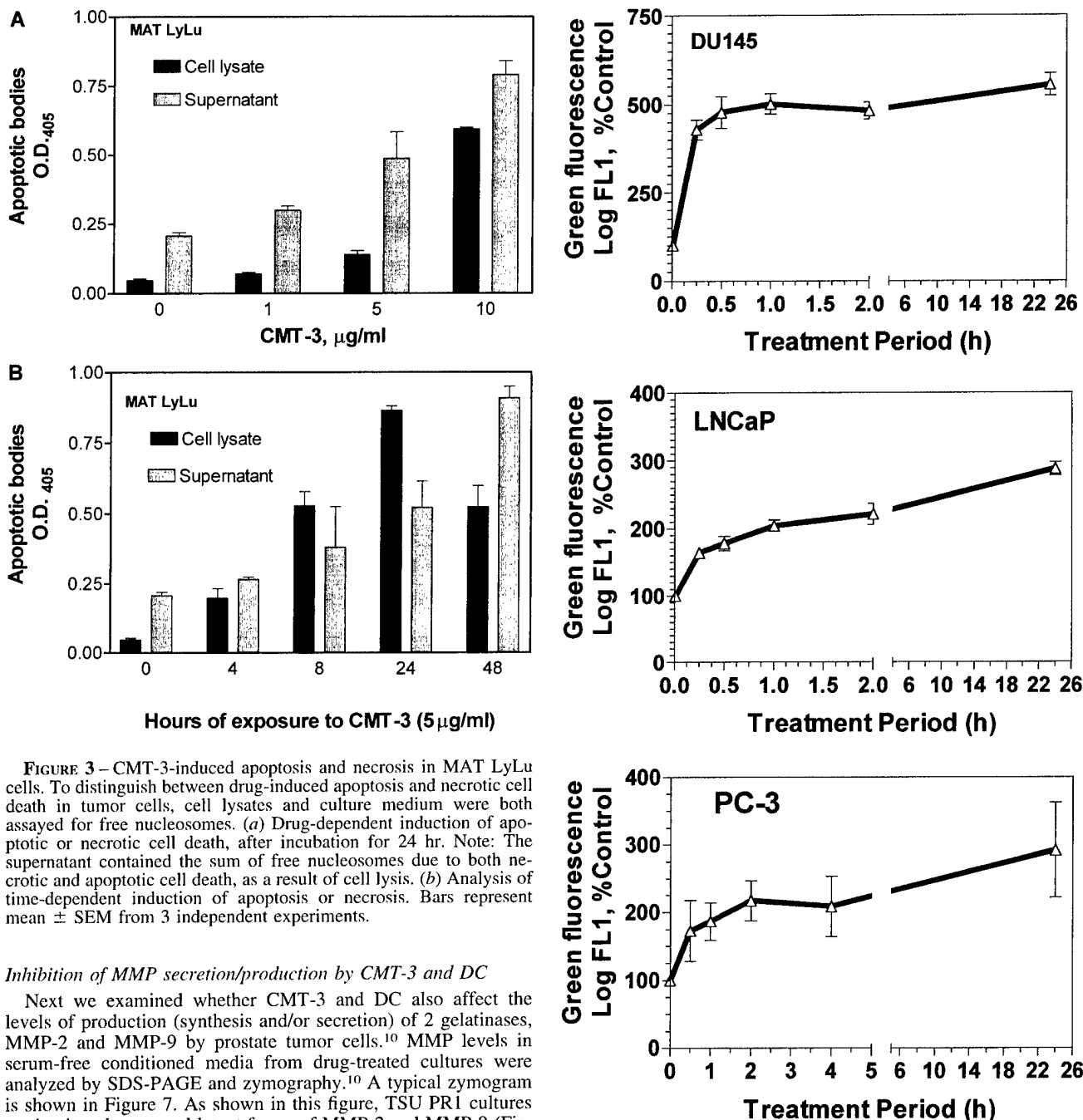


FIGURE 3—CMT-3-induced apoptosis and necrosis in MAT LyLu cells. To distinguish between drug-induced apoptosis and necrotic cell death in tumor cells, cell lysates and culture medium were both assayed for free nucleosomes. (a) Drug-dependent induction of apoptotic or necrotic cell death, after incubation for 24 hr. Note: The supernatant contained the sum of free nucleosomes due to both necrotic and apoptotic cell death, as a result of cell lysis. (b) Analysis of time-dependent induction of apoptosis or necrosis. Bars represent mean \pm SEM from 3 independent experiments.

Inhibition of MMP secretion/production by CMT-3 and DC

Next we examined whether CMT-3 and DC also affect the levels of production (synthesis and/or secretion) of 2 gelatinases, MMP-2 and MMP-9 by prostate tumor cells.¹⁰ MMP levels in serum-free conditioned media from drug-treated cultures were analyzed by SDS-PAGE and zymography.¹⁰ A typical zymogram is shown in Figure 7. As shown in this figure, TSU PR1 cultures predominantly secreted latent forms of MMP-2 and MMP-9 (Fig. 7a,b), whereas the MAT LyLu cells secreted activated MMP-2 (62 kDa form) and little MMP-9 (Fig. 7c,d). Incubation with CMT-3 or DC decreased the secretion of MMPs in a dose-dependent manner. As appears in Figure 7, cells treated with CMT-3 secreted significantly less MMP than the cells treated with DC. Moreover, MMP-9 levels did not decrease significantly even at the highest concentration of DC tested (50 μ g/ml). Presence of the drug in the conditioned medium used in the gel did not interfere with the digestion of gelatin after electrophoresis; most likely all the bound CMT-3 or DC had diffused out of the gel during electrophoresis and washing steps.

To establish further that the observed decreases in MMP levels in conditioned medium are indeed due to the drug-induced inhibition of MMP production/secretion, protein levels of MMPs were measured by an ELISA that uses a monoclonal anti-MMP-2 antibody. Initial measurement of MMP-2 protein levels in TSUPR1

FIGURE 4—Decrease in mitochondrial membrane potential in cells treated with CMT-3. Fluorescence intensity of CaP cells incubated with CMT-3 (5 μ g/ml) for various periods and with JC-1 for 30 min was estimated by flow cytometry as described previously.³¹ Median fluorescence intensity, log FL1 (green fluorescence, narrow pass filter $\lambda = 530$ nm) is taken as that proportional to the amount of JC-1 present inside the cells in an unaggregated form. Unaggregated JC-1 accumulation is indicative of a decrease in mitochondrial membrane potential, $\Delta\Psi$.³² Bars represent mean \pm SEM from 3 independent determinations.

conditioned medium exhibited levels of MMP below the detection limits (<10 ng/ml). However, MMP-2 protein levels were measurable in a primary prostate tumor-derived culture, CaP 139. As we have reported before, the primary cultures typically secrete a 10-fold higher amount of MMP-2 than that of common established

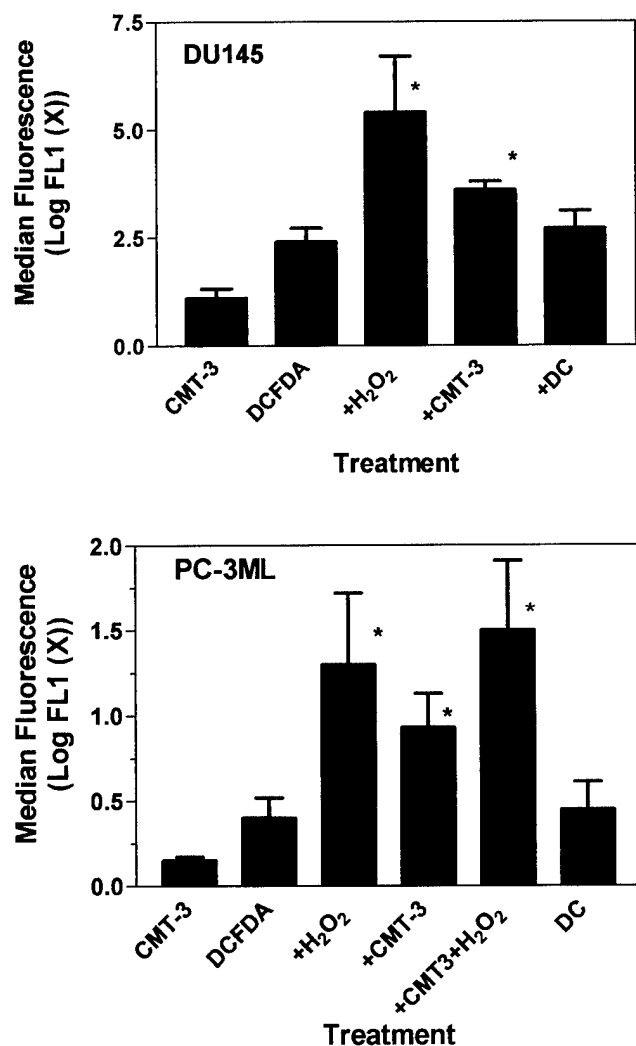


FIGURE 5—Increase in free radical generation in CMT-3-treated cells. Fluorescence intensity of cells incubated with CMT-3 (5 μ g/ml), DC (10 μ g/ml) and CM-DCFDA (10 μ g/ml), alone or together, was compared by flow cytometry. Cells incubated with CMT-3 and DC emitted weak green fluorescence. Histograms in the top panel represent the fluorescence intensity of DU 145 cells incubated with CMT-3 alone, DCFDA alone or DCFDA + H₂O₂, CMT-3 + DCFDA or DC + DCFDA. Cells incubated with DCFDA alone fluoresced significantly; this was further increased significantly when a free radical-generating agent (hydrogen peroxide) was added. Data are from 3 independent experiments. *, fluorescence levels significantly different from that of control ($p < 0.04$).

CaP cell lines.¹⁰ We found a dose-dependent decrease in the levels of MMP-2 secreted by the CaP 139 cells treated with CMT-3 or DC. MMP-2 levels decreased by 51 and 74% at 20 μ g/ml DC and 10 μ g/ml CMT-3, respectively (Table V). Although traces of MMP-9 were detected by zymography, MMP-9 levels even in 10 \times concentrated medium were below the minimum detection levels of ELISA.

Levels of TIMP-1 and TIMP-2 in CMT-3- and DC-treated cultures

Since the MMP-dependent invasion process may also depend on the levels of their endogenous inhibitors, TIMP-1 and TIMP-2, we measured TIMP-1 and TIMP-2 levels in CMT-3- and DC-treated cells (Table V). We observed a decrease in the levels of TIMPs secreted by CaP 139 cells treated with CMT-3 or DC. The de-

creases in TIMP-1 levels were 33 and 38% at 10 and 20 μ g/ml of CMT-3 or DC, respectively. These decreases are significantly less than those determined for MMP-2 ($p < 0.05$, t -test). Similarly, levels of TIMP-2 were also decreased by 10.27 and 21.75% respectively, in CMT-3 (10 μ g/ml) and DC (20 μ g/ml) treated cultures. As noted above for TIMP-1, decreases in TIMP-2 levels were also significantly less than the decrease in MMP-2 levels under comparable treatment conditions ($p < 0.04$, t -test).

Effect of DC and CMT-3 on Dunning tumor growth and lung metastasis

Due to the multiple effects of CMT-3 and DC on prostate cancer cells, we next examined whether CMT-3 and DC show antitumor activity *in vivo*. Although CMT-2 was comparable in efficacy, it was not tested *in vivo* because of its poor bioavailability (Golub *et al.*, unpublished observation). In the first experiment, we started treating the animals with drugs on the same day as we implanted 1×10^6 tumor cells. Tumors were palpable (≥ 0.1 cm³) after 6 days in more than 50% of the animals in all treatment groups. Tumors increased in volume rapidly, reaching >10 cm³ at 15 days post implant. Regression analysis of tumor volumes showed no significant difference in the primary tumor growth between the control group and the DC- or CMT-3-treated groups (Fig. 8a).

The mean duration for the growth of a 1 cm³ tumor was 10.3 ± 2.12 days in the control group and 12.0 ± 1.9 days in the CMT-3-treated group. Tumors in the control group, as well as from the drug-treated groups, developed a highly necrotic center as the tumors grew to a size of ≥ 10 cm³.

Tumor foci were visible in lungs fixed in Bouin's fluid. Typically, they were ≤ 1 mm in diameter from all the treatment groups. As illustrated in Figure 8b, lungs in the control group had 59.5 ± 13.9 metastatic tumor foci (MTF)/rat (mean \pm SD). The animals treated with DC had 39.7 ± 17.2 and 43.6 ± 18.8 MTF/rat in the low-dose (20 mg/kg) and high-dose (40 mg/kg) treatment groups, respectively. The most significant reduction in lung MTF (28.9 ± 15.4 MTF/rat) occurred in those rats treated with a high dose of CMT-3 (40 mg/kg): 51% reduction in MTF as compared with that of the control group ($p < 0.01$, Tukey-Kramer multiple comparison test). Histologic examination of the tumor foci did not reveal any apparent differences among the various treatment groups (data not shown).

In an attempt to increase the efficacy of therapy, a predosing drug regimen was next employed and combined with a reduction in the number of tumor cells implanted. Since recent studies indicate rapid extravasation of tumor cells from the capillaries,⁵ we reasoned that a sustained serum level of the drugs should reduce the incidence of growth and metastasis of the injected tumor cells. In addition, we thought that reducing the tumor cell inoculum should increase the tumor latency. Therefore, 2 modifications to the first experiment were introduced: (i) rats were predosed with DC or CMT-3, both at 40 mg/kg, with daily gavage for 7 days; and (ii) the tumor cell inoculum was reduced to 2×10^5 cells/animal from the previous dose of 1×10^6 cells/site. Due to the decrease in the cell inocula, the tumor latency increased from 6 to 9 days in the control group. However, there was no change in the tumor growth rate in the control group, once the tumors became palpable (see below).

As shown in Figure 9a, tumor incidence was $>90\%$ in control and DC-treated groups in 3 independent experiments. Interestingly, the tumor incidence in CMT-3-treated rats varied from 28% (2/7) to 85% (6/7) in 4 separate experiments. This was significantly lower ($55 \pm 9\%$) than that for control or DC-treated groups. The rats with no primary tumor incidence remained tumor-free for up to 6 months, at which time they were euthanized. No histologically identifiable tumor focus was observed at the site of injection or in the lungs. In addition, among the rats in the CMT-3-treated group that developed measurable tumors ($\leq 50\%$), tumor growth in the CMT-3-treated group was significantly slower, 20.2 ± 3.5 days (CMT-3-treated) versus 15.9 ± 2.0 days (control) versus $16.7 \pm$

TABLE III - CELL CYCLE PHASE COMPOSITION OF CMT-3- AND DC-TREATED CELLS¹

Phase	Untreated (control)	CMT-3		DC		
		5 µg/ml	10 µg/ml	5 µg/ml	10 µg/ml	20 µg/ml
LNCaP cells						
G0–G1	51.8 ± 4.8	74.5 ± 4.1	78.0 ± 4.2	75.0 ± 4.1	75.2 ± 3.8	70.0 ± 5.6
S	32.7 ± 4.8	6.6 ± 4.1	5.1 ± 4.1	10.4 ± 4.2	5.0 ± 3.8	5.5 ± 5.6
G2–M	15.5 ± 4.8	18.9 ± 4.8	17.0 ± 4.1	14.8 ± 4.1	20.0 ± 5.0	24.6 ± 5.6
DU 145 cells						
G0–G1	47.5 ± 5.2	78.6 ± 5.4	85.3 ± 5.5	59.4 ± 5.2	79.2 ± 5.4	79.1 ± 5.4
S	34.9 ± 5.2	15.9 ± 5.6	5.1 ± 4.1	26.7 ± 5.7	5.8 ± 5.4	5.5 ± 5.6
G2–M	17.6 ± 1.8	5.6 ± 5.6	7.0 ± 5.5	13.9 ± 5.2	15.0 ± 5.4	12.8 ± 5.6

¹Cell cycle phase composition of prostate cancer cells treated with either CMT-3 or DC was determined by flow cytometric analysis of propidium iodide (PI)-stained nuclei as described in Material and Methods. Data for each phase were extracted from analyzing histograms obtained from flow analysis of long-pass red filter PMT signals (PI staining) using ModFit LT software (Verity Software House). Percent of cells in a given phase shown is from 3 independent experiments for both cell lines.

1.9 days (DC, 40 mg/kg) to reach a tumor volume of 3 cm³. Interestingly, in 2 separate experiments, we observed tumor regression in 20 and 30% of CMT-3-treated groups. In these animals tumors were palpable (volume ≤ 0.01 cm³) at 8–10 days after tumor cell injection at the primary site but did not increase in volume and disappeared (impalpable) 4–7 days later. These animals remained tumor-free for up to 6 months. Although there was a significant reduction in tumor incidence and growth rate, pre-dosing the animals with CMT-3 did not further enhance the inhibition of tumor metastasis to lungs. The MTF in CMT-3-treated animals was 46.3 ± 6.7 versus 74.2 ± 6.4 in control, a 37.6% reduction ($p \leq 0.01$).

Toxicity and adverse reactions to DC and CMT-3

None of the 142 animals used in our study demonstrated adverse effects of drug treatments, such as irritability, hypersensitivity to light, hair loss or diarrhea. As a gross measure of normal tissue injury, plausibly caused by DC or CMT-3, animals were weighed before, during and after treatment. In all experiments, we found no significant weight loss in any groups. The animals gained 1.5–3.2% of their weight during the 4-week treatment (with tumor measurement) and gained an additional 8–12% of their weight during the 6 months of posttreatment observation. These weight gains were similar to the weight gain in naive animals of matching age.

DISCUSSION

The results presented above show that DC and various CMTs inhibit multiple aggressive activities of tumor cells including cell proliferation, invasion, secretion of MMPs, primary tumor growth and metastasis. Possible mechanisms of these actions are discussed.

Tetracycline and cytotoxicity

In bacteria and protozoa the principal toxic action of tetracycline is disruption of 30S ribosomal protein synthesis,⁴⁷ a component that is absent in higher eukaryotes. We propose that tetracycline and CMTs may induce inhibition of cell proliferation of mammalian cells by at least 2 mechanisms, occurring in both cytoplasmic and mitochondrial compartments. Kroon and colleagues^{16,20} hypothesized that tetracycline acts as a cytostatic drug since it inhibits protein synthesis in mitochondria and decreases the activity of cytochrome C oxidase. Results presented here show that tetracycline and its nonantibiotic derivatives (e.g., CMT-3) are cytotoxic. Reduction of tumor cell viability (reduction in MTT reduction) and increase in apoptotic activity both support this conclusion. Decrease in conversion of MTT into insoluble formazan may be the result of DC and CMT-3 inhibiting mitochondrial function and reducing the cytoplasmic pyridine nucleotide pool, NADH and NADPH.^{48,49} Furthermore, we have reported previously that CMTs and DC inhibit clonal survival of prostate tumor cells.⁵⁰ Cytotoxic activity shown by analogs of tetracycline, with or with-

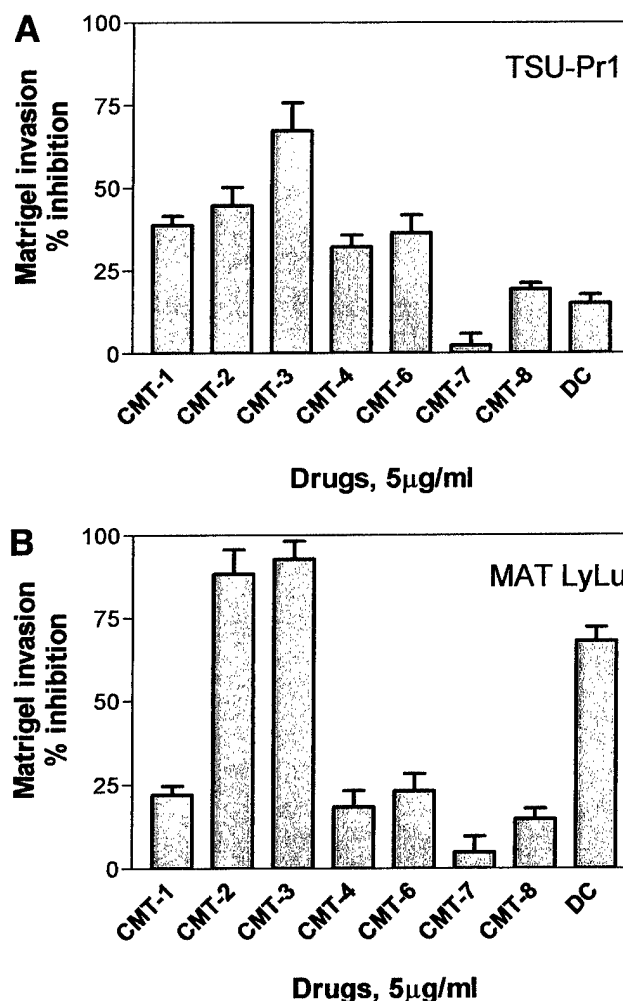


FIGURE 6 - Inhibition of invasive potential of tumor cells by DC and CMTs. Cells in the top chamber and those that had invaded the Matrigel-coated filter after 48 hr were quantitated (invasion index) using the MTT assay. The invasion index was defined as the ratio between the OD of the reduced MTT (formazan) in the bottom wells to the total OD (bottom plus the top wells). The invasion index of the control (0.1% DMSO) wells was 22 ± 8.3 % for TSU PR1 cells (a), and 17 ± 4.2 for MAT LyLu cells (b). DMSO (0.1%) had a negligible effect on the invasion index. Results presented are from 3 independent experiments.

TABLE IV - INHIBITION OF MMP ACTIVITY BY CMT-3 AND DC

Drug concentration (μM)	% Inhibition (mean \pm SEM) ¹			
	CMT-3		Doxycycline	
	1 mM CaCl_2 ²	10 mM CaCl_2 ³	1 mM CaCl_2 ²	10 mM CaCl_2 ³
0.25	47.2 \pm 3.6	20.7 \pm 4.9	35.3 \pm 2.7	0.0
0.50	64.4 \pm 8.3	31.7 \pm 6.5	44.8 \pm 7.6	0.0
1.0	84.8 \pm 10.1	37.8 \pm 7.5	54.8 \pm 0.6	0.0
2.0	96.7 \pm 4.6	45.1 \pm 2.9	77.4 \pm 2.9	32.7 \pm 11.4
10	97.2 \pm 2.9	52.4 \pm 3.5	87.5 \pm 2.8	64.3 \pm 19.5
20	100	69.9 \pm 10.5	91.15 \pm 3.3	75.5 \pm 3.3
100.0	100	94.2 \pm 3.3	100	93.2 \pm 2.7

¹Inhibition of gelatinase activity by CMT-3 or DC was calculated from the activity (expressed as ng of [³H]gelatin solubilized/min/ml) of MAT LyLu conditioned medium. Culture-conditioned medium was incubated with [³H]gelatin in the presence of various concentrations (0–100 μM) of either CMT-3 or DC and 1 or 10 mM CaCl_2 , at 37°C for 4 hr. The assay was conducted as described in Material and Methods. Data presented are from 3 independent experiments. Inhibition of gelatinase activity was significantly different between 1 and 10 mM Ca^{2+} concentrations for both CMT-3 and DC at 0.25–20 μM concentrations, tested independently for both drugs ($p < 0.05$ for all groups, t-test). ²Total gelatinase activity in the presence of 1 mM CaCl_2 , without inhibitors (control), was 18.95 \pm 3.18 ng [³H]gelatin digested/min/ml of the dialyzed culture-conditioned medium. ³Total gelatinase activity in the presence of 10 mM CaCl_2 without inhibitors (control) was 48.92 \pm 2.7 ng/min/ml.

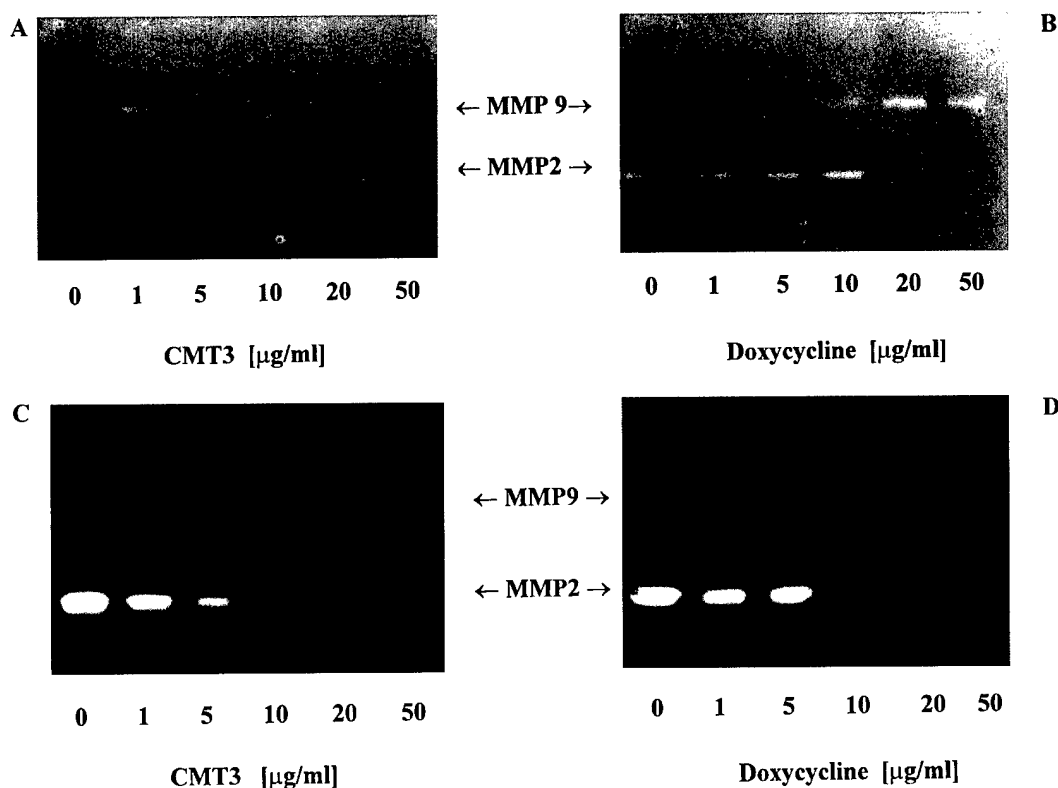


FIGURE 7 - Zymographic detection of gelatinases secreted into the conditioned media from cultures treated with CMT-3 or DC. Culture conditioned media (15 $\mu\text{l}/\text{lane}$, equivalent to 5×10^3 cells) from TSU PR1 (a,b) and MAT LyLu (c,d) cells were separated by SDS-PAGE (8% polyacrylamide) on a gelatin-embedded (1 mg/ml) gel and zymography. The positions of purified MMP-2 and MMP-9 are indicated. Note: the major fraction of MMP-2 from MAT LyLu (bottom) cell conditioned media was active ($M_r \sim 64,000$), whereas most of the TSU PR1 (top) MMP-2 was in the latent form ($M_r 72,000$).

out antimicrobial activity, shows that tumor cell cytotoxicity is independent of its antibiotic action.

We report here that CMT-3 is a specific and potent inducer of apoptotic cell death. Our selection of the assay system to measure apoptosis, the Cell Death ELISA-Plus kit, facilitated distinction between CMT-3- and DC-induced programmed cell death and necrosis. CMT-3 not only induced apoptosis but also caused necrotic cell death; the latter was increased at higher concentrations of the drug ($\geq 10 \mu\text{g}/\text{ml}$). Although necrotic cell death is often

termed "nonspecific cell death," tetracycline-induced cell lysis may be attributable to the ability to complex and sequester divalent cations such as Ca^{2+} , Fe^{2+} and Zn^{2+} , thus leading to cell lysis.^{51–53} The minimum incubation time required for CMT-3 to induce apoptosis was 4 hr (Table II), similar to the time interval for detectable depolarization of mitochondria (a decrease in $\Delta\Psi$, Fig. 4). This time range was also similar to the maximum increase observed in cellular $[\text{OH}^-]$ (Fig. 5). The cellular $[\text{OH}^-]$ levels in cells exposed to CMT-3 for 4 hr or more were comparable to those

TABLE V - INHIBITION OF MMP-2 AND TIMP-1 PRODUCTION BY CAP 139 CELLS BY CMT-3 AND DC¹

Drug ($\mu\text{g/ml}$)	MMP-2	TIMP-1 ²	TIMP-2 ³
No drug, control	65.9 \pm 2.2 (0) ⁴	230 \pm 11.2 (0)	18.2 \pm 1.15
CMT-3			
1.0	43.1 \pm 1.6 (35)	187.3 \pm 5.5 (18.5)	17.64 \pm 0.5 (3.13)
5.0	28.6 \pm 1.1 (56.7)	170.0 \pm 7.5 (26.3)*	16.53 \pm 0.84 (9.22)
10.0	17.3 \pm 8.3 (74.0)	144.3 \pm 2.4 (37.9)*	16.59 \pm 0.61 (10.27)
DC			
1.0	58.9 \pm 1.64 (10.6)	193.3 \pm 17.3 (16.0)	17.29 \pm 0.38 (5.05)
5.0	63.8 \pm 1.1 (3.0)	188.1 \pm 2.8 (18.2)	16.1 \pm 0.46 (11.87)
10.0	52.7 \pm 0.8 (20.0)	169.0 \pm 5.68 (26.5)	15.86 \pm 1.64 (12.9)
20.0	32.3 \pm 1.3 (50.9)	156.1 \pm 3.8 (32.7)	14.25 \pm 0.79 (21.75)

¹MMP-2 and TIMPs in the drug-treated CaP 139 culture-conditioned medium were measured using ELISA kits (Oncogene Sciences). Amount of MMP-2 or TIMP proteins in the assay medium was calculated from a standard graph using amount standards provided in the kits. MMP-9 levels measured using a similar but separate assay kit was below the detection limit of the kit (<10 ng/ml conditioned medium). Data are ng/mg (mean \pm SD), with percent reduction in parentheses.²In data marked with an asterisk, the levels were significantly different from untreated cultures (control) ($p < 0.05$, t -test).³TIMP-2 levels from drug-treated cultures did not significantly differ from control levels ($p > 0.05$, t -test).⁴Data shown are from a single experiment with replicate (4) samples.

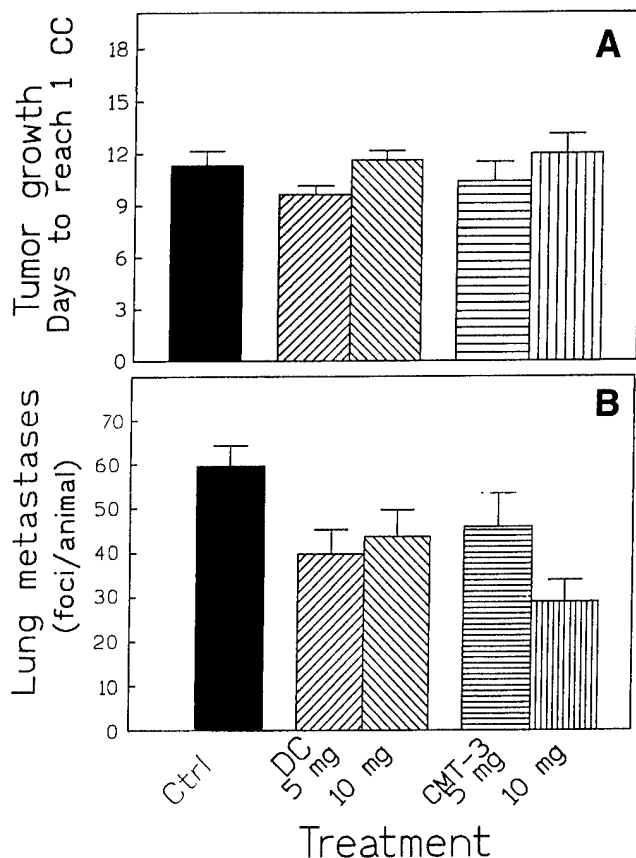


FIGURE 8 - Effect of DC and CMT-3 on growth and metastasis of Dunning tumor in rats. Tumor growth was initiated by injection of 1×10^6 tumor cells s.c. Drug dosing began the same day. (a) Growth profile of all tumors. (b) Number of metastatic tumor foci in lungs (mean \pm SD). The doses of drugs, 5 and 10 mg/day, are actual amounts used in the dosage for a rat weighing ~ 250 g; this amounts to 20 and 40 mg/kg/day, respectively.

found in unexposed cells, indicating possible interaction of $[\text{OH}^-]$ with their cellular targets and destruction of polarity of mitochondrial membrane. As shown in many types of cells including cardiac myocytes, release of reactive oxygen species is accompanied by mitochondrial depolarization.⁵⁴ Mitochondrial depolarization is

frequently observed in cells undergoing apoptosis.⁵² Therefore, it is compelling to conclude that CMT-3-induced apoptosis in CaP cells is associated with depolarization of mitochondria. Cytotoxic activity of CMTs by necrotic mechanisms may be irrelevant to their clinical application; in preclinical trials the peak plasma levels rarely reached ≤ 5 $\mu\text{g/ml}$ without causing severe toxicity.⁵⁵ Therefore, induction of apoptosis is likely to be of major significance to potential application of CMTs in the clinic.

In addition to the induction of apoptosis, cell cycle progression was blocked in cultures exposed to CMT-3 and DC. A significant increase in accumulation at the G_0/G_1 phase and a decrease in S-phase fractions was observed in both androgen-sensitive LNCaP and androgen-insensitive DU145 cells. This G_1/S transition block is indicative of the inhibition of biochemical processes such as inhibition of cell cycle phase transition-related cyclin-dependent kinases.⁵⁶

CMTs and antiinvasive activity

We have presented results showing evidence of the antiinvasive activity of DC and CMTs. DC and several CMTs inhibited invasive activity in both human and rat CaP cells. Since the invasion process is complex and involves both tumor cell motility and the ability to degrade basement membrane, our evidence suggests that the antiinvasive activity of CMT and DC is predominantly due to their anti-MMP activity. CMT-3 and DC not only inhibited the activity of secreted MMPs (MMP-2 and MMP-9) but also significantly decreased the production and/or secretion of these enzymes (Table V, Fig. 6). Interestingly, both TIMP-1 and TIMP-2 levels were much less inhibited by DC or CMT-3 than that for MMPs (Table V). This suggests that CMT-3 reduces invasive activity of tumor cells not only by binding to active MMPs and inhibiting their synthesis/secretion, but also by not affecting TIMP-1 and TIMP-2 levels significantly. Stearns *et al.*⁵⁷ have reported that the cytokine interleukin-10 (IL-10) decreases MMP levels in CaP cells, while simultaneously increasing TIMP-1 expression. Preliminary studies in our laboratory indicate that CMT-3 actually reduces the expression of IL-10 and other immunomodulatory cytokines such as IL-1 β in some CaP cells such as the PC-3 cell line (unpublished observations). It is thus possible that the decrease in MMP-2 levels in CMT-3-treated cells is primarily due to the effect of CMT-3 and is not mediated by cytokine-mediated pathways.

We observed that CMT-3 and DC significantly reduced but did not abolish invasive activity (Fig. 7). This partial inhibition could be attributable to other proteinases secreted by tumor cells that are not inactivated by these drugs. An example is urokinase-like plasminogen activator (uPA), a serine proteinase that also facilitates invasion and metastasis.⁴⁰ It has been reported that DC or CMTs do not inhibit uPA secretion or activity.⁵⁸ However, they

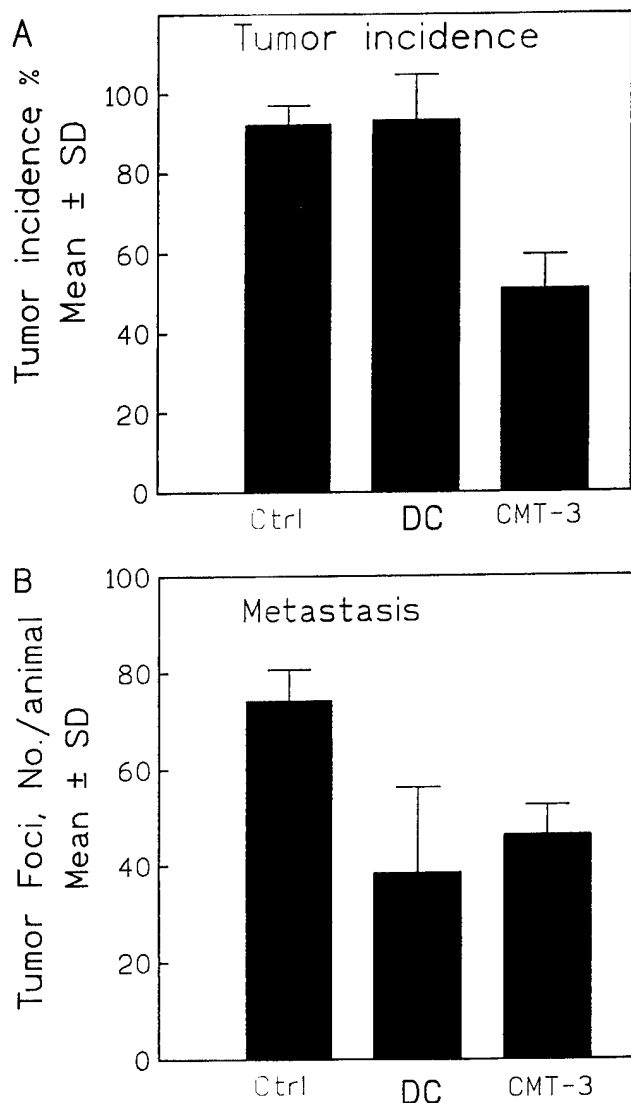


FIGURE 9 – Effect on tumor incidence and metastasis of predosing the rats with DC and CMT-3. (a) Tumor incidence. The experiments were conducted as described in Material and Methods. Animals without palpable tumors at the site of injection were considered tumor-free. The percentage of animals belonging to the CMT-3 treatment group in which tumors were resorbed varied between 20 and 30% in 3 separate experiments (2/10, 2/7 and 3/10, respectively). No tumor resorption was observed in other experimental groups. Data are mean \pm SD. (b) Tumor foci in lungs. Data are mean \pm SD from all animals in which the primary tumors grew to a size of ≥ 10 cm³. Tumor foci were counted manually under a 2.5 \times magnifying lens. Specimens were selected randomly to avoid bias.

may inhibit other serine proteinases that activate MMPs, such as trypsinogen-2.⁵⁹ Recently, Meng *et al.*⁶⁰ showed that CMT-3 and CMT-8 also inhibit proliferation and invasive potential of MDAMB-468 human breast tumor cells. In addition, CMT-3 increased the expression of E-cadherin, catenins and BRACA1, a tumor suppressor. That report, along with ours, suggests a potential application of CMTs in early treatment for metastatic disease.

CMT and antitumor activity

A combined antitumor and antimetastatic efficacy of CMT-3, an orally administered tetracycline analog, is a significant finding of our study. Although administration of DC or CMT after tumor implant caused insignificant inhibition of primary tumor growth,

inhibition of tumor metastasis was significant (Figs. 8,9). However, predosing rats with the drug caused a delay in primary tumor growth. It is unclear at present why primary tumor growth was unaffected if the dosing began after tumor implant. It is plausible that a significant fraction of tumor cells survive *in vivo* if drug dosing is initiated after tumor cells are implanted. However, predosing may result in significantly higher plasma levels of CMT-3 (>10 μ g/ml), would be sufficient to kill most of the tumor cells. The selection of 7 days as the predosing period was arbitrary. Rodman *et al.*⁵⁵ (using the alternate term COL-3 for CMT-3) have shown that the absorption half-life is 5.4 hr and the elimination half-life is 7.1 hr after a single oral dose in rats. Furthermore, they reported that a significant amount remained in the circulation after 48 hr. In their studies, the plasma levels of CMT-3, after a single daily gavage of CMT-3 (30 mg/kg), exceeded the concentration required to inhibit the gelatinases by more than 2-fold. Taking our results together with these findings, it is possible to conclude that the enhanced efficacy of CMT-3 against tumor growth and metastasis over DC or other tetracyclines could be due to sustained high levels of CMT-3 in plasma.

Predosing the animals for 7 days with CMT-3 before implanting tumor cells also caused significant tumor remission and a remarkable reduction in tumor incidence. Tumor cell cytotoxicity combined with disruption of MMP-dependent early extravasations and angiogenesis^{61,62} might have contributed to the reduced tumor incidence and tumor remission. It is possible that an immune-mediated response may play a part in abolishing tumor incidence in predosed animals. Although at present MAT LyLu cells are poorly immunogenic in syngenic Copenhagen (COP) rats, both bilateral tumors and regrowth of ablated tumors have been observed in this system, indicating a lack of tumor immunity in this model.⁶³ The absence of these effects by DC is not surprising. Although DC was able to inhibit invasive activity of MAT LyLu cells *in vitro* (present report) and is capable of inhibiting angiogenic activity,⁶⁴ its low tumor cell cytotoxicity and low peak plasma levels (≤ 2.5 μ g/ml²²) may have limited its efficacy in this model. An enhanced efficacy of CMT-3 upon predosing shows that CMT-3 treatment can be effective if dosing is started even before clinical signs are apparent. This dosing schedule may be efficacious in situations such as immediately after surgical removal of malignant prostate or as adjuvant to radiation in the palliative treatment of metastatic disease.

The overall effectiveness of CMT-3 (demonstrated by a reduction in tumor incidence, tumor remission and decreased tumor metastasis in the Dunning MAT LyLu model) indicates that it also has a potential application in advanced hormone-refractory prostate cancer in men. Oral bioavailability, with minimal adverse reactions within a tolerable dose, suggests that it could be used as an adjuvant to hormone ablation or radiation therapy in prostate cancer. Similar studies in other models of cancer, notably melanoma and sarcoma, have also shown efficacy of CMTs as antitumor and antimetastatic drugs.^{65,66} Fife *et al.*⁶⁷ have reported that DC induces apoptosis and antiinvasive activities in PC-3 and DU 145 cells *in vitro*, although the concentrations (≥ 10 μ g/ml) at which these activities were elicited were higher than those that could be achieved safely by oral administration.

While our work was in progress, a multicenter phase I clinical trial of CMT-3 (trade name COL-3, Metastat; CollaGenex Pharmaceuticals) was conducted by the Investigational Drug Branch, Cancer Therapy Evaluation Program (National Cancer Institute, Bethesda, MD). The study evaluated maximum tolerated dose (MTD) and dose-limiting toxicities in patients with refractory solid tumors. The study, initially involving 35 patients, demonstrated disease stabilization for up to 26 months in patients with nonepithelial types of malignancy. In addition, there was a significant reduction in plasma MMP-2 levels in the group that showed disease stabilization. The major dose-limiting toxicity was photosensitivity. Drug-induced photosensitivity to both UV-A and UV-B radiation was reported in 40–70% of patients receiving

COL-3 at a dose ≥ 70 mg/m²/day. Based on the results of this study, the investigators have recommended a daily dose of 36 mg/m² for a phase II clinical trial.⁶⁸

Several other inhibitors of MMPs also reduce experimental tumor growth and metastasis in animal tumor models.^{14,69,70} For example, 2 synthetic inhibitors of MMPs, Batimastat and Marimastat (British Biotechnology and Pharmaceutical, Cowley, Oxford, UK) have shown significant antitumor activity in several experimental tumor models including ovarian,¹⁴ colon,⁷¹ breast⁷⁰ and melanoma models.⁷¹ Recent experience, gained from clinical trials of various MMP inhibitors, however, shows a lack of significant efficacy in most of the human cancers and, furthermore, some are contraindicated.⁷²⁻⁷⁵ A few, however, have been shown to be capable of stabilizing the disease.⁷⁵

Some have argued that this was an anticipated result in the light of the stage and timing of the therapeutic intervention. For example, Zucker *et al.*⁷⁶ have postulated that the therapeutic benefit of MMP inhibitors is seen in early-stage disease, in some tumors as soon as malignancy is detected. Furthermore, they have expressed concern that anti-MMP therapy at an advanced stage in any human cancer

is likely to be ineffective, akin to "closing the barn door after the horses have escaped." Although this may be a valid concern for conventional anti-MMP agents in cancer therapy, CMTs may be potentially more effective if treatment begins at first diagnosis of cancer, even in situations in which clinical manifestations of the disease are not apparent. CMT-3 or its close derivatives have a potential advantage over other anti-MMP agents in that CMTs show antiproliferative activity against tumor cells. The antimetastatic and antiproliferative activity, as well as the oral bioavailability, makes this class of drug potentially more powerful than synthetic MMP inhibitors.

ACKNOWLEDGEMENTS

The authors are grateful to Prof. A. Krishnan for many suggestions and advice, Dr. N. Altman, Department of Pathology University of Miami, for help with histology and Mr. R. Ashley and Dr. B. Zerler of CollaGenex Pharmaceuticals (Newtown, PA) for a generous supply of CMTs. B.L.L. is grateful to Dr. V.B. Lokeshwar for encouragement, patience and understanding. BLL is grateful to NY Academy of Sciences for permission to reproduce Fig 2.

REFERENCES

- Kamardt J, Smith DC, Pienta KJ. Hormone refractory prostate cancer: national comprehensive cancer network guidelines. *Adv Oncol* 1998; 14:14-21.
- Vogelzang NJ. One hundred thirteen men with hormone-refractory prostate cancer died today (editorial). *J Clin Oncol* 1996;14:1753-5.
- Liotta LA, Stetler-Stevenson WG. Principles of molecular cell biology of cancer: cancer metastasis. In: De Vita VT, Hellman S, Rosenberg SA, eds. *Cancer: principles and practice of oncology*, 4th ed. Philadelphia: JB Lippincott, 1993. 134-49.
- Stetler-Stevenson WG, Aznavoorian S, Liotta LA. Tumor cell interactions with the extra cellular-matrix during invasion and metastasis. *Annu Rev Cell Biol* 1993;9:541-73.
- Chambers AF, MacDonald IC, Schmidt EE, et al. Steps in tumor metastasis: new concepts from intravital videomicroscopy. *Cancer Metastasis Rev* 1995;14:279-301.
- Lawrence JA, and Steeg PS. Mechanism of tumor invasion and metastasis. *World J Urol* 1996;14:124-30.
- Liotta LA, Stetler-Stevenson WG. Metalloproteinase and cancer invasion. *Semin Cancer Biol* 1990;1:99-106.
- Liotta LA, Steeg PS, Stetler-Stevenson WG. Cancer metastasis and angiogenesis: an imbalance of positive and negative regulation. *Cell* 1991;64:327-36.
- McCawley LJ, Matrisian LM. Matrix metalloproteinases: multifunctional contributors to tumor progression. *Mol Med Today* 2000;6: 149-56.
- Lokeshwar BL, Selzer MG, Block NL, et al. Secretion of matrix metalloproteinase and their inhibitors (TIMPs) by human prostate in explant cultures: reduced tissue inhibitor of metalloproteinase secretion by malignant tissues. *Cancer Res* 1993;53:4493-8.
- Pajouh MS, Nagle RB, Breathnach R, et al. Expression of metalloproteinase genes in human prostate cancer. *Cancer Res Clin Oncol* 1991;17:144-50.
- Stearns ME, Wang M. Type IV collagenase (Mr 72,000) expression in human prostate: benign and malignant tissue. *Cancer Res* 1993;53: 878-83.
- DeClerck YA, Perez N, Shimada H, et al. Inhibition of invasion and metastasis in cells transfected with an inhibitor of metalloproteinase. *Cancer Res* 1992;52:701-8.
- Davies B, Brown PD, East N, et al. A synthetic matrix metalloproteinase inhibitor decreases tumor burden and prolongs survival of mice bearing human ovarian carcinoma xenografts. *Cancer Res* 1993; 53:2087-91.
- Zucker S, Lysik RM, Ramamurthy NS, et al. Diversity of melanoma plasma membrane proteinases: inhibition of collagenolytic and cytolytic activities by minocycline. *J Natl Cancer Res* 1985;75:517-25.
- Kroon AM, Dontje BHJ, Holtrop M, et al. The mitochondrial genetic system as a target for chemotherapy: tetracycline as cytostatic. *Cancer Lett* 1984;25:33-80.
- Golub LM, Ramamurthy NS, McNamara TF. Tetracyclines inhibit connective tissue breakdown: new therapeutic implications for an old family of drugs. *Crit Rev Oral Biol Med* 1991;2:297-322.
- Sipos EP, Tamargo RJ, Weingart JD, et al. Inhibition of tumor angiogenesis. *Ann NY Acad Sci* 1994;732:263-72.
- Golub LM, Soummlainen K, Sorsa T. Host modulation with tetracyclines and their chemically modified analogues. *Curr Opin Dentist* 1992;2:80-90.
- van den Bogert C, Dontje BHJ, Holtrop M, et al. Arrest of the proliferation of renal and prostate carcinomas of human origin by inhibition of mitochondrial protein synthesis. *Cancer Res* 1986;46: 3283-9.
- Golub LM, McNamara TF, D'Angelo GD, et al. A non-antibacterial chemically modified tetracycline inhibits mammalian collagenase activity. *J Dent Res* 1987;66:1310-4.
- Yu Z, Leung MK, Ramamurthy NS, et al. HPLC determination of a chemically modified non-antimicrobial tetracycline: biological implications. *Biochem Med Metab Biol* 1992;47:10-20.
- Paemen L, Martens E, Nogra K, et al. The gelatinase inhibitory activity of tetracyclines and chemically modified tetracycline analogues as measured by a novel micro titer assay for inhibitors. *Biochem Pharmacol* 1996;52:105-11.
- Ryan ME, Ramamurthy NS, Golub LM. Matrix metalloproteinases and their inhibition in periodontal treatment. *Curr Opin Periodontol* 1996;3:85-96.
- Greenwald RA, Golub LM, Ramamurthy NS, et al. In vitro sensitivity of three mammalian collagenases to tetracycline inhibition: relationship to bone and cartilage degradation. *Bone* 1998;22:33-8.
- Isaacs JT, Isaacs WB, Feitz WFJ, et al. Establishment and characterization of seven Dunning rat prostatic cancer cell lines and their use in developing methods for predicting metastatic abilities of prostatic cancers. *Prostate* 1986;9:261-81.
- Lokeshwar BL, Ferrell SM, Block NL. Enhancement of radiation response of prostatic carcinoma by taxol: therapeutic potential for late-stage malignancy. *Anticancer Res* 1995;15:93-8.
- Hayward SW, Dahiya R, Cunha GR, et al. Establishment and characterization of an immortalized but non-transformed human prostate epithelial cell line: BPH-1. *In Vitro Cell Dev Biol* 1995;31A:14-24.
- Mossman T. Rapid colorimetric assay for cellular growth and survival: application to proliferation and cytotoxicity assays. *J Immunol Methods* 1983;65:55-63.
- Lokeshwar BL, Lokeshwar VB, Block NL. Expression of CD44 in prostate cancer cells: association with cell proliferation and invasive potential. *Anticancer Res* 1995;15:1191-8.
- Boehringer Mannheim handbook on apoptosis and cell proliferation, 2nd ed. Mannheim: Boehringer Mannheim, 1998.
- Cossarizza A, Baccarani-Contri M, Kalashnikova G, et al. A new method for cytofluorimetric analysis of mitochondrial membrane potential using the J-aggregate forming lipophilic cation 5,5',6,6'-tetrachloro-1,1',3,3'-tetraethylbenzimidazol carbocyanine iodide (JC-1). *Biochem Biophys Res Commun* 1993;197:40-5.
- Lokeshwar BL, Escatel E, Zhu B-Q. Cytotoxic activity and inhibition of tumor cell invasion by derivatives of a chemically modified tetracycline CMT-3. *Curr Med Chem* 2001;8:271-9.
- Haughland RP. Handbook of fluorescent probes and research chemicals, 6th ed. Eugene, OR: Molecular Probes, 1996. 491-7.
- Ubezio P, Civoli F. Flow cytometric detection of hydrogen peroxide production induced by doxorubicin in cancer cells. *Free Radic Biol Med* 1994;16:509-16.
- Model MA, Kukuruga MA, Todd RF III. A sensitive flow cytometric

- method for measuring the oxidative burst. *J Immunol Methods* 1997; 202:105-11.
37. Krishan A. Rapid DNA content analysis by propidium iodide-hypotonic citrate method. *Methods Cell Biol* 1990;33:121-5.
 38. Bagwell CB. Theoretical aspects of flow cytometry data analysis. In: Bauer KD, Duque RE, Shanky TV, eds. *Clinical flow cytometry*, 1st ed. Baltimore: Williams and Wilkins, 1993. 117-142.
 39. Albini A, Iwamoto Y, Kleinman HK, et al. A rapid in vitro assay for quantitating the invasive potential of tumor cells. *Cancer Res* 1987; 47:3239-45.
 40. Houssein NM, Boyd DD, Hollas WJ, et al. Involvement of urokinase and its receptor in the invasiveness of human prostatic carcinoma cell lines. *Cancer Commun* 1991;3:255-64.
 41. Dean DD, Woessner JF Jr. A sensitive, specific assay for tissue collagenases using telopeptide-free ³H-acetylated collagen. *Anal Biochem* 1985;148:174-81.
 42. Dean DD, Curry TE, LeMaire WJ, et al. Determination of metalloproteinase activity after selective destruction of tissue inhibitor of metalloproteinases. In: *Transactions of the 33rd Annual Meeting of the Orthopedic Research Society* 1987;12:248.
 43. Lehninger AL. *Biochemistry*, 2nd ed. New York: Worth, 1975. 783.
 44. Woessner JF Jr. Matrix metalloproteinase and their inhibitors in connective tissue remodeling. *FASEB J* 1991;5:2145-54.
 45. Benckroun NM, Myers CE, Sinha BK. Free radical formation by anisoyl benzoylquinone in human breast tumor cells: implication for cytotoxicity resistance. *Free Radic Biol Med* 1994;17:191-200.
 46. Kamesaki H. Mechanisms involved in chemotherapy induced-apoptosis and their implications in cancer chemotherapy. *Int J Hematol* 1998;68:29-43.
 47. Sande MA, Mandel GL. Antimicrobial agents: tetracyclines, chloramphenicol, erythromycin, and miscellaneous antibacterial agents. In: Gilman AG, Rall TW, Nies AS, et al (eds.). *Goodman and Gilman's the pharmacological basis of therapeutics*. New York: Pergamon Press, 1990. 117-1125.
 48. Slater TF, Sawyer B, Strauli UD. Studies on succinate-tetrazolium reductase systems. *Biochim Biophys Acta* 1983;77:383-93.
 49. Berridge MV, Tan AS, McCoy KA, et al. The biochemical and cellular basis of cell proliferation assays that uses tetrazolium salts. *Biochemica* 1996;4:15-9.
 50. Lokeshwar BL. MMP inhibition in prostate cancer. *Ann NY Acad Sci* 1999;878:271-89.
 51. Grenier D, Hout MP, Maynard D. Iron-chelating activity of tetracyclines and its impact on the susceptibility of actinobacillus actinomycetemcomitans to these antibiotics. *Antimicrob Agents Chemother* 2000;44:763-6.
 52. Lemasters JJ, Nieminen A-L, Quian T, et al. The mitochondrial permeability transition in cell death: a common mechanism in necrosis, apoptosis and autophagy. *Biochem Biophys Acta* 1998, 1366: 177-96.
 53. Starke PE, Hoek JB, Farber JL. Calcium-dependent and calcium-independent mechanisms of irreversible cell injury in cultured hepatocytes. *J Biol Chem* 1986;261:3006-12.
 54. Zorov DB, Filburn CR, Klotz LO, et al. Reactive oxygen species (ROS)-induced ROS-release: a new phenomenon accompanying induction of mitochondrial permeability transition in cardiac myocytes. *J Exp Med* 2000;192:1001-14.
 55. Rodman L, Farnell D, Tomaszewski J, et al. Pre-clinical dose range-finding studies of COL-3 (NSC-683551) in rats and monkeys. *Proc Am Assoc Cancer Res* 1997;38:3999a, 4021a, 596.
 56. Sher CJ, Roberts JM. CDK inhibitors: positive and negative regulators of G1-phase progressions. *Genes Dev* 1999;13:1501-12.
 57. Stearns ME, Rhim J, Wang M. Interleukin 10 (IL-10) Inhibition of primary human prostate cell-induced angiogenesis: IL-10 stimulation of tissue inhibitor of metalloproteinase-1 and inhibition of matrix metalloproteinase (MMP)-2/MMP-9 secretion. *Clin Cancer Res* 1999; 5:189-196.
 58. Chang K, Rani, AS, Chang K, et al. Plasminogen activator activity is decreased in rat gingiva during diabetes. *J Periodontol* 1996;67: 743-7.
 59. Lukkonen A, Sorsa T, Salo T, et al. Down-regulation of trypsinogen-2 expression by chemically modified tetracyclines: association with reduced cancer cell migration. *Int J Cancer* 2000;86:577-81.
 60. Meng Q, Xu J, Goldberg ID, et al. Influence of chemically modified tetracyclines on proliferation, invasion, and migration properties of MDA-MB468 human breast cancer cells. *Clin Exp Metastasis* 2000; 18:130-46.
 61. Tamargo RJ, Bok RA, Brem H. Angiogenesis inhibition by minocycline. *Cancer Res* 1991;51:672-5.
 62. Teicher BA, Sotomayor EA, Huang ZD. Antiangiogenic agents potentiate cytologic cancer therapies against primary and metastatic disease. *Cancer Res* 1992;52:6702-4.
 63. Vieweg J, Heston WDW, Giloa E, et al. An experimental model stimulating local recurrence and pelvic lymph node metastasis following orthotopic induction of prostate cancer. *Prostate* 1994;24: 291-8.
 64. Fife RS, Sledge GW Jr, Sission S, et al. Effects of tetracyclines on angiogenesis in vitro. *Cancer Lett* 2000;153:75-8.
 65. Masumori N, Tsukamoto T, Miyao N, et al. Inhibitory effects of minocycline on in vitro invasion and experimental metastasis of mouse renal adenocarcinoma. *J Urol* 1994;151:1400-4.
 66. Seftor REB, Seftor EA, De Larco JE, et al. Chemically modified tetracyclines inhibit human melanoma cell invasion and metastasis. *Clin Exp Metastasis* 1998;16:217-225.
 67. Fife RS, Sledge GW, Roth BJ, et al. Effects of doxycycline on human prostate cancer cells in vitro. *Cancer Lett* 1998;127:37-41.
 68. Rudek MA, Figg WB, Dyer C, et al. Phase I clinical trial of oral COL-3, a matrix metalloproteinase inhibitor, in patients with refractory metastatic cancer. *J Clin Oncol* 2001;19:584-92.
 69. Brown PB. Matrix metalloproteinase inhibitors: a novel class of anticancer agents. *Adv Enzyme Res* 1995;35:293-301.
 70. Sledge GW Jr, Quali M, Goulet R, et al. Effect of metalloproteinase inhibitor Batimastat on breast cancer regrowth and metastasis in athymic mice. *J Natl Cancer Inst* 1995;87:1546-50.
 71. Wang X, Fu X, Brown PD, et al. Matrix metalloproteinase inhibitor BB-94 (Batimastat) inhibits human colon tumor growth and spread in a patient-like orthotopic model in nude mice. *Cancer Res* 1994;54: 4726-8.
 72. Kirov RG, Garofalo A, Crimmin MJ, et al. Inhibition of the metastatic spread and growth of B16-BL6 murine melanoma by a synthetic matrix metalloproteinase inhibitor. *Int J Cancer* 1994;58:460-4.
 73. Brown PD. Ongoing trials with matrix metalloproteinase inhibitors. *Expert Opin Investig. Drugs* 2000;9:2167-77.
 74. Dimitroff CJ, Sharma A, Bernacki RJ. Cancer metastasis: a search for therapeutic inhibition. *Cancer Invest* 1998;16:279-90.
 75. Levitt NC, Ferry AL, Eskins M, et al. Phase I and pharmacological study of the oral matrix metalloproteinase inhibitor, MMI270 (CGS27023A) in patients with advanced solid tumor. *Clin Cancer Res* 2001;7:1912-22.
 76. Zucker S, Cao J, Chen W-T. Critical appraisal of the use of matrix metalloproteinase inhibitors in cancer treatment. *Oncogene* 2000;19: 6642-50.
 77. Lokeshwar BL. MMP inhibition in prostate cancer. In: Greenwald RA, Zucker S, Golub LM, eds. *Inhibition of matrix metalloproteinases therapeutic potential*. Annals of the New York Academy of Sciences, vol. 878. New York: New York Academy of Sciences, 1999. 284.

Miami Nature Biotechnology Short Reports - Volume 14

PROGRAM AND SHORT REPORTS

50 YEARS ON: FROM THE DOUBLE HELIX TO MOLECULAR MEDICINE

February 1-5, 2003

<http://www.med.miami.edu/mnbws>

**Radisson Deauville Resort
Miami Beach, Florida, USA**

miami
nature
biotechnology
**winter
symposia**

Proceedings of the 2003
Miami Nature Biotechnology Winter Symposium

Organized by
the University Biochemistry &
Molecular Biology Foundation, Inc.,
The Sylvester Comprehensive Cancer Center,
Nature Biotechnology and Nature Medicine

DAMD 17-98-1-8526

P. I.: B. L. Lokeshwar, Ph.D.

2002-2003 Annual Report

Appendix 1-4

This Symposium
is in celebration of the
50th Anniversaries of the
Double Helix and the
Founding of the
University of Miami
School of Medicine

Editors

*Murray P. Deutscher
Sandra Black
Kermit Carraway
Dalton Dietrich
Frans Huijting
Luca Inverardi
Robert Keane
Andrew Marshall
Eckhard Podack
Beatrice Renault
and
William J. Whelan*

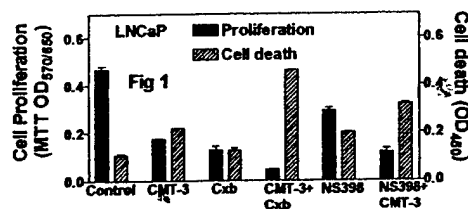
NOVEL THERAPY FOR PROSTATE CANCER: IMPROVED EFFICACY OF AN ANTIMETASTATIC DRUG COMBINED WITH AN ANTI-INFLAMMATORY DRUG

Bal L. Lokeshwar*, Devendra S. Dandekar, Monica Lopez
Dep. Urology and Sylvester Cancer Center, U. Miami, Miami, FL.
*blokeshw@med.miami.edu.

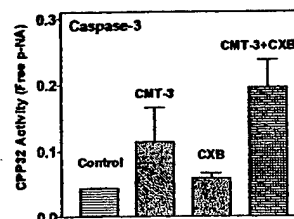
INTRODUCTION: Existing therapies for metastatic prostate cancer (CaP) are largely ineffective, partly due to the acquired drug resistance (ADR)(1). CMT-3 (COL-3), a non-antimicrobial tetracycline analog has potent cytotoxic and anti-metastatic action on prostate tumors (2). Celecoxib (CXB), a strong inhibitor of cyclooxygenase-2 (COX-2), has shown to kill tumor cells by many mechanisms (3). The objective of this investigation was to demonstrate the potential of combined efficacy of CMT-3 and CXB in the treatment of prostate cancer using CaP cells in culture.

METHODS: Viability of cells treated with CMT-3 or CXB, or both were quantified with MTT assay. Drug-induced apoptosis and death-inducible caspase activity were tested by ELISAs(2). Cell cycle fractionation was done by flow cytometry. Differential gene expression analysis was performed on a 10,800-cDNA microarray using InCyte GEM Tool software.

RESULTS: Treatment of CaP cells (PC-3ML and LNCaP) with CMT-3 (5µg/mL), CXB (10µM) or CMT3+CXB (10µM) all decreased tumor cell viability by >50%, the drug combination killed >80% of cells (Fig1). As shown in Fig 1, CMT-3 alone inhibited cell proliferation (62%) and induced apoptosis (2-fold). Although, CXB inhibited cell proliferation (73%) it did not induce significant apoptosis. However, CMT-3 and CXB combination inhibited cell proliferation by 80% and caused a 4.6-fold increase in apoptosis. The fraction of cells in G0/G1 phase in CMT-3 (5 µg/ml) treated samples ($75.6 \pm 6.5\%$) was significantly higher compared to untreated control ($54.4 \pm 3.4\%$). CXB (10µM) also caused some G0/G1 phase arrest (63.2 ± 5.0). However, the G0/G1 fraction of CXB+CMT-3 combination (78.9 ± 5.2) was not significantly different than that of CMT-3 treated samples. Increased cytotoxicity of CMT-3 and CXB combination found to be correlated with increased activation of Caspase-3 (>70% increase in drug combination, compared to single drug alone (Fig 2)). Gene expression by microarray revealed ≥ 2 fold decrease in 22 genes in CMT-3 treated, 89 genes in CXB treated and 77 genes in CMT-3+CXB combination treated PC-3ML cells. The key genes that were down regulated in combination treatment include COX-2 (4.2x), IL-1 β (7.6x), IL-8 (2.5x), VEGF-c (2.1x), and Cx3C (14.5x).



CONCLUSION: These results demonstrate the enhanced cytotoxicity of the CMT-3+CXB combination may be mediated via enhanced activation of caspases, and suppression of survival promoting cytokines. Further, these results suggest that use of CMT-3 and CXB together could lead to an improved therapy in advanced prostate cancer. (NIH R01CA61038 ; DAMD1718526)



REFERENCES:

1. Fidler, I.J. (1999) Cancer Chemother Pharmacol. 43, :S3-10.
2. Lokeshwar B.L., Selzer M.G., Zhu, B-Q., Block, N.L., Golub, L.M (2002). Internat. J Cancer; 98, 297-309
3. Thun MJ, Henley SJ, Patrono C. (2002) JNCI, 94, 252-66

#3723 Synergistic increase in efficacy of an antimetastatic drug (CMT-3) combined with an anti-inflammatory drug (celecoxib) in prostate cancer. Balakrishna L. Lokeshwar, Devendra S. Dandekar, and Monica Lopez. *University of Miami School of Medicine, Miami, FL.*

INTRODUCTION: The median survival of patients with androgen-refractory prostate cancer is less than two years, therefore, an opportunity exists to improve the efficacy of existing therapies or develop new therapies (1). CMT-3 (COL-3), a non-antimicrobial tetracycline analog has potent cytotoxic and anti-metastatic action on prostate tumors (2). Celecoxib (CXB), a strong inhibitor of cyclooxygenase-2 (COX-2), has shown to kill tumor cells by many mechanisms. The objective of this investigation was to demonstrate the potential of combined efficacy of CMT-3 and CXB in the treatment of prostate cancer using CaP cells in culture.

METHODS: Viability of cells treated with CMT-3 or CXB, or both were quantified with MTT assay. Drug-induced apoptosis and death-inducible caspase activity were tested by ELISAs (2). Cell cycle fractionation was done by flow cytometry. Differential gene expression analysis was performed on a 10,800-cDNA microarray using InCyte GEM Tool software.

RESULTS: Treatment of CaP cells (PC-3ML and LNCaP) with CMT-3 (5 µg/mL), CXB (10 µM) or CMT3 + CXB (10 µM) all decreased tumor cell viability by >50%, the drug combination killed >90% of cells in 48 hours. CMT-3 alone inhibited cell proliferation (62%) and induced apoptosis (2-fold). Although, CXB inhibited cell proliferation (73%) it did not induce significant apoptosis. However, CMT-3 and CXB combination inhibited cell proliferation by 90% and caused a 4.6-fold increase in apoptosis. The fraction of cells in G0/G1 phase in CMT-3 (5 µg/ml) treated samples ($75.6 \pm 6.5\%$) was significantly higher compared to untreated control ($54.4 \pm 3.4\%$). CXB (10 µM) also caused some G0/G1 phase arrest (63.2 ± 5.0). However, the G0/G1 fraction of CXB + CMT-3 combination (78.9 ± 5.2) was not significantly different than that of CMT-3 treated samples. Increased cytotoxicity of CMT-3 and CXB combination was found to be correlated with increased activation of Caspase-3 (>70% increase in drug combination, compared to single drug alone. Gene expression by microarray revealed ≥ 2 fold decrease in 22 genes in CMT-3 treated, 89 genes in CXB treated and 77 genes in CMT-3 + CXB combination treated PC-3ML cells. The key genes that were down regulated in combination treatment include COX-2 (4.2x), IL-1 β (7.6x), IL-8 (2.5x), VEGF-c (2.1x), and Cx α cytokine5 (14.5x).

CONCLUSION: These results demonstrate the enhanced cytotoxicity of the CMT-3 + CXB combination may be mediated via enhanced activation of caspases, and suppression of survival promoting cytokines. Further, these results suggest that use of CMT-3 and CXB together could lead to an improved therapy in advanced prostate cancer. (Supported by grants from NIH R01CA61038 and U.S Army DAMD1718526).

REFERENCES: 1. Hellerstedt BA, Pienta KJ. (2002) CA-Cancer J Clin. 52, 154-179 2. Lokeshwar B.L., Selzer M.G., Zhu, B-Q, Block, N.L., Golub, L.M (2002). *Internat. J Cancer*; 98, 297-309

Original Article

An orally active Amazonian plant extract (BIRM) inhibits prostate cancer growth and metastasis

Devendra S. Dandekar · Vinata B. Lokeshwar · Edwin Cevallos-Arellano · Mark S. Soloway · Balakrishna L. Lokeshwar (✉)

D. S. Dandekar · V. B. Lokeshwar · M. S. Soloway · B. L. Lokeshwar
Department of Urology, McKnight Vision Research Building, University of Miami School of Medicine, Miami, Florida, 33101, USA

D. S. Dandekar · V. B. Lokeshwar · M. S. Soloway · B. L. Lokeshwar
Sylvester Comprehensive Cancer Center, University of Miami School of Medicine, Miami, Florida, 33101, USA

E. Cevallos-Arellano
Instituto de Tumores, Quito, Ecuador

✉ B. L. Lokeshwar
Phone: +1-305-2431012
Fax: +1-305-2436893
E-mail: BLOKESHW@med.miami.edu

Received: 26 December 2002 / Accepted: 6 March 2003

Abstract *Purpose* Poor efficacy of conventional chemotherapeutic drugs against metastatic hormone-refractory prostate cancer (CaP) drives patients to try “alternative medicine”. The antitumor activity of one such agent, “BIRM” (biological immune response modulator; “Simple Ecuadorian Oral Solution: an extract of an Amazonian plant”), was characterized in vitro and in vivo using established CaP cell lines and a tumor model.

Methods The cytotoxicity of BIRM in four human and one rat CaP cell line was evaluated using cell proliferation-inhibition and clonogenic survival assays. BIRM-induced apoptosis, alterations in cell cycle phase progression and inhibition of the extracellular matrix-degrading enzyme hyaluronidase were also investigated in these cells. The in vivo efficacy of BIRM was evaluated in rats with subcutaneous tumor implants of Dunning EGFP-MAT LyLu cells. The active species in BIRM were characterized by gel filtration chromatography.

Results BIRM inhibited cell proliferation and clonogenic growth of the CaP cells (IC_{50} about 8.0 μ l/ml). It increased cell accumulation in the G_0/G_1 phase by 33.8% and decreased the proportion of cells in S phase by 54.6%. Apoptotic cell death in BIRM-treated cells was associated with activation of cell death-associated caspases. BIRM inhibited the activity of hyaluronidase, a hyaluronic acid-degrading enzyme, at 1 μ l/ml. Treatment of MAT LyLu tumor-bearing rats with BIRM by oral gavage resulted in a significant decrease in tumor incidence (50%), tumor growth rate (18.6 ± 1.3 days for 1 ml tumor growth in control rats and 25.7 ± 2.6 days in BIRM-treated rats), and only one out of six BIRM-treated rats versus four out of six in the control group developed lung metastasis. Three active ingredients in BIRM with a relative molecular mass (M_r) of ≥ 3500 were identified by ultracentrifugation and gel filtration chromatography and were found to be resistant to proteinase and heat ($100^\circ C$).

Conclusion The plant extract BIRM contains antitumor compounds of $M_r \geq 3500$ with potent antiproliferative activity in vitro and in vivo against prostate cancer cells.

Keywords Natural herbal anticancer products · Prostate cancer · Invasion and metastasis · Chemoprevention · Apoptosis

Abbreviations

CaP Prostate cancer/cancer of the prostate

EGFP Enhanced green fluorescence protein

HA Hyaluronic acid

HAase Hyaluronidase

MTT Methyl thiozoyl tetrazolium bromide [(3-[4,5-demethylthiozol-2-y]-2,5-diphenyl tetrazolium bromide]

This work was supported in part by PHS grants R01 CA 61038 (B.L.L.), CA 72821 (V.B.L.), and DoD Grants DAMD 179818526 (B.L.L.) and DAMD 170210005 (V.B.L.).

Introduction

Cancer of the prostate (CaP) is the most frequently diagnosed malignant cancer in American men with an estimated 189,000 new cases in 2002 [13]. The majority of CaP-related deaths,

estimated to be 30,200 in 2002, are the result of failure of all currently available conventional treatments. Besides undergoing conventional therapy, CaP patients often seek treatment by unproven therapeutic approaches [12]. It is estimated that 30–40% of men with CaP experiment with one or more complementary therapies which include high-dose vitamins and minerals, herbal preparations and supplements of soy, saw palmetto etc. [14]. Moreover, there is a dramatic increase in the number of patients moving towards complementary and alternative medicine and consuming plant extracts from “folklore medicine” [26]. We have come across one such natural herbal medicine “BIRM” (biological immune response modulator; “Simple Ecuadorian Oral Solution: an extract of an Amazonian plant”) formulated by a physician (E.C.-A.), promoted in South America, and based on the local folklore of the Ecuadorian native population. The formulation is dispensed as a natural remedy for a variety of maladies including HIV-1 infection and cancer [1, 3, 4]. Very little systematic information is currently available on BIRM, and no studies have been undertaken to investigate the structure-function correlations in the ingredients of BIRM. Therefore, we decided to evaluate the efficacy and antiproliferative effects of BIRM in a CaP model.

Materials and methods

Test compound

BIRM was a gift from BIRM (Quito, Ecuador). BIRM is an aqueous extract of dried roots of a plant of the genus *Dulcamara* (family Solanaceae) grown in Ecuador, and marketed as a greenish-brown suspension with a mild bittersweet smell. The inactive ingredients in BIRM comprise 16% solid particles, likely root fibers, and the remainder, a lipid-free liquid. BIRM is prepared by aqueous extraction of dried roots followed by oxidation/reduction of the extract. During this process, the amount of roots and the timing of oxidation/reduction are carefully controlled to minimize batch-to-batch variation. Prior to initiation of this project, the efficacy of BIRM samples from five different batches were selected randomly and tested in two different cell lines (PC-3ML and LNCaP) by the MTT assay to determine the degree of interbatch variation. We found no interbatch variation in the potency of BIRM for induction of cytotoxicity. In the present study, BIRM samples from lot number 011-2000 were used. For all the studies reported here, BIRM clarified by centrifugation at 10,000 *g* was used.

Cells and tumor lines

Established human CaP cell lines (LNCaP and DU-145) were obtained from the ATCC (Rockville, Md.). A recently established bone metastatic PSA⁺ CaP line (VCaP) was generously provided by Drs. Pienta and Cooper (Karmanos Cancer Center, University of Michigan, Ann Arbor, Mich.) [11, 17, 23]. A metastatic variant of a PC-3 cell line, PC-3ML, was a gift from Dr. M.E. Stearns (Allegheny University Hospitals, Philadelphia, Pa.) [15, 27]. All cultures were maintained in a complete medium containing RPMI-1640 basal medium, 10% fetal bovine serum (Atlanta Biologicals, Atlanta, Ga.), and 10 µg/ml gentamicin. The EGFP-MAT LyLu cell line was generated by stable transfection of Dunning MAT LyLu rat CaP cells with pEGFP-1 plasmid DNA (Clontech, Palo Alto, Calif.) and was maintained in complete medium with 250 nM dexamethasone as described previously [19, 28]

Growth inhibition assay

A ³H-thymidine incorporation assay was performed as described previously [8]. Following incubation in medium containing BIRM or without BIRM, the cells were pulse-labeled with ³H-thymidine (1 µCi/ml) for 2 h. Incorporation of ³H-thymidine into cellular DNA was stopped by the addition of 10% trichloroacetic acid and the acid-precipitable radioactivity was determined by liquid scintillation counting [8]. Clonogenic survival of CaP cells exposed to BIRM for 24 h was assayed by the colony assay as described previously [8].

Determination of apoptotic activity

BIRM-induced apoptosis was assayed using a cell death ELISA kit (Cell Death ELISA-Plus kit; Roche Molecular Biochemicals, Mannheim, Germany). The assay measured the amount of free nucleosomes in cell lysate resulting from programmed cell death [9]. The relative amount of free nucleosomes present in cell lysates from cultures incubated with BIRM for 4 h was estimated according to the supplier's instructions.

Cell cycle analysis

CaP cells (1×10^5) were cultured in 60-mm culture dishes. After an overnight culture, the cells were treated with 10 µl/ml of BIRM for 24 h. BIRM-treated and untreated cells were harvested and stained with 50 µg/ml propidium iodide. The amount of propidium iodide bound to DNA was profiled in an EPICS XL flow cytometer as described previously [19].

The fraction of dead cells at the time of harvesting was about 16% as determined by trypan blue exclusion. The majority of these cells were floating, so were discarded at the time of washing. The remaining dead cells were gated out using the forward angle light scatter and side scatter gatings during flow cytometry. About 20,000 propidium iodide-stained cells were analyzed in the flow cytometer from each sample. The MODFIT LT program (Verity Software House, Topsham, Me.) was used for the cell cycle phase analysis [29].

Determination of activation of cell death caspases

Caspase activation in CaP cells treated with BIRM was determined using a kit (Homogeneous Caspases Assay, fluorimetric; Roche) which determined collectively activated caspases nos. 2, 3, 6, 7, 8, 9 and 10. The assay measured the free rhodamine 110 (R110) resulting from the cleavage of a common caspase substrate, DEVD, conjugated with R110. The amount of free R110 was determined fluorimetrically at an excitation wavelength of 499 nm and an emission wavelength of 528 nm, and is expressed as relative fluorescence units (RFU) [25].

HAase assay

We tested whether BIRM affects HAase activity secreted in DU-145 culture-conditioned medium and partially purified HYAL1 using a HAase activity ELISA-like assay [20, 22]. HYAL1-type HAase was partially purified from the urine of patients with high-grade bladder cancer as described previously [20]. The assay was performed in a 96-well microtiter plate coated with HA (200 µg/ml, ICN Biomedicals). Wells were incubated with various concentrations of BIRM or column fractions from a Sephadex G-50 gel-filtration column (see below) in a HAase assay buffer at 37°C for 15 h [20]. Following incubation, HA degraded by HAase was washed off and the HA remaining in the microtiter wells was estimated using a biotinylated bovine nasal cartilage HA-binding protein, and an avidin-biotin detection system (Vector Laboratories, Burlingame, Calif.) [21].

Biochemical characterization of cytotoxic activity in BIRM

To study heat inactivation, BIRM was heated at 100°C for 5 min in a water bath. BIRM was digested with proteinase K (10 U/ml) at 37°C for 18 h. For size fractionation studies, clarified BIRM was loaded into ultrafiltration mini-Centriprep tubes (Millipore, Bedford, Mass.) with membrane barriers with different molecular weight cut-off points (i.e. about 3.5, 10 and

30 kDa). Following three cycles of centrifugation and separation of the low molecular weight fractions, both the filtrate and the retentate were assayed for cytotoxic activity. BIRM solution was also treated with charcoal-dextran (50 mg/ml) at 4°C for 12 h to remove lipids and steroids (if any). Following the various treatments, BIRM was centrifuged and various concentrations of the supernatant were added to PC3-ML cells cultured in 24-well plates (2×10^4 cells/well). BIRM-induced cytotoxicity was estimated using the MTT reduction assay following a 24-h treatment [19].

Gel filtration chromatography

Particle-free BIRM was loaded onto a G-50 Sephadex column (1.5×120 cm) equilibrated with 20 mM Tris-HCl, pH 7.4, containing 150 mM NaCl buffer (Tris/NaCl buffer) [20]. The column was eluted in Tris/NaCl buffer at 7 ml/h and 3-ml fractions were collected. Each fraction was assayed for protein (BCA-BioRad), uronate [2], inhibition of cell growth (MTT assay) [19] and inhibition of HAase activity (HAase ELISA-like assay).

Tumor generation and BIRM administration

This experiment was performed according to a protocol approved by the University of Miami Animal Care and Use Committee and as stipulated in the NIH Guide to the Humane Care and Use of Laboratory Animals. A suspension (1×10^5 cells, 0.5 ml) of growing EGFP-MAT LyLu cells was implanted subcutaneously into the dorsal flank of adult (about 250 g) male Copenhagen rats (Harlan Sprague Dawley, Indianapolis, Ind.) under mild anesthesia [19]. The rats were housed in a room under a 12-h light/12-h dark cycle and provided with food and water ad libitum throughout the experiment. Following implantation, the rats were randomly divided into two groups of six animals and gavaged with 1 ml of either distilled water (vehicle control, group 1) or BIRM (group 2) using a 3-inch stainless-steel intubation cannula on day 1 of tumor implantation and then daily for 30 days. Tumor growth was examined by palpating the skin around the site of injection. After the tumors became palpable (about day 5), they were measured three times a week using calipers, and the volumes calculated assuming approximation to an ellipsoid ($\text{length} \times \text{height} \times \text{width} \times 0.524$). Animals were killed when the tumor volume was about 10 ml or the tumor became significantly necrotic. At necropsy, lungs were collected and viewed under a Nikon stereomicroscope with a fluorescence attachment (SMZ 1500) to examine the presence of fluorescent metastatic tumor foci.

Statistical analysis

Triplicate samples were assayed in all in vitro experiments. Statistical analysis was performed using parametric and nonparametric Student's *t*-tests.

Results

BIRM inhibits cell proliferation in CaP cells

BIRM inhibited cell proliferation in all the CaP cell lines tested in a dose-dependent manner (Fig. 1). The concentration of BIRM causing 50% growth inhibition (IC_{50}) was 8 μ L/ml (i.e. 0.8% v/v). Furthermore, the inhibitory activity of BIRM was comparable among all CaP cell lines regardless of their androgen sensitivity (androgen-sensitive LNCaP and VCaP cells versus androgen-resistant PC-3ML and DU-145 cells). Similar results were obtained by cell counting and Trypan blue exclusion assays (data not shown). The results presented in Fig. 1 and similar observation from other assays suggested that BIRM-induced inhibition of cell proliferation led to either cell death (cytotoxicity) or arrest of cell proliferation (cytostasis). To distinguish between these mechanisms, we investigated the colony-forming efficiency of CaP cells treated with BIRM. The clonogenic assay revealed a dose-dependent inhibition of colony formation in BIRM-treated CaP cells. Neither cell colonies nor cell clusters were observed in cultures exposed to BIRM at doses of 10 μ L/ml and above for 24 h (Fig. 2A). The IC_{50} of BIRM for inhibiting clonogenic survival was also 8 μ L/ml, the same as the value obtained in the 3 H-thymidine assay (Fig. 2B).

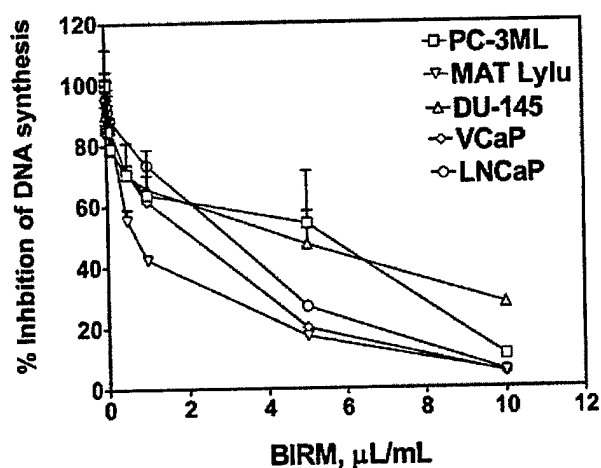


Fig. 1. Cytotoxicity of BIRM against prostate tumor cell lines. CaP cells cultured in growth medium (1×10^4 cells/well, 48-well plates) were exposed to various concentrations of BIRM. Following incubation for 24 h, DNA synthesis was determined by measuring ^3H -thymidine incorporation in the proliferating cells (vertical bars means \pm SEM from three independent assays)

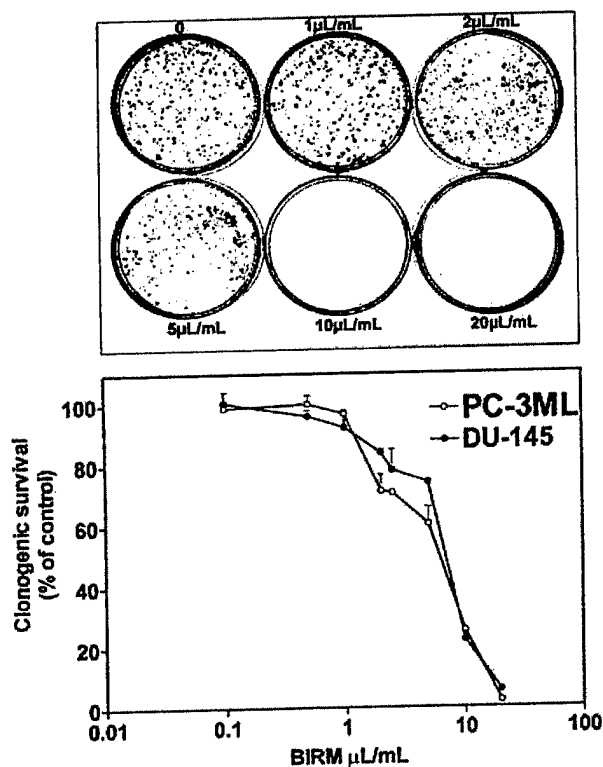


Fig. 2a, b. Effect of BIRM on the growth of CaP cells. Cells cultured at low density in 60-mm culture dishes were exposed to BIRM for 24 h. Surviving cells at the end of incubation were allowed to form adherent cell colonies during the next 7–10 days. Cell colonies stained with 0.1% crystal violet and colonies containing >50 cells were counted manually using a hand-held electronic counter in a blinded fashion. **a** Colonies of surviving PC3-ML cells exposed to BIRM for 24 h. **b** Clonogenic survival of CaP cells cultured with BIRM. The results are presented as means \pm SEM from three independent experiments

BIRM causes cell cycle arrest in CaP cells

As shown in Table 1, the proportion of cells in G_0/G_1 phase increased significantly from $56.4 \pm 0.9\%$ in control to $75.5 \pm 2.2\%$ in cultures treated with BIRM at $25 \mu\text{L/mL}$. The increase in the G_0/G_1 phase fraction in the BIRM-treated cells was contrasted with a decrease in the S-phase fraction. The S-phase fraction in BIRM-treated cells was $13.1 \pm 2.9\%$ compared to

28.9±2.1% in the control. A small decrease of 15–22% in the G₂/M fraction was also observed in BIRM-treated cells.

[Table 1. will appear here. See end of document.]

BIRM induces apoptosis in CaP cells

We did not observe a significant difference in the levels of free nucleosomes in BIRM-treated cells during 4 h of treatment, but after 24 h of treatment the intracellular levels of free nucleosomes showed a two- to threefold dose-dependent increase (Fig. 3).

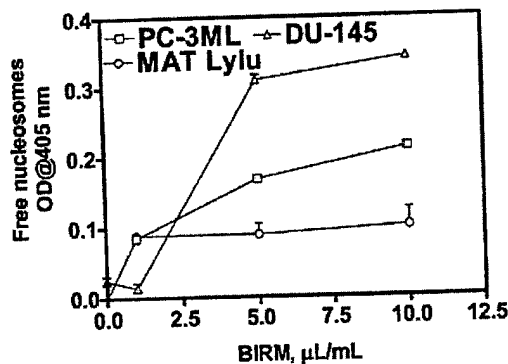


Fig. 3. BIRM kills tumor cells by induction of apoptosis. PC-3ML, DU-145 and Mat Lylu CaP cells cultured in growth medium (1×10^4 cells/well; 48-well plates) with or without BIRM at various concentrations for 24 h were analyzed for apoptotic activity using the Cell Death ELISA Plus assay kit, which allowed measurement of soluble nucleosomes by spectrophotometry. The data presented as means±SEM from three independent experiments

Activation of cell death-associated caspases

As shown in Fig. 4, the activities of one or more of caspases 2, 3, 7, 8, 9 and 10 were increased significantly in BIRM-treated cells as compared to the activities in control cells. We initially detected a time-dependent increase in combined caspase activity, beginning at 4 h of exposure to BIRM and peaking at 18 h. The dose-dependent increase in caspase activities showed a 50% increase in cells treated at 5 μl/ml BIRM over the activity in control cells following incubation for 18 h or longer (Fig. 4).

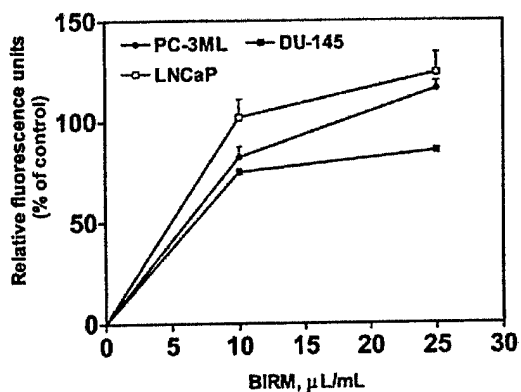


Fig. 4. BIRM induced increases in caspase activity. CaP cells were treated with BIRM for 4 to 24 h and the total activities of cell death-associated caspases were measured using a kit that employed a rhodamine110-conjugated peptide substrate common to all cell death-related caspases. The results are presented as means \pm SEM from three independent experiments in each of which cell lysates incubated with BIRM for 24 h were used for caspase activity determination. Caspase activity in untreated control cultures was detectable, but was typically ten times less than the activity detected in the positive controls provided with the assay kit

BIRM inhibits tumor growth and metastasis

As shown in Fig. 5, following tumor implantation, oral administration of BIRM (4 ml/kg body weight) to rats resulted in slow tumor growth. While the tumor incidence was 100% in the control group, only four out of six BIRM-treated animals (67%) developed tumors. The tumor growth rate estimated using non-linear regression analysis of tumor volumes over time for each animal confirmed a decreased growth rate in BIRM-treated animals. The times taken for tumors to reach 1 ml was 18.6 ± 1.3 days in control animals and 25.7 ± 2.6 days in BIRM-treated animals (mean \pm SE from four animals). A 38% delay in tumor growth was observed in BIRM-treated animals compared with control animals. The difference in the growth rate between control and BIRM-treated animals was statistically significant (unpaired *t*-test: $P=0.03$, $t=2.773$, $df=6$, 95% CI 0.835–13.36). Fluorescence imaging of the lungs at necropsy revealed that only one out of six BIRM-treated animals had metastatic lung foci, whereas five out of six control animals had tumor metastasis to the lungs. Furthermore, the tumor foci in the lungs of the BIRM-treated animal were significantly smaller than those in control animals (Fig. 6). These results indicate that ingredients in BIRM either delay or block spontaneous lung metastasis.

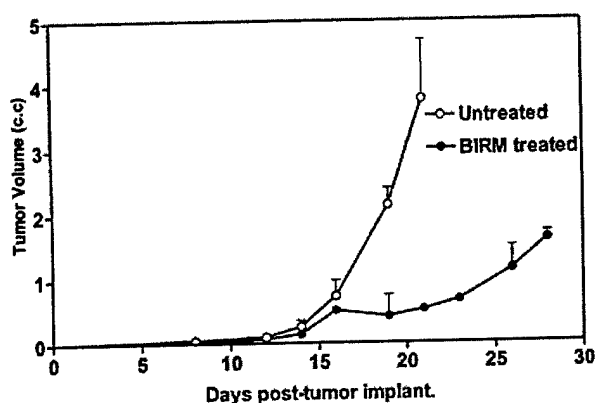


Fig. 5. Effect of daily dosing of BIRM on growth and metastasis of Dunning MAT LyLu tumors in rats. Tumor growth in rats with subcutaneous tumor implant with EGFP-MAT LyLu cells (2×10^5 cells/animal). The data are presented as means \pm SEM of each treatment group over time. Data from the control group include measurements from six tumor bearing rats, whereas the BIRM-treated group had only four animals; the other two animals in this group did not develop tumors

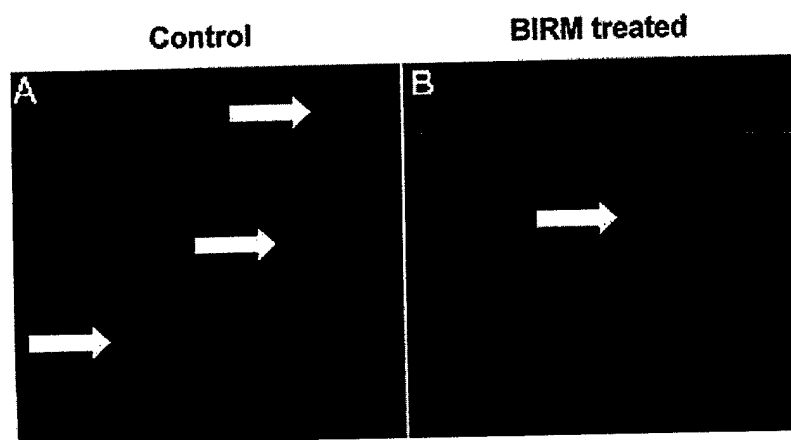


Fig. 6A, B. EGFP-MAT LyLu rat prostate tumors metastatic to lungs. The figure shows rat lungs with fluorescent tumor foci (arrows). A Control animals ($\times 40$); B a typical tumor metastatic to the lung in a BIRM-treated animal ($\times 20$). Tumor foci in the lungs of BIRM-treated animals were typically ten times smaller or absent

BIRM inhibits the activity of HYAL1-type HAase

Investigation of inhibition of matrix metalloproteinase activity by BIRM using a ^3H -labeled collagen-degradation assay [18] showed no changes in matrix metalloproteinase activity following BIRM treatment (data not shown). We next examined whether BIRM could inhibit the activity of HYAL1-type HAase. We have previously shown that HYAL1 is the major

HAase expressed in cancers of the prostate and bladder [21, 22]. Furthermore, invasive tumor cells express high levels of HYAL1 [5, 21, 22]. As shown in Fig. 7, BIRM potently inhibited HAase activity. BIRM inhibited the HAase activity present in the culture-conditioned medium of DU-145 cells (a good source of HYAL-1 [21]) and the activity of partially purified HYAL1, in a dose-dependent manner (IC_{50} 0.25 μ l/ml).

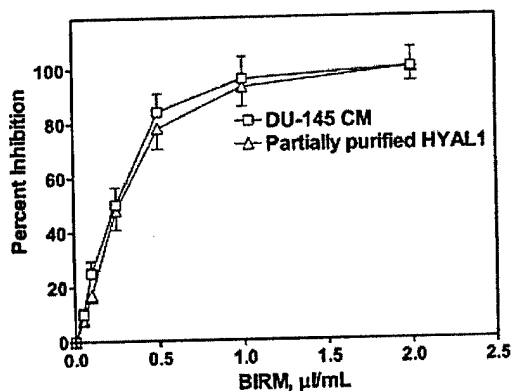


Fig. 7. BIRM inhibits tumor-derived HAase. Effect of BIRM on the HAase activity present in DU-145 cell-conditioned medium and partially purified preparation of HYAL1 was carried out using an HAase ELISA-like assay as described in Materials and methods. The data shown are from a typical experiment. Similar results were obtained in three other experiments using LNCaP cells (data not shown)

Characterization of active ingredients in BIRM solution

BIRM retained its full cytotoxic activity after boiling for 5 min or digestion with proteinase K, indicating that reactive species present in BIRM most likely are heat-stable proteinase-resistant compounds. Similarly, charcoal-dextran extraction also did not result in any loss in the cytotoxic activity associated with BIRM, suggesting that the active species present in BIRM are not lipid-soluble compounds such as alkaloids or steroids. No loss in cytotoxic activity was found upon ultrafiltration through a 3.5-kDa membrane barrier. However, a 40% loss in activity was observed after ultrafiltration through 10-kDa and 30-kDa membranes (Fig. 8). These results indicate that BIRM contains at least two species with different molecular mass, i.e. one with a molecular mass between 3500 and 10,000 and a second with a molecular mass of $\geq 30,000$, with cytotoxic activity against CaP cells. The possibility of the growth-inhibitory activity being associated with carbohydrate derivatives was investigated using the Bitter and Muir modified carbazole assay to measure glycosaminoglycans and proteoglycans containing D-glucuronic acid (i.e. uronate) [23]. The

results showed that BIRM is rich in uronate-containing carbohydrates (19.5 mg/ml). Gel filtration chromatography on a Sephadex G-50 column also showed two active fractions (fraction nos. 28 and 42, Fig. 9).

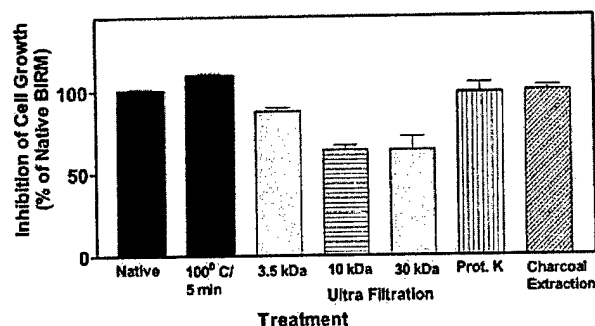


Fig. 8. Cytotoxicity of modified BIRM as assayed by MTT assay and compared with unmodified BIRM. BIRM solution was treated with proteinases (proteinase K), heated for 5 min in a bath of boiling water or subjected to ultrafiltration as described in Materials and methods. Following treatment, untreated and treated BIRM solutions were tested for cytotoxic activity in PC3-ML cells by MTT assay, as described in Materials and methods (vertical bars means \pm SEM from four independent assays)

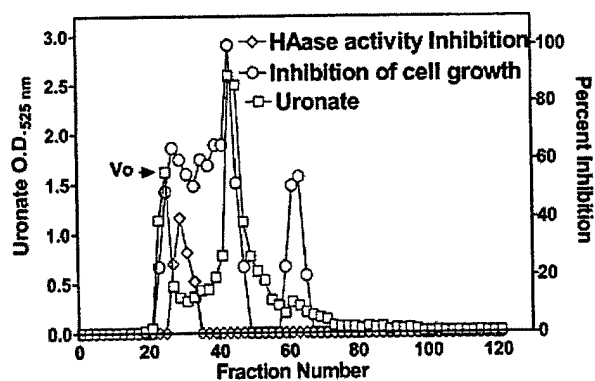


Fig. 9. Fractionation of antineoplastic ingredients present in BIRM by gel filtration chromatography. Clarified BIRM (5 ml) was fractionated on a Sephadex G-50 column. The column fractions were assayed for protein ($A_{280 \text{ nm}}$), uronate concentration (Bitter and Muir assay), HAase activity (HAase activity ELISA) and cytotoxicity (MTT assay). A single protein peak was detected in fraction no. 20, which had neither cytotoxic activity nor HAase-inhibitory activity

Discussion

A systematic investigation of promising plant products has led to the discovery and development of antineoplastic agents with unique modes of action and striking efficacy (e.g. paclitaxel, vinblastine, etoposide, etc) [7]. In this report, we present evidence of the antineoplastic activity of a plant-derived nutritional supplement, BIRM. BIRM with medicinal value is believed to be associated only with the plant variety found in Dulcamara in the upper Amazon basin where the micronutrients present in the soil promote the synthesis of the medicinal compounds in the plant. BIRM inhibited cell proliferation and clonogenic survival (Figs. 1 and 2) and caused apoptotic cell death via the caspase activation pathway (Figs. 3 and 4). In vivo studies on the growth and metastasis of Dunning MAT LyLu tumors suggested that oral dosing with BIRM resulted in lower tumor incidence, slower tumor growth and reduced spontaneous metastasis to the lungs (Figs. 5 and 6). A preliminary biochemical characterization and size-exclusion chromatography suggested that there were at least four active species present in BIRM, three with cytotoxic activity and one with HAase-inhibitory activity. We have not yet determined whether the three cytotoxic species present in BIRM have the same chemical composition but different polymer length. Nonetheless, all four active ingredients were heat-stable and unlikely to be proteins or lipid-soluble compounds.

Inhibition of tumor growth in the rat CaP model following the oral administration of BIRM clearly suggests that the active ingredient(s) of BIRM are absorbed in the gastrointestinal tract. The reduction in tumor incidence (33%) and the number of tumor foci in the lungs (>80%) in BIRM-treated animals suggest that BIRM may exert both antiproliferative and antimetastatic activities. It is estimated that 20–40% of patients initially diagnosed with local CaP have either locally advanced disease (stage C) or metastatic disease (stage D) [10, 16], and the cure of metastatic disease still remains a challenge. Our observation that CaP cell cultures treated with BIRM showed a significant reduction in cell proliferation and undergo apoptosis (Figs. 1, 2, and 3) indicates that the active ingredients present in BIRM have potential for use in controlling advanced hormone-refractory prostate cancer. We investigated whether the BIRM-induced cytotoxic effect was due to inhibition of mitotic spindle separation. This would lead to mitotic inhibition and arrest of cells in the G_2/M phase. Contrary to our expectation, incubation with BIRM arrested CaP cells in G_0/G_1 , which was compensated for by a significant decrease (i.e. –56%) in the proportion of cells in S phase and a modest decrease in G_2/M , indicating lack of mitotic arrest or cytokinesis (Table 1).

This finding is novel in the sense that most plant-derived compounds used in cancer therapy interfere with tubulin polymerization (e.g. vinblastine and vincristine) or depolymerization (paclitaxel), or inhibit topoisomerase I activity (e.g. irinotecan, topotecan, 9-aminocamptothecin and 9-nitrocamptothecin) [6] or topoisomerase II activity, leading to cell cycle arrest in the G₂/M phase (e.g. paclitaxel, etoposide and teniposide) [24].

Apoptotic cell death may be one of the mechanisms involved in BIRM-induced cytotoxicity. BIRM increased the apoptosis in three CaP cell lines (Fig. 3). Furthermore, induction of apoptosis in BIRM-treated CaP cells was coincident with activation of cell-death caspases (Fig. 4). In addition to its cytotoxic effects, BIRM appeared to be a potent inhibitor of metastasis. Although, the mechanism by which it may inhibit metastasis is unknown at present, our results suggests that BIRM is a potent inhibitor of HAase, a class of matrix-degrading enzymes whose levels have been shown to correlate with CaP progression [20, 22].

The recommended minimum dose of BIRM for human consumption is 4 ml/day (as indicated on the bottle label), a significantly lower dose than that used in the current study. We based the dosage to rats on the observed efficacy in vitro. We found no observable systemic toxicity in rats at a dose of 4 ml/kg. Given its effect on tumor growth and metastasis and no systemic toxicity, inclusion of BIRM as an adjuvant to standard therapy has potential to reduce/halt disease progression.

In summary, our study demonstrated that BIRM shows cytotoxic activity against both androgen-dependent and androgen-independent CaP cells in vitro. More importantly, it reduced tumor incidence, delayed tumor growth and caused a significant reduction in metastasis in an experimental model of late-stage CaP. Furthermore, no systemic toxicity was seen following continuous administration of BIRM in an in vivo rat model. These useful properties of BIRM indicate that further investigation of its mechanism of action and clinical trials involving its use in advanced CaP are warranted.

Acknowledgements The authors are indebted to Mr. Christian DeGetau von Forckenbeck for introducing us to BIRM. The authors thank Rita Mourelatos, Monica Lopez and Dr. Tie Yan Shang for technical assistance and Dr. A. Krishan for the use of his flow cytometry facility.

References

1. BIRM Carbohydrate of low molecular weight ECA10-142 controls AIDS (1994) Tenth International Conference on AIDS (Yokohama, Japan). Abstracts, vol 2 (abstract no. 0291)

2. Bitter T, Muir H (1966) Mucopolysaccharides of whole human spleens in generalized amyloidosis. *J Clin Invest* 45:963-975
3. Cevallos EA (1994) Binational experience in the treatment of AIDS with a low molecular weight natural carbohydrate (ECA-10-142), as a stimulant of the immune system. Tenth International Conference on AIDS (Yokohama, Japan). Abstracts, vol 1 (abstract no. 0294)
4. Cevallos EA (1996) "BIRM: La estrategia terapeutica del futuro". Abstract of Congresso Mundial de SIDA en Vancouver
5. Delpech B, Girard N, Bertrand P (1997) Hyaluronan: fundamental principles and applications in cancer. *J Intern Med* 242:41-48
6. Dennis RAM, Adriana BN, Rocha DA, Gilberto S (2000) Anti-cancer drug discovery and development in Brazil: targeted plant collection as a rational strategy to acquire candidate anti-cancer compound. *Oncologist* 5:185-198
7. Donehower RC, Rowinsky EK (1993) Anticancer drugs derived from plants. In: DeVita VT Jr, Hellman S, Rosenberg SA (eds) *Principles and practice of oncology*, 4th edn. Lippincott, New York
8. Dudak SD, Lopez A, Block NL, Lokeshwar BL (1996) Enhancement of radiation response of prostatic carcinoma by lonidamine. *Anticancer Res* 16:3665-3671
9. Eisel D, Fertig G, Fischer B, Manzow S, Schmelig K (eds) (2000) *Guide to cell proliferation and apoptosis methods*, 2nd edn (technical manual). Roche Applied Science, Mannheim, Germany
10. Harris K, Reese DM (2001) Treatment options in hormone-refractory prostate cancer: current and future approaches. *Drugs* 61:2177-2192
11. Horoszewicz JS, Leong SS, Kawinski E, Karr JP, Rosenthal H, Chu TM, Mirand EA, Murphy GP (1983) LNCaP model of human prostatic carcinoma. *Cancer Res* 43:1809-1818
12. Jacobson JS, Chetty AP (2001) Complementary and alternative medicine in prostate cancer. *Curr Oncol Rep* 3:448-452
13. Jamel A, Thomas A, Murray T, Thun M (2002) Cancer statistics 2000. *CA Cancer J Clin* 52:23-47
14. Jones HA, Metz JM, Devine P, Hahn SM, Whittington R (2002) Rates of unconventional medical therapy use in patients with prostate cancer: standard history versus directed questions. *Urology* 59:272-276
15. Kaighn ME, Narayan KS, Ohnuki Y, Lechner JF, Jones LW (1979) Establishment and characterization of a human prostatic carcinoma cell line (PC-3). *Invest Urol* 17:16-23
16. Kojima M, Troncoso P, Babaian RJ (1995) Use of prostate-specific antigen and tumor volume in predicting needle biopsy grading error. *Urology* 45:807-812
17. Korenchuk S, Lehr JE, Mclean L, Lee YG, Whitney S, Vessella R, Lin DL, Pienta KJ (2001) VCaP, a cell-based model system of human prostate cancer. *In Vivo* 15:163-168
18. Lokeshwar BL, Selzer MG, Block NL, Gunja-Smith Z (1993) Secretion of matrix metalloproteinases and their inhibitors (tissue inhibitor of metalloproteinases) by human prostate in explant cultures: reduced tissue inhibitor of metalloproteinase secretion by malignant tissues. *Cancer Res* 53:4493-4498
19. Lokeshwar BL, Selzer MG, Zhu BQ, Block NL, Golub LM (2002) Inhibition of cell proliferation, invasion, tumor growth and metastasis by an oral non-antimicrobial tetracycline analog (COL-3) in a metastatic prostate cancer model. *Int J Cancer* 98:297-309
20. Lokeshwar VB, Lokeshwar BL, Pham HT, Block NL (1996) Association of elevated levels of hyaluronidase, a matrix-degrading enzyme, with prostate cancer progression. *Cancer Res* 56:651-657
21. Lokeshwar VB, Young MJ, Goudarzi G, Iida N, Yudin AI, Cherr GN, Selzer MG (1999) Identification of bladder tumor-derived hyaluronidase: its similarity to HYAL1. *Cancer Res* 59:4464-4470
22. Lokeshwar VB, Rubinowicz D, Schroeder GL, Forgacs E, Minna JD, Block NL, Nadji M, Lokeshwar BL (2001) Stromal and epithelial expression of tumor markers hyaluronic acid and hyaluronidase in prostate cancer. *J Biol Chem* 276:11922-11932

23. Mickey DD, Stone KR, Wunderli H, Mickey H, Paulson DF (1980) Characterization of a human prostate adenocarcinoma cell line (DU 145) as a monolayer culture and as a solid tumor in athymic mice. *Prog Clin Biol Res* 37:67-84
24. Pienta KJ, Naik HN, Jeffrey EL (1996) Effect of estramustine, etoposide and taxol on prostate cancer cell growth in vitro and in vivo. *Urology* 48:164-170
25. Roche Applied Science (2002) Homogeneous caspases assay, fluorimetric (pack insert/product instruction). Roche Applied Science, Mannheim Germany
26. Smith M, Mills EJ (2001) Select complementary/alternative therapies for prostate cancer: the benefits and risks. *Cancer Pract* 9:253-255
27. Wang M, Stearns ME (1991) Isolation and characterization of PC-3 human prostatic sublines, which preferentially metastasize to select organs in S.C.I.D. mice. *Differentiation* 48:115-125
28. Wenger AS, Mickey DD, Hall M, Silverman LM, Mickey GH, Fried A (1984) In vitro characterization of MAT LyLu: a Dunning rat prostate adenocarcinoma tumor subline. *J Urol* 131:1232-1236
29. Yamamura Y, Rodriguez N, Schwartz A, Eylar E, Bagwell B, Yano N (1995) A new flow cytometric method for quantitative assessment of lymphocyte mitogenic potentials. *Cell Mol Biol (Noisy-le-grand)* 41:121-132

Table 1. Flow cytometric cell cycle fractionation analysis of PC-3ML cells treated with BIRM for 24 h. The distributions of cells in the various cell cycle phases were calculated from the DNA content of propidium iodide-labeled cells using the MODFIT program. Values are mean \pm SE percentages from three independent experiments. Similar results were obtained from the cell cycle fractionation analysis of LNCaP cells exposed to BIRM

Treatment	G ₀ /G ₁ phase		S phase		G ₂ /M phase	
		Difference (%) [*]		Difference (%) [*]		Difference (%) [*]
Control	56.37 \pm 0.9		28.9 \pm 2.1		14.6 \pm 1.2	
BIRM (10 μ l/ml)	67.93 \pm 2.1	+20.5	19.5 \pm 2.4	-32.5	12.5 \pm 0.28	-15
BIRM (25 μ l/ml)	75.46 \pm 2.2	+33.8	13.1 \pm 2.9	-54.6	11.39 \pm 0.29	-22

^{*}Calculated as [(% of cells in respective phase of untreated samples - % of cells in respective phase in BIRM-treated samples) / (% of cells in respective phase in untreated control)] \times 100